

USING CARBOHYDRATE-BINDING MODULES AS TOOLS FOR *IN VIVO*  
VISUALIZATION/MODULATION OF PLANT CELL WALL POLYSACCHARIDES

by

TIANTIAN ZHANG

(Under the direction of Michael G Hahn)

ABSTRACT

Plant cell walls are highly complex and dynamic cell compartments. Until now, most knowledge of cell wall is derived from the biochemical analysis of fractionated walls and immunolabeling of fixed tissues. Consequently, the majority of temporal and developmental information is lost. Recently, Carbohydrate-Binding Modules (CBMs) from microbial cell wall polysaccharides hydrolases have been developed as probes for cell wall analysis *in vitro*. CBMs are particularly attractive as *in vivo* cell wall probes because of their intrinsic specificities toward polysaccharides, ease of heterologous expression, and convenience of modification with fluorescent protein markers.

Preliminary research found xylan-binding CBM is more suitable to be utilized as *in vivo* tagging xylan tool since expression of fluorescent protein mCherry tagged CBM2b-1-2 has no deleterious effect on plant morphology or development. The heterologously expressed fluorescent protein-tagged CBM2b-1-2 selectively labels cell walls that contain xylan, including those of xylem vessels and interfascicular fibers associated with phloem in wild-type *Arabidopsis* plants. As a functional *in vivo* visualization tool, we were interested in testing whether fluorescent protein-tagged CBM2b-1-2 would allow us observe effects that arise from

mutations in genes that affect the synthesis and deposition of xylan *in vivo*. Mutation of a WRKY transcription factor causes ectopic xylan deposition in pith cells of Arabidopsis. The plant line carrying a mutation in this WRKY gene was crossed with the stable CBM2b-1-2:mCherry expression line. Examination of F2 plants resulting from this cross demonstrated that the ectopic deposition of xylan can be observed simply and conveniently via hand sectioning. These results suggest that the fluorescent protein-tagged xylan-binding CBM2b-1-2 is a functional *in vivo* visualization tool to follow xylan dynamics during plant development.

In contrast, heterologous expression of cellulose-binding CBM3a affected plant cell wall polysaccharides network and modulated plant growth and developmental processes. Transgenic CBM3a:mCherry plants displayed a dwarfed phenotype, had reduced cellulose and xylan content, and showed changes in glycan epitope extractability patterns. These results indicate that expression of a specific CBM in Arabidopsis may lead to changes in the composition and/or structure of the cell wall, which in turn, may have an impact on the development of the plant.

INDEX WORDS: Carbohydrate-Binding Module (CBM), Plant Cell Wall, *in vivo* Visualization Tool, CBM2b-1-2, modulation, CBM3a

USING CARBOHYDRATE-BINDING MODULES AS TOOLS FOR *IN VIVO*  
VISUALIZATION/MODULATION OF PLANT CELL WALL POLYSACCHARIDES

by

TIANTIAN ZHANG

(Under the direction of Michael G Hahn)

B.S. Nanjing Normal University, China, 2004

M.S. Texas Tech University, Texas, United States, 2008

A Dissertation Submitted to the Graduate Faculty of The University of Georgia in Partial  
Fulfillment of the Requirements for the Degree

DOCTOR OF PHILOSOPHY

ATHENS, GEORGIA

2014

© 2014

TIANTIAN ZHANG

All Rights Reserved

USING CARBOHYDRATE-BINDING MODULES AS TOOLS FOR *IN VIVO*  
VISUALIZATION/MODULATION OF PLANT CELL WALL POLYSACCHARIDES

by

TIANTIAN ZHANG

Major Professor: Michael G Hahn

Committee: Debra Mohnen

Kelly Dawe

William S York

Wolfgang Lukowitz

Electronic Version Approved:

Julie Coffield

Interim Dean of the Graduate School

The University of Georgia

December 2014

## DEDICATION

This dissertation is dedicated to my parents and my husband for their forever love and unconditional support.

## ACKNOWLEDGEMENTS

First and most importantly, I would like to express my gratitude and appreciation to my advisor, Dr. Michael G Hahn, for giving me the opportunity to study and work in his group with an extraordinary environment. I am really grateful to his constant guidance, support and encouragement throughout all the years of my graduate study.

I would like to thank my committee, Dr. Debra Mohnen, Dr. Kelly Dawe, Dr. William York and Dr. Wolfgang Lukowitz for their invaluable time and expertise. I would also like to thank Dr. Harry Gilbert, for his countless help.

Many thanks go to the past and present members of the Complex Carbohydrate Research Center: Yingzhen Kong, Sivakumar Pattathil, Utku Avci, Fangfang Fu, Claudia L. Cardenas, Ron Clay, Christina Hopper, Sivasankari Venketachalam, Sindhu Kandemkavil, Lei Zhao, Supriya Ratnaparkhe, Xiaoyang Zhang, Ann (Zhangyin) Hao, Li Tan, Melani Atmodjo. Best wishes in their future endeavors.

Last but not least, I would like to thank my family and all my friends for their love and support.

## TABLE OF CONTENTS

	Page
ACKNOWLEDGEMENTS.....	v
LIST OF TABLES.....	vii
LIST OF FIGURES.....	viii
CHAPTER	
1 INTRODUCTION AND LITERATURE REVIEW.....	1
2 CHARACTERIZATION OF THE BINDING SPECIFICITIES OF FLUORESCENT PROTEIN TAGGED CBMS.....	32
3 <i>IN VIVO</i> VISUALIZATION OF XYLAN IN WILD-TYPE AND MUTANT PLANTS USING CBM2B-1-2.....	64
4 HETEROLOGOUS EXPRESSION OF CRYSTALLINE CELLULOSE DIRECTED- CARBOHYDRATE BINDING MODULE 3A IN ARABIDOPSIS MODULATES PLANT CELL WALLS AND DEVELOPMENT.....	95
5 CONCLUSIONS.....	130

## LIST OF TABLES

	Page
Table 1.1: List of CBMs.....	15
Table 2.1: List of CBMs in this project.....	34
Table 2.2: Size of the fluorescent protein mCherry tagged CBMs in this study.....	38

## LIST OF FIGURES

	Page
Figure 1.1: Schematic representation of the polysaccharides in plant cell walls.....	3
Figure 1.2: Cartoon of network models of the primary cell wall.....	8
Figure 1.3: The genes encoding polysaccharide synthases involved in xyloglucan biosynthesis in Arabidopsis.....	9
Figure 2.1: Expression of mCherry fluorescent protein tagged CBMs.....	38
Figure 2.2: Binding specificity of CBM2a:mCherry towards 55 plant polysaccharide antigens..	40
Figure 2.3: Binding specificity of CBM3a:mCherry towards 55 plant polysaccharide antigens..	41
Figure 2.4: Binding specificity of CBM2b-1-2:mCherry towards 55 plant polysaccharide antigens.....	43
Figure 2.5: Binding specificity of CBM35:mCherry towards 55 plant polysaccharide antigens..	44
Figure 2.6: Binding specificity of CBMXG34/1-X:mCherry towards 55 plant polysaccharide antigens.....	45
Figure 2.7: Binding specificity of CBMXG34/1-X:mCherry towards 55 plant polysaccharide antigens.....	46
Figure 2.8: Cellulose Pull-Down Assay of mCherry tagged CBMs.....	48
Figure 2.9: Labeling of Arabidopsis stem sections <i>in vitro</i> with tagged CBM fusion proteins.....	49
Figure 2.10: Binding studies of fluorescent protein tagged CBMs on Arabidopsis cell wall extracts.....	51

Figure 3.1: Outline of heterologous expression of CBM2b-1-2:mCherry in transgenic plants....	72
Figure 3.2: Observation of WT plants <i>in vivo</i> and <i>in vitro</i> .....	75
Figure 3.3: Observation of transgenic SP:mCherry plants <i>in vivo</i> and <i>in vitro</i> .....	76
Figure 3.4: Observation of transgenic CBM2b-1-2:mCherry plants <i>in vivo</i> and <i>in vitro</i> .....	77
Figure 3.5: Identification and phenotypic characterization of CBM2b-1-2:mCherry X <i>wrky12-1</i> , CBM2b-1-2:mCherry and SP:mCherry plants.....	79
Figure 3.6: Observation of CBM2b-1-2:mCherry X <i>wrky12-1</i> plants <i>in vivo</i> and <i>in vitro</i> .....	82
Figure 3.7: Observation of <i>wrky12-1</i> plants <i>in vivo</i> and <i>in vitro</i> .....	83
Figure 3.8: <i>In vivo</i> localization of CBM2b-1-2:mCherry/SP:mCherry proteins in maturation zone of 3-day-old CBM2b-1-2:mCherry x <i>wrky12-1</i> , CBM2b-1-2:mCherry, <i>wrky12-1</i> , SP:mCherry and WT plants.....	85
Figure 4.1: (A) Outline of heterologous expression of CBM3a:mCherry in transgenic plants; (B) Agarose gels showing the presence of transgene <i>CBM3a</i> by RT-PCR in T1 plants; (C) RT-PCR analysis confirming equal expression of <i>CBM3a</i> gene in the T3 plants used in this study.....	105
Figure 4.2: Morphological phenotypes of transgenic CBM3a:mCherry plants.....	107
Figure 4.3: Fluorescent images of root and stem of transgenic Arabidopsis plants expressing CBM3a:mCherry and of wild type plants.....	108
Figure 4.4: Compositional analysis of plant cell walls from wild type and transgenic CBM3a:mCherry plants.....	111
Figure 4.5: Detection of cellulose in stem sections of 2-month-old WT plant (Upper) and transgenic CBM3a:mCherry plant (Lower).....	112

Figure 4.6: Glycome Profiling of sequential cell wall extracts from 2-month-old Wild-Type and transgenic CBM3a:mCherry plants.....114

## **CHAPTER 1**

### **INTRODUCTION AND LITERATURE REVIEW**

Plant cells are surrounded by a highly complex and dynamic cell compartment known as the cell wall. This cell wall plays important roles in the physiology, growth and development of plants, and provides structural integrity and mechanical protection for plant cells (Carpita and McCann, 2000). Plant cell walls are also important sources for human nutrition, animal feedstock, natural textile fibers, paper and wood products, and raw materials for biofuel production (Somerville, 2007). The major polysaccharide components of plant cell walls are currently classed as cellulose, hemicelluloses (e.g., xyloglucan, xylan, mannan, and mixed-linkage glucan), and pectic polysaccharides (e.g., homogalacturonan, rhamnogalacturonan I and rhamnogalacturonan II). In the primary cell walls, which surround growing cells, cellulose is thought to form load-bearing microfibrils that are cross-linked by, or are co-extensive with xyloglucan and pectin (Carpita and Gibeaut, 1993). Secondary cell wall polysaccharides surround cells that have stopped growing and are differentiated; these walls often contain cellulose, xylan and/or mannan and lignin. Increasing knowledge of the structure and function of the polysaccharide components of plant cell walls, and how their synthesis is coordinated and regulated, is required to understand how plant cell wall polysaccharide components form a functional wall.

## **The structure and biosynthesis of the plant cell wall**

Combinations of genetic, biochemical and functional genomic approaches have led to the identification of hundreds of genes that are involved in the biosynthesis and modification of cell wall components. However, a detailed understanding about how these genes impact the construction and maintenance of cell walls during plant development and how the corresponding proteins function in the cellular context is still limited. Here, we will briefly overview the current state of knowledge in relation to the structure and biosynthesis of cellulose, xyloglucan and xylan, which are the main focus of the studies reported in this thesis.

### Cellulose structure and function

On average, primary cell walls contain between 20 and 30% cellulose, while secondary cell walls can contain up to 50% cellulose (Albersheim et al., 2010). Cellulose is the most stable wall polysaccharide and is thought to be the major load-bearing constituent of plant cell walls. Cellulose is a relatively simple polysaccharide in that it is composed of unsubstituted  $\beta$ -1-4-glucan chains (Figure 1.1). Each cellulose polymer is arranged in 3-nm thick microfibrils, which are currently thought to contain roughly 36 crystalline, parallel  $\beta$ -1-4-glucan chains (Carpita and McCann, 2000). Cellulose provides the major mechanical resistance to external stresses and internal osmotic pressure (Brown, 2004) and also serves as scaffold for other cell wall polysaccharides such as hemicelluloses and pectins (Carpita and McCann, 2000).

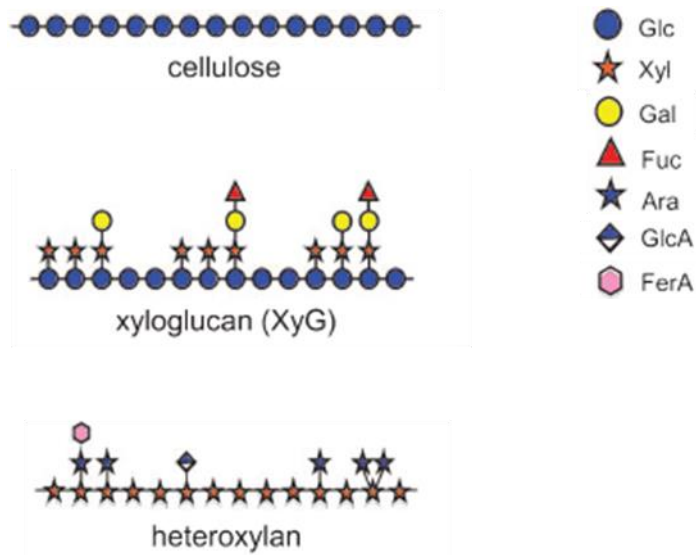


**Figure 1.1. Schematic representation of three polysaccharides in plant cell walls.** Cellulose and xyloglucan have a backbone based on glucose (Glc), heteroxylan has a backbone based on xylose (Xyl). Xylose, galactose (Gal) and fucose (Fuc) are incorporated into xyloglucan side chains. Arabinose (Ara), glucuronic acid (GlcA) and ferulic acid ester (FerA) are incorporated into heteroxylan side chains. Adapted from Figure 2 (Doblin et al., 2010).

### Biosynthesis of cellulose

Cellulose is synthesized at the plasma membrane by rosette-like cellulose synthase enzyme complexes (CSCs). A CSC is organized as hexamer of hexamers, thought to consist of 36 individual cellulose synthase (CESA) proteins. The CSCs are assembled in the Golgi and then exported to the plasma membrane via exocytosis (Somerville, 2006). Importantly, mutant analyses in *Arabidopsis* revealed that at least three different CESA proteins are required to form a functional CSC (Taylor et al., 2000; Desprez et al., 2007). In *Arabidopsis*, CESA1, 3, 6 or 6-like (CESA2, 5, 9 are partially redundant with these proteins) are required for primary wall cellulose synthesis, and CESA4, 7, 8 are required for secondary wall cellulose synthesis (Taylor et al., 2000; Persson et al., 2005; Desprez et al., 2007). Secondary wall CESAs are equally

important for cellulose biosynthesis in secondary walls, as *CESA4*, *CESA7*, *CESA8* have the same expression pattern in xylem and display interactions in the BiFc and co-immunoprecipitation assays (Atanassov et al., 2009; Timmers et al., 2009). The *cesa4*, *cesa7* and *cesa8* mutants were initially identified by collapsed xylem phenotypes and the xylem defect was associated with an up to eightfold reduction in the total amount of cellulose in stems (Turner and Somerville, 1997). On the other hand, the three primary wall CESAs have unequal contributions to cellulose biosynthesis. No null mutants have been reported for either *CESA1* or *CESA3* (Persson et al., 2007). Missense mutations in *CESA1* or *CESA3* result in severely retarded growth phenotypes and missense mutations in the catalytic domain of *CESA1* cause embryo-lethal phenotypes (Beeckman et al., 2002; Gillmor et al., 2002). However, null mutations for *CESA6* exhibit relatively mild phenotypes such as anisotropic cell swelling (Fagard et al., 2000).

Live-cell imaging of a yellow fluorescent protein (YFP) fusion to *CESA6* in *Arabidopsis* has greatly advanced understanding of how cellulose is synthesized (Paredez et al., 2006). Such YFP-tagged *CESA6* shows that CESA rosettes move with an average velocity of  $300 \text{ nm min}^{-1}$  *in vivo* (Paredez et al., 2006). To further observe the spatial relationship between microtubules and membrane-localized cellulose synthase complexes, the YFP tagged *CESA6* line was crossed with a CFP-tagged tubulin (*TUA1*) marker line. Co-localization of YFP:*CESA* and CFP:*TUA1* showed that CESA localization and guidance are spatially and temporally coupled to microtubules (Paredez et al., 2006). In the absence of cortical microtubules by treatment with MT-destabilizing drug Oryzalin, the same velocities of CESA complexes were maintained as in untreated samples (Paredez et al., 2006). This observation demonstrated that MTs might not be required for cellulose synthase motility and the motive force for CSC motility is likely provided

by cellulose polymerization (Paredes et al., 2006). Interestingly, in the disorganized MT resulting from treatment with Morlin, the velocities of CESA complexes were significantly reduced (DeBolt et al., 2007). Therefore, Morlin affects an unknown agent that is possibly involved in mediating interactions between the CESA complex and MTs, or a signaling mediator that coordinates the CSC and MT activities (Hematy et al., 2007).

Apart from the CESA proteins, other proteins in the CSC also participate in cellulose biosynthesis. These include the KORRIGAN (KOR1) glucanase, the KOBITO1 (KOB1) protein, the COBRA (COB) glycosylphosphatidylinositol-anchored protein, and the Tracheary Element Differentiation-Related (TED)-6 protein. Several mutations in the *KOR1* gene lead to a marked reduction in cellulose content, lateral organ swelling, and altered pectin composition, which may arise as a compensation for the loss of cellulose (Nicol et al., 1998; Zuo et al., 2000; Sato et al., 2001). There are three hypotheses about KOR1: first, KOR1 functions in removing the growing cellulose chain from some type of primer or initiator (Peng et al., 2002); second, KOR1 alters the crystallization properties within microfibrils (Szyjanowicz et al., 2004; Takahashi et al., 2009); or third, KOR1 participates in the release of completed cellulose microfibrils from the CSC (Szyjanowicz et al., 2004). The KOB1 protein appears to be involved directly in cellulose biosynthesis. *kob1* deletion mutants show a dwarf phenotype with swollen roots, and random deposition of cellulose microfibrils (Pagant et al., 2002). COB is anchored to the extracellular face of the plasma membrane and contains a motif with some similarities to a cellulose-binding domain (Roudier et al., 2002). *cob* mutants exhibit defects in anisotropic expansion due to altered cellulose microfibril orientations (Roudier et al., 2002; Roudier et al., 2005). TED6 interacts with the CESA7 subunit of the secondary wall CSC *in vivo* (Endo et al., 2009). Suppression of *TED6* results in defects of secondary cell-wall formation in vessels (Endo et

al.2009). However, the specific functions of these proteins involved in cellulose synthesis are still unclear.

### Xyloglucan structure and function

Of the hemicelluloses in dicot and non-grass monocot primary cell walls, xyloglucan is the most abundant hemicellulosic polysaccharide, representing approximately 20% of leaf cell walls in dicots (Zabackis et al., 1995). Xyloglucan consists of a  $\beta$ -1,4-linked glucan backbone that is highly branched, with substitutions of  $\alpha$ -1,6-linked xylosyl residue or side chains composed of xylosyl, galactosyl and fucosyl residues (Figure 1.1). Some acetylated xyloglucans have also been found in plant cell walls (Jia et al., 2005). A new discovery reports that *Arabidopsis* root hair walls contain a previously unidentified xyloglucan that is composed of both neutral and galacturonic acid-containing side chains (Peña et al., 2012). Xyloglucan was believed to work as a tether between cellulose microfibrils. Therefore, xyloglucan was hypothesized to contribute to the rigidity of cell walls when it associates with and non-covalently links adjacent microfibrils, and to the loosening of the cell wall when it degrades (Hayashi et al., 1988) (Figure 1.2A). Xyloglucan has been proposed to regulate cell expansion, to control cell growth, and to prevent self-association of cellulose microfibrils (Liepman et al., 2010).

However, recent studies argue against a major mechanical role for xyloglucan tethers spanning the space between adjacent microfibrils, since *xxt1 xxt2* double mutant and *xxt1 xxt2 xxt5* triple mutant plants, which lack detectable xyloglucan in their cell walls, can survive with minor defects in root hairs (Cavalier et al., 2008; Park and Cosgrove, 2012; Zabolina et al., 2012). The study of the structure and interactions of plant cell wall polysaccharides by two- and three-dimensional magic-angle-spinning Solid-State NMR revealed that load bearing in plant cell

walls is accomplished by a single network of all three types of polysaccharides instead of a cellulose-xyloglucan network (Dick-Perez et al., 2011). Upon treating cucumber hypocotyl walls with a set of homologous endoglucanases with varying substrate specificities: xyloglucan-specific endoglucanase (XEG from *Aspergillus aculeatus*) and cellulose-specific endoglucanase (CEG from *Aspergillus niger*) failed to induce cell wall creep, either by themselves or in combination, whereas an endoglucanase that hydrolyzes both xyloglucan and cellulose (Cel12A from *Hypocrea jecorina*) induced high cell wall creep (Park and Cosgrove, 2012). Measurements of elastic and plastic compliance revealed that both XEG and Cel12A hydrolyzed xyloglucan in intact walls, and Cel12A could hydrolyze a minor xyloglucan compartment recalcitrant to XEG digestion (Park and Cosgrove, 2012). Therefore, these results point to a revised model for primary cell wall networks (Figure 1.2B) in which only a minor xyloglucan component is located in the limited regions of tight contact between cellulose fibers to form load-bearing connections (Park and Cosgrove, 2012).

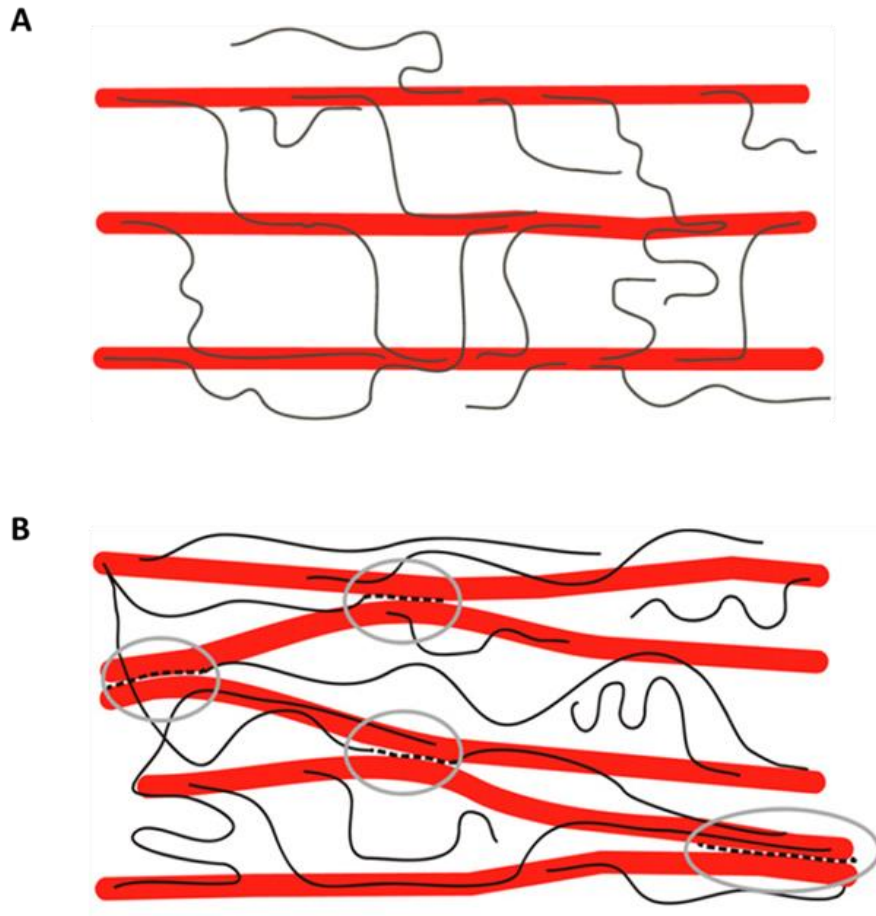


**Figure 1.2.** Cartoon of network models of the primary cell wall. **(A)** The tethered network model: xyloglucans (thin strands) bind to the surface of cellulose microfibrils (thick rods), forming a load-bearing network. **(B)** Revised model: load-bearing xyloglucans are represented as broken lines between cellulose microfibrils (thick rods) and are highlighted by the gray circles. These xyloglucans may work as a molecular binder to connect two adjacent cellulose microfibrils. The other non-load-bearing xyloglucans are shown as thin strands. Adapted from Figure 1 and Figure 10 (Park and Cosgrove, 2012).

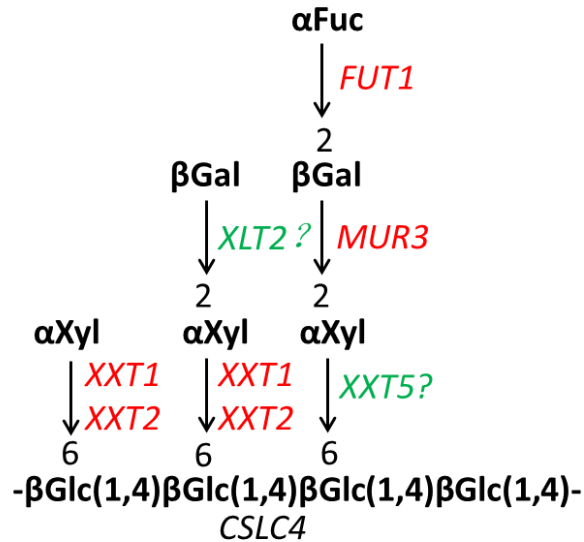


**Figure 1.3.** The genes encoding polysaccharide synthases involved in xyloglucan biosynthesis in Arabidopsis. The catalytic activities of XXT5 and XLT2 have not been confirmed. Redrawn from Figure 1 (Zabotina, 2012).

### Biosynthesis of xyloglucan

Biosynthesis of xyloglucan requires at least four types of enzymatic activities to synthesize this highly branched polysaccharide in the Golgi (Figure 1.3). (1) UDP-glucose-dependent  $\beta$ -1,4-glucan synthase, CELLULOSE SYNTHASE-LIKE C4 (CSL4), a member of the CAZy glycosyltransferase (GT) family GT2, is believed to be involved in xyloglucan backbone biosynthesis in Arabidopsis (Cantarel et al., 2009). (2) UDP-xylose-dependent  $\alpha$ -1,6-xylosyltransferases attaches xylosyl residues to selected glucosyl residues of the glucan backbone: AtXXT1 and its homolog AtXXT2, members of GT34, have been demonstrated to participate in xyloglucan biosynthesis since *txt1 txt2* double mutant plants lack detectable xyloglucan (Cavalier et al., 2008). XXT1 and XXT2 have also been demonstrated to xylosylate cellohexaose *in vitro* (Cavalier and Keegstra, 2006). Within the GT34 family, XXT5 is also

involved in xyloglucan biosynthesis, but its activity has not been demonstrated *in vitro* (Zabotina et al., 2008). (3) UDP-galactose-dependent  $\beta$ -1,2-galactosyltransferase attaches galactosyl residues to selected xylosyl residues: a screen for mutants with significant reduction in the fucose content of cell walls identified *AtMUR3*, which encodes a GT47 galactosyltransferase (Reiter et al., 1997). Recently, a second xyloglucan galactosyltransferase named Xyloglucan L-side Chain Galactosyltransferase (XLT2) was found to be required for galactosylation of the second xylose in the xyloglucan subunit, although the catalytic activity of XLT2 has not been confirmed (Jensen et al., 2012). (4) GDP-fucose-dependent  $\alpha$ -1,2-fucosyltransferase attaches fucosyl residues to selected galactosyl residues: the *AtFUT1* gene from the GT37 family encodes a xyloglucan  $\alpha$ -1,2-fucosyltransferase that terminally fucosylates xyloglucan (Perrin et al., 1999). *Arabidopsis fut1* T-DNA knock-out mutants exhibit complete elimination of fucosylated xyloglucan subunits (Perrin et al., 1999).

### Xylan structure and function

Xylan consists of a linear backbone of  $\beta$ -1,4-linked xylose residues substituted with acetyl, glucuronic acid (GlcA), 4-*O*-methylglucuronic acid (Me-GlcA), and arabinose residues (Figure 1.1). Depending on the plant species and even tissues in the same species, there is variation in xylan structures (Rennie and Scheller, 2014). In dicots, xylan is the second most abundant polysaccharide after cellulose in plant secondary cell walls, and it is also found at much lower level in primary walls. Dicot xylans contain the tetrasaccharide reducing-end sequence, known as  $\beta$ -D-Xyl-(1,3)- $\alpha$ -L-Rhap-(1,2)- $\alpha$ -D-GalA-(1,4)-D-Xyl, which has been proposed to serve either as an initiator or terminator of xylan backbone biosynthesis (York and O'Neill, 2008). In *Arabidopsis*, the ratio of Me-GlcA to GlcA is 2:1 and Me-GlcA substitution occurs on one out of eight xylose residues on average (Bromley et al., 2013). No or very few arabinosyl

substitutions have been reported in Arabidopsis and Poplar; hence these xylans are referred to as Glucuronoxylans (GX) (Rennie and Scheller, 2014). In contrast, grass xylans are typically substituted with arabinosyl residues, and are referred to as Glucuronoarabinoxylans (GAX).

Xylans have been proposed to coat cellulose microfibrils and crosslink with other polysaccharides via hydrogen bonds. Xylans are believed to link to lignin via ester bonds to GlcA and/or ether bonds to Xyl or Ara (Imamura et al., 1994; Balakshin et al., 2011). A recent study discovered that within Arabidopsis, a large proteoglycan complex, Arabinoxylan Pectin Arabinogalactan Protein 1 (APAP1) has short stretches of arabinoxylan/xylan that appear to be covalently linked to both pectin and arabinogalactans (Tan et al., 2013).

Xylan provides shape, structural strength and protection for plant cells, and is required for normal plant growth and development. Xylan makes up a large fraction of plant biomass. However, xylan is composed almost entirely of pentose sugars, which cannot be efficiently fermented. Therefore, plants that have reduced amounts of xylan, but still maintain normal growth and development, are desired for converting biomass to biofuel (Petersen et al., 2012).

### Biosynthesis of xylan

GX biosynthesis involves at least three types of glycosyltransferase activities: (1) formation of the  $\beta$ -1,4-linked xylose backbone; (2) formation of the sequence  $\beta$ -D-Xyl-(1,3)- $\alpha$ -L-Rhap-(1,2)- $\alpha$ -D-GalA-(1,4)-D-Xyl at the reducing end (at least in those plants that make this sequence); (3) addition and modification of GlcA and Me-GlcA side chains.

Two members of GT43, *Irregular Xylem (IRX) 9* and *IRX14*, and one member of GT47, *IRX10*, which encode putative xylosyltransferases, are required to synthesize the xylan backbone (Brown et al., 2005; Brown et al., 2007; Lee et al., 2007). Mutations in *IRX9* and *IRX14* result in

decreases in xylan contents and length of the xylan chains. *IRX9* and *IRX14* are not functionally redundant in backbone synthesis and are suggested to work cooperatively, since *IRX9* did not rescue the *irx14* phenotype (Lee et al., 2010). However, the catalytic activities of *IRX9* and *IRX14* have not been demonstrated *in vitro*. Mutations in *IRX10/GUT2* and its homolog *IRX10-L/GUT1* lead to a reduction in xylan content and the proteins encoded by these genes are thought to function redundantly in synthesizing the xylan backbone, as the reduction in xylan content is much greater in *irx10 irx10-L* double mutants (Brown et al., 2009; Wu et al., 2009). *IRX10-L* has recently been demonstrated to have UDP-Xyl:β-(1,4)-xylosyl transferase activity and has been renamed XYLAN SYNTHASE-1 (XYS1) (Urbanowicz et al., 2014). Interestingly, the authors also showed that *TBL29/ESK1* catalyzes the subsequent addition of O-acetyl groups from acetyl-CoA to the 2-position of xylosyl backbone residues (Urbanowicz et al., 2014). A recent study found that an *IRX10* homolog from the moss, *Physcomitrella patens*, and an *IRX10* homolog from the dicot plant, *Plantago ovate*, are conserved in having xylan β-1,4-xylosyltransferase activities (Jensen et al., 2014).

The *Arabidopsis* genes *IRX7/FRA8* (GT47), a homolog of *IRX7/FRA8* termed *F8H*, *GAUT12/IRX8* (GT8), and *GATL1/PARVUS* (GT8) have been implicated in the synthesis of the xylan reducing end sequencing (Zhong et al., 2005; Brown et al., 2007; Peña et al., 2007; Persson et al., 2007; Kong et al., 2009; Lee et al., 2009). Mutations in these genes cause reduced amounts of the reducing-end tetrasaccharide, more heterogeneous distribution of xylan chain length, and yet microsomal extracts exhibit no change in xylan synthase activity. There are two proposed functions of this reducing end tetrasaccharide in xylan biosynthesis, either acting as a GX chain terminator or acting as a GX primer, assuming that GX chain elongation occurs by sequential addition of xylosyl residues to this sequence (York and O'Neill, 2008).

The GlcA side chains are added by Glucuronic Acid Substitution of Xylan (GUX) 1 and GUX2, two members of GT8 that catalyze the transfer of  $\alpha$ -GlcA onto the *O*-2 position of xylose in xylan (Mortimer et al., 2010). The *gux1 gux2* double mutant has almost no detectable GlcA substitution on xylan, yet shows a visibly normal phenotype (Mortimer et al., 2010). A recent detailed study further points out that GUX1 is responsible for adding GlcA to evenly spaced xylose residues, while GUX2 is responsible for adding GlcA to both evenly and oddly spaced xylose residues of the xylan backbone (Bromley et al., 2013). 4-*O*-Methyl groups are transferred from S-adenosylmethionine (SAM) to GlcA by Glucuronoxylan Methyltransferase 1 (GXMT1), a protein containing a Domain of Unknown Function 579 (DUF579) (Urbanowicz et al., 2012). The *gxmt1* mutants have a 75% reduction in Me-GlcA residues in their secondary cell wall xylan (Urbanowicz et al., 2012).

### **Using Carbohydrate Binding Modules (CBMs) as tools for analysis of cell wall polysaccharides**

To degrade the highly complex and dynamic cell wall structure, microorganisms produce an extensive repertoire of polysaccharide-degrading enzymes, including glycoside hydrolases, polysaccharide lyases, carbohydrate esterases and polysaccharide oxidases (Gilbert, 2010). These enzymes often contain protein domains called Carbohydrate-Binding Modules (CBMs). CBMs display no hydrolytic function and it has been suggested that CBMs enhance the efficiency of hydrolytic enzymes by mediating prolonged and intimate contact between their catalytic modules and their target substrates (Boraston et al., 2004; Herve et al., 2010). Based on sequence comparisons, CBMs have been grouped into 69 families (<http://www.cazy.org/Carbohydrate-Binding-Modules.html>). Recently, CBMs have been used as

probes to assess and document the cell biological contexts of polysaccharides and cell wall diversity *in vitro* (Knox, 2008). CBMs that have been used to study polysaccharides include those that bind to cellulose, xylan, mannan, xyloglucan and pectin according to their binding specificities, as listed in Table 1.1. CBM binding specificity for pectin was underrepresented until recently, when a new family of CBMs, CBM61, was identified (Cid et al., 2010).

The capacity of these CBMs to recognize polysaccharides in cell walls was usually assessed using an indirect triple labeling immunofluorescence procedure (His-tagged CBM, anti-His mouse-Ig, anti-mouse Ig fluorescein isothiocyanate) on sections of plant tissues (Blake et al., 2006; McCartney et al., 2006). Within the same polysaccharide-directed CBM group, diverse origins of CBMs displayed differential binding capacities to cell walls depending on cell type, tissue, and taxon of origin (Blake et al., 2006; McCartney et al., 2006). For instance, the xylan-directed CBM2b-1-2 targets all of the secondary cell walls of specific cell types such as xylem vessels and sclerechyma fibers associated with phloem in sections of a range of dicotyledonous plant materials (tobacco, pea and flax) (McCartney et al., 2006). However, xylan-directed CBM35 did not bind to all secondary cell walls of xylem vessels, exhibiting a preference for an unmethylated form of xylan (GlcA not Me-GlcA) in tobacco sections (McCartney et al., 2006). CBM35 bound specifically to the secondary cell walls of pea sections, but to both primary and secondary cell walls of flax (McCartney et al., 2006). This diversity reveals that a variety of polysaccharide microstructures exists in plants, and points out a biological rationale for the large number of CBMs: different CBMs have the capacity to target appended catalytic modules to specific cell wall structures in diverse species (McCartney et al., 2006).

Compared to another set of cell wall probes, antibodies, CBMs have the advantages that gene sequences and protein structures are often known (Knox, 2008). This information

generates great opportunities for the engineering of CBM specificities and the generation of fluorescent protein-tagged CBMs. To date, the only existing xyloglucan CBMs were created by protein engineering of the xylan-binding CBM4-2, by modification of the CBM protein through random mutagenesis of the corresponding gene in combination with phage display technology (Gunnarsson et al., 2006; von Schantz et al., 2009). By fusing the xylan-binding CBM2b-1-2 and/or cellulose-directed CBM3a to the xylanases Xyl11A/Xyl10B (either by appending single CBM or tandem CBMs), degradation of xylan polysaccharides in secondary cell walls was potentiated (Herve et al., 2010). A recent study also found that cellulose-binding CBM3a and mannan-binding CBM27 have a great impact on the removal of mannan from tobacco and *Physcomitrella* cell walls, respectively, by fusion to GH5 and GH26 mannanases and CE2 esterases (Zhang et al., 2014). Although the functions of CBMs in cell wall degrading processes are still not fully understood, these studies proposed a mechanism that polysaccharide degrading enzymes are bound to the cell wall through their appended CBM(s), and that the CBM(s) greatly increase the concentration of the enzymes in the vicinity of the substrate by targeting polysaccharides that are in close proximity to the substrate of the catalytic module, leading to the observed increase in polysaccharide hydrolysis (Herve et al., 2010).

**Table1.1. List of CBMs**

<b>Group</b>	<b>Protein</b>	<b>Source enzymes</b>	<b>Organism</b>	<b>Type</b>	<b>Reference</b>
A. Cellulose-Binding group	CBM1	Cellulase	<i>Trichoderma reesei</i>	crystalline cellulose	(Reinikainen et al., 1992)
	CBM2a	Xylanase 10A	<i>Cybister japonicus</i>	crystalline cellulose	(Bolam et al., 1998)

	CBM3a	Scaffoldin	<i>Clostridium thermocellum</i>	crystalline cellulose	(Tormo et al., 1996)
	CBM10	Xylanase 10A	<i>Cybister japonicas</i>	crystalline cellulose	(Gill et al., 1999)
	CBM4-1	Cellulase 9B	<i>Cellulomonas fimi</i>	amorphous cellulose	(Tomm e et al., 1996)
	CBM17	Cellulase 5A	<i>Clostridium cellulovorans</i>	amorphous cellulose	(Borast on et al., 2000)
	CBM28	Cellulase 5A	<i>Bacillus sp.1139</i>	amorphous cellulose	(Borast on et al., 2002)
	CBM9-2	Xylanase 10A	<i>Thermotoga maritima</i>	the ends of cellulose chain	(Borast on et al., 2001)
B. Xylan-Binding group	CBM2b-1-2	Xylanase 11A	<i>Cellulomonas fimi</i>	both decorated and unsubstituted xylan	(Bolam et al., 2001)
	CBM4-2	Xylanase 10A	<i>Rhodothermus marinus</i>	both decorated and unsubstituted xylan	(Abou Hache m et al., 2000)
	CBM6	Xylanase 11A	<i>Clostridium thermocellum</i>	both decorated and unsubstituted xylan	(Czjzek et al., 2001)
	CBM15	Xylanase 10C	<i>Cybister japonicus</i>	both decorated and unsubstituted xylan	(Szabo et al., 2001)
	CBM22-2	Xylanase 10B	<i>Clostridium thermocellum</i>	both decorated and unsubstituted xylan	(Charno ck et al., 2000)

	CBM35	Arabinofuranosidase 62A	<i>Cybister japonicus</i>	unsubstituted xylan	(Bolam et al., 2004)
C. Mannan-binding group	CBM27 <sub>T</sub> mMan5	Mannanase 5C	<i>Thermotoga maritima</i>	mannan	(Filonova et al., 2007)
	CBM35 <sub>Cj</sub> man5C	Mannanase 5C	<i>Cybister japonicus</i>	mannan	(Filonova et al., 2007)
D. Xyloglucan-Binding group	CBMXG 34	Modified Xylanase 10A	<i>Rhodothermus marinus</i>	non-fucosylated xyloglucan	(Gunnarsson et al., 2006)
	CBMXG 34/1-X	Modified Xylanase 10A	<i>Rhodothermus marinus</i>	non-fucosylated xyloglucan	(von Schantz et al., 2009)
	CBMXG 34/2-VI	Modified Xylanase 10A	<i>Rhodothermus marinus</i>	non-fucosylated xyloglucan	(von Schantz et al., 2009)
	CBMXG 35	Modified Xylanase 10A	<i>Rhodothermus marinus</i>	non-fucosylated xyloglucan	(Gunnarsson et al., 2006)
E. Pectin-Binding group	TmCBM 61	GH53 endo- $\beta$ -1,4-galactanase	<i>Thermotoga maritima</i>	$\beta$ -1,4-galactan	(Cid et al., 2010)

### Summary of the studies described in this thesis

We plan to develop fluorescent protein tagged CBMs and express those constructs in plants. Our hypothesis is that fluorescent protein tagged CBMs will bind to their specific binding targets and thereby “tag” specific wall components and permit them to be tracked in

living plants. There are two potential outcomes: **A)** The binding of the fluorescent tagged CBM to the polysaccharide *in vivo* is benign, that is, has no effect on polysaccharide function and therefore the incorporation of the tag will allow us track the dynamics of plant cell wall polysaccharides during plant growth and development; or **B)** The binding of the fluorescent tagged CBMs to the polysaccharide *in vivo* is NOT benign, that is, has an effect on the bound polysaccharide and leads to changes in the function or structure of the wall, which in turn, may have an impact on the development of the plant. Before setting up the specific objectives, we verified the binding specificities of fluorescent protein tagged CBMs *in vitro* and examined the morphological and developmental effects of the expression of these CBMs in Arabidopsis. Our preliminary data suggest that BOTH outcomes **A AND B** mentioned above occur, depending on the CBM and the polysaccharide that the CBM binds to. Even within the same group, expression of different CBMs can lead to different results. It appears that the xylan-binding CBM group is more suitable to be utilized as an *in vivo* tagging tool for xylans, since expression of either CBM2b-1-2 (see Chapter 3) or CBM35 (data not shown) has no deleterious effect on plant morphology and development. On the other hand, cellulose binding CBMs appear to have deleterious effects when expressed in plants, making them tools for selectively modulating cell wall function(s) (see Chapter 4).

## References

- Abou Hachem M, Nordberg Karlsson E, Bartonek-Roxa E, Raghothama S, Simpson PJ, Gilbert HJ, Williamson MP, Holst O** (2000) Carbohydrate-binding modules from a thermostable *Rhodothermus marinus* xylanase: cloning, expression and binding studies. *Biochem J* **345 Pt 1**: 53-60
- Albersheim P, Darvill A, Roberts K, Sederoff R, Staehelin A** (2010) *Plant Cell Walls*. Garland Science, New York
- Atanassov, II, Pittman JK, Turner SR** (2009) Elucidating the mechanisms of assembly and subunit interaction of the cellulose synthase complex of *Arabidopsis* secondary cell walls. *J Biol Chem* **284**: 3833-3841
- Balakshin M, Capanema E, Gracz H, Chang HM, Jameel H** (2011) Quantification of lignin-carbohydrate linkages with high-resolution NMR spectroscopy. *Planta* **233**: 1097-1110
- Beeckman T, Przemeck GK, Stamatiou G, Lau R, Terryn N, De Rycke R, Inze D, Berleth T** (2002) Genetic complexity of cellulose synthase a gene function in *Arabidopsis* embryogenesis. *Plant Physiol* **130**: 1883-1893
- Blake AW, McCartney L, Flint JE, Bolam DN, Boraston AB, Gilbert HJ, Knox JP** (2006) Understanding the biological rationale for the diversity of cellulose-directed carbohydrate-binding modules in prokaryotic enzymes. *J Biol Chem* **281**: 29321-29329
- Bolam DN, Ciruela A, McQueen-Mason S, Simpson P, Williamson MP, Rixon JE, Boraston A, Hazlewood GP, Gilbert HJ** (1998) *Pseudomonas* cellulose-binding domains mediate their effects by increasing enzyme substrate proximity. *Biochem J* **331 ( Pt 3)**: 775-781

- Bolam DN, Xie H, Pell G, Hogg D, Galbraith G, Henrissat B, Gilbert HJ** (2004) X4 modules represent a new family of carbohydrate-binding modules that display novel properties. *J Biol Chem* **279**: 22953-22963
- Bolam DN, Xie H, White P, Simpson PJ, Hancock SM, Williamson MP, Gilbert HJ** (2001) Evidence for synergy between family 2b carbohydrate binding modules in *Cellulomonas fimi* xylanase 11A. *Biochemistry* **40**: 2468-2477
- Boraston AB, Bolam DN, Gilbert HJ, Davies GJ** (2004) Carbohydrate-binding modules: fine-tuning polysaccharide recognition. *Biochem J* **382**: 769-781
- Boraston AB, Chiu P, Warren RA, Kilburn DG** (2000) Specificity and affinity of substrate binding by a family 17 carbohydrate-binding module from *Clostridium cellulovorans* cellulase 5A. *Biochemistry* **39**: 11129-11136
- Boraston AB, Creagh AL, Alam MM, Kormos JM, Tomme P, Haynes CA, Warren RA, Kilburn DG** (2001) Binding specificity and thermodynamics of a family 9 carbohydrate-binding module from *Thermotoga maritima* xylanase 10A. *Biochemistry* **40**: 6240-6247
- Boraston AB, Ghaffari M, Warren RA, Kilburn DG** (2002) Identification and glucan-binding properties of a new carbohydrate-binding module family. *Biochem J* **361**: 35-40
- Bromley JR, Busse-Wicher M, Tryfona T, Mortimer JC, Zhang Z, Brown DM, Dupree P** (2013) GUX1 and GUX2 glucuronyltransferases decorate distinct domains of glucuronoxylan with different substitution patterns. *Plant J* **74**: 423-434
- Brown DM, Goubet F, Wong VW, Goodacre R, Stephens E, Dupree P, Turner SR** (2007) Comparison of five xylan synthesis mutants reveals new insight into the mechanisms of xylan synthesis. *Plant J* **52**: 1154-1168

- Brown DM, Zeef LA, Ellis J, Goodacre R, Turner SR** (2005) Identification of novel genes in Arabidopsis involved in secondary cell wall formation using expression profiling and reverse genetics. *Plant Cell* **17**: 2281-2295
- Brown DM, Zhang Z, Stephens E, Dupree P, Turner SR** (2009) Characterization of IRX10 and IRX10-like reveals an essential role in glucuronoxylan biosynthesis in Arabidopsis. *Plant J* **57**: 732-746
- Brown RM** (2004) Cellulose structure and biosynthesis: What is in store for the 21st century? *Journal of Polymer Science Part A: Polymer Chemistry* **42**: 487-495
- Carpita NC, Gibeaut DM** (1993) Structural models of primary cell walls in flowering plants: consistency of molecular structure with the physical properties of the walls during growth. *Plant J* **3**: 1-30
- Cavalier DM, Keegstra K** (2006) Two xyloglucan xylosyltransferases catalyze the addition of multiple xylosyl residues to cellohexaose. *J Biol Chem* **281**: 34197-34207
- Cavalier DM, Lerouxel O, Neumetzler L, Yamauchi K, Reinecke A, Freshour G, Zabolina OA, Hahn MG, Burgert I, Pauly M, Raikhel NV, Keegstra K** (2008) Disrupting two Arabidopsis thaliana xylosyltransferase genes results in plants deficient in xyloglucan, a major primary cell wall component. *Plant Cell* **20**: 1519-1537
- Charnock SJ, Bolam DN, Turkenburg JP, Gilbert HJ, Ferreira LM, Davies GJ, Fontes CM** (2000) The X6 "thermostabilizing" domains of xylanases are carbohydrate-binding modules: structure and biochemistry of the Clostridium thermocellum X6b domain. *Biochemistry* **39**: 5013-5021

- Cid M, Pedersen HL, Kaneko S, Coutinho PM, Henrissat B, Willats WG, Boraston AB** (2010) Recognition of the helical structure of beta-1,4-galactan by a new family of carbohydrate-binding modules. *J Biol Chem* **285**: 35999-36009
- Czjzek M, Bolam DN, Mosbah A, Allouch J, Fontes CM, Ferreira LM, Bornet O, Zamboni V, Darbon H, Smith NL, Black GW, Henrissat B, Gilbert HJ** (2001) The location of the ligand-binding site of carbohydrate-binding modules that have evolved from a common sequence is not conserved. *J Biol Chem* **276**: 48580-48587
- DeBolt S, Gutierrez R, Ehrhardt DW, Melo CV, Ross L, Cutler SR, Somerville C, Bonetta D** (2007) Morlin, an inhibitor of cortical microtubule dynamics and cellulose synthase movement. *Proc Natl Acad Sci U S A* **104**: 5854-5859
- Desprez T, Juraniec M, Crowell EF, Jouy H, Pochylova Z, Parcy F, Hofte H, Gonneau M, Vernhettes S** (2007) Organization of cellulose synthase complexes involved in primary cell wall synthesis in *Arabidopsis thaliana*. *Proc Natl Acad Sci U S A* **104**: 15572-15577
- Dick-Perez M, Zhang Y, Hayes J, Salazar A, Zobotina OA, Hong M** (2011) Structure and interactions of plant cell-wall polysaccharides by two- and three-dimensional magic-angle-spinning solid-state NMR. *Biochemistry* **50**: 989-1000
- Doblin MS, Pettolino F, Bacic A** (2010) Plant cell walls: the skeleton of the plant world. *Functional Plant Biology* **37**: 357-381
- Endo S, Pesquet E, Yamaguchi M, Tashiro G, Sato M, Toyooka K, Nishikubo N, Udagawa-Motose M, Kubo M, Fukuda H, Demura T** (2009) Identifying new components participating in the secondary cell wall formation of vessel elements in zinnia and *Arabidopsis*. *Plant Cell* **21**: 1155-1165

- Fagard M, Desnos T, Desprez T, Goubet F, Refregier G, Mouille G, McCann M, Rayon C, Vernhettes S, Hofte H** (2000) PROCUSTE1 encodes a cellulose synthase required for normal cell elongation specifically in roots and dark-grown hypocotyls of Arabidopsis. *Plant Cell* **12**: 2409-2424
- Filonova L, Kallas AM, Greffe L, Johansson G, Teeri TT, Daniel G** (2007) Analysis of the surfaces of wood tissues and pulp fibers using carbohydrate-binding modules specific for crystalline cellulose and mannan. *Biomacromolecules* **8**: 91-97
- Gilbert HJ** (2010) The biochemistry and structural biology of plant cell wall deconstruction. *Plant Physiol* **153**: 444-455
- Gill J, Rixon JE, Bolam DN, McQueen-Mason S, Simpson PJ, Williamson MP, Hazlewood GP, Gilbert HJ** (1999) The type II and X cellulose-binding domains of Pseudomonas xylanase A potentiate catalytic activity against complex substrates by a common mechanism. *Biochem J* **342** ( Pt 2): 473-480
- Gillmor CS, Poindexter P, Lorieau J, Palcic MM, Somerville C** (2002) Alpha-glucosidase I is required for cellulose biosynthesis and morphogenesis in Arabidopsis. *J Cell Biol* **156**: 1003-1013
- Gunnarsson LC, Zhou Q, Montanier C, Karlsson EN, Brumer H, 3rd, Ohlin M** (2006) Engineered xyloglucan specificity in a carbohydrate-binding module. *Glycobiology* **16**: 1171-1180
- Hayashi T, Koyama T, Matsuda K** (1988) Formation of UDP-Xylose and Xyloglucan in Soybean Golgi Membranes. *Plant Physiol* **87**: 341-345

- Hematy K, Sado PE, Van Tuinen A, Rochange S, Desnos T, Balzergue S, Pelletier S, Renou JP, Hofte H** (2007) A receptor-like kinase mediates the response of Arabidopsis cells to the inhibition of cellulose synthesis. *Curr Biol* **17**: 922-931
- Herve C, Rogowski A, Blake AW, Marcus SE, Gilbert HJ, Knox JP** (2010) Carbohydrate-binding modules promote the enzymatic deconstruction of intact plant cell walls by targeting and proximity effects. *Proc Natl Acad Sci U S A* **107**: 15293-15298
- Imamura T, Watanabe T, Kuwahara M, Koshijima T** (1994) Ester linkages between lignin and glucuronic acid in lignin-carbohydrate complexes from *Fagus crenata*. *Phytochemistry* **37**: 1165-1173
- Jensen JK, Johnson NR, Wilkerson CG** (2014) Arabidopsis thaliana IRX10 and two related proteins from psyllium and *Physcomitrella patens* are xylan xylosyltransferases. *The Plant Journal* **80**: 207-215
- Jensen JK, Schultink A, Keegstra K, Wilkerson CG, Pauly M** (2012) RNA-Seq analysis of developing nasturtium seeds (*Tropaeolum majus*): identification and characterization of an additional galactosyltransferase involved in xyloglucan biosynthesis. *Mol Plant* **5**: 984-992
- Jia Z, Cash M, Darvill AG, York WS** (2005) NMR characterization of endogenously O-acetylated oligosaccharides isolated from tomato (*Lycopersicon esculentum*) xyloglucan. *Carbohydr Res* **340**: 1818-1825
- Knox JP** (2008) Revealing the structural and functional diversity of plant cell walls. *Current Opinion in Plant Biology* **11**: 308-313

- Kong Y, Zhou G, Avci U, Gu X, Jones C, Yin Y, Xu Y, Hahn MG** (2009) Two poplar glycosyltransferase genes, PdGATL1.1 and PdGATL1.2, are functional orthologs to PARVUS/AtGATL1 in Arabidopsis. *Mol Plant* **2**: 1040-1050
- Lee C, O'Neill MA, Tsumuraya Y, Darvill AG, Ye ZH** (2007) The irregular xylem9 mutant is deficient in xylan xylosyltransferase activity. *Plant Cell Physiol* **48**: 1624-1634
- Lee C, Teng Q, Huang W, Zhong R, Ye ZH** (2009) The F8H glycosyltransferase is a functional paralog of FRA8 involved in glucuronoxylan biosynthesis in Arabidopsis. *Plant Cell Physiol* **50**: 812-827
- Lee C, Teng Q, Huang W, Zhong R, Ye ZH** (2010) The Arabidopsis family GT43 glycosyltransferases form two functionally nonredundant groups essential for the elongation of glucuronoxylan backbone. *Plant Physiol* **153**: 526-541
- Liepman AH, Wightman R, Geshi N, Turner SR, Scheller HV** (2010) Arabidopsis - a powerful model system for plant cell wall research. *Plant J* **61**: 1107-1121
- McCartney L, Blake AW, Flint J, Bolam DN, Boraston AB, Gilbert HJ, Knox JP** (2006) Differential recognition of plant cell walls by microbial xylan-specific carbohydrate-binding modules. *Proceedings of the National Academy of Sciences of the United States of America* **103**: 4765-4770
- Mortimer JC, Miles GP, Brown DM, Zhang Z, Segura MP, Weimar T, Yu X, Seffen KA, Stephens E, Turner SR, Dupree P** (2010) Absence of branches from xylan in Arabidopsis gux mutants reveals potential for simplification of lignocellulosic biomass. *Proceedings of the National Academy of Sciences* **107**: 17409-17414

- Nicol F, His I, Jauneau A, Vernhettes S, Canut H, Höfte H** (1998) A plasma membrane-bound putative endo-1,4- $\beta$ -d-glucanase is required for normal wall assembly and cell elongation in Arabidopsis, Vol 17
- Pagant S, Bichet A, Sugimoto K, Lerouxel O, Desprez T, McCann M, Lerouge P, Vernhettes S, Hofte H** (2002) KOBITO1 encodes a novel plasma membrane protein necessary for normal synthesis of cellulose during cell expansion in Arabidopsis. *Plant Cell* **14**: 2001-2013
- Paredez AR, Somerville CR, Ehrhardt DW** (2006) Visualization of Cellulose Synthase Demonstrates Functional Association with Microtubules. *Science* **312**: 1491-1495
- Park YB, Cosgrove DJ** (2012) A Revised Architecture of Primary Cell Walls Based on Biomechanical Changes Induced by Substrate-Specific Endoglucanases. *Plant Physiology* **158**: 1933-1943
- Peña MJ, Kong Y, York WS, O'Neill MA** (2012) A Galacturonic Acid-Containing Xyloglucan Is Involved in Arabidopsis Root Hair Tip Growth. *The Plant Cell Online* **24**: 4511-4524
- Peña MJ, Zhong R, Zhou G-K, Richardson EA, O'Neill MA, Darvill AG, York WS, Ye Z-H** (2007) Arabidopsis irregular xylem8 and irregular xylem9: Implications for the Complexity of Glucuronoxylan Biosynthesis. *The Plant Cell Online* **19**: 549-563
- Peng L, Kawagoe Y, Hogan P, Delmer D** (2002) Sitosterol-beta-glucoside as primer for cellulose synthesis in plants. *Science* **295**: 147-150
- Perrin RM, DeRocher AE, Bar-Peled M, Zeng W, Norambuena L, Orellana A, Raikhel NV, Keegstra K** (1999) Xyloglucan fucosyltransferase, an enzyme involved in plant cell wall biosynthesis. *Science* **284**: 1976-1979

- Persson S, Caffall KH, Freshour G, Hilley MT, Bauer S, Poindexter P, Hahn MG, Mohnen D, Somerville C** (2007) The Arabidopsis irregular xylem8 mutant is deficient in glucuronoxytan and homogalacturonan, which are essential for secondary cell wall integrity. *Plant Cell* **19**: 237-255
- Persson S, Paredez A, Carroll A, Palsdottir H, Doblin M, Poindexter P, Khitrov N, Auer M, Somerville CR** (2007) Genetic evidence for three unique components in primary cell-wall cellulose synthase complexes in Arabidopsis. *Proceedings of the National Academy of Sciences* **104**: 15566-15571
- Persson S, Wei H, Milne J, Page GP, Somerville CR** (2005) Identification of genes required for cellulose synthesis by regression analysis of public microarray data sets. *Proc Natl Acad Sci U S A* **102**: 8633-8638
- Petersen PD, Lau J, Ebert B, Yang F, Verhertbruggen Y, Kim JS, Varanasi P, Suttangkakul A, Auer M, Loque D, Scheller HV** (2012) Engineering of plants with improved properties as biofuels feedstocks by vessel-specific complementation of xylan biosynthesis mutants. *Biotechnol Biofuels* **5**: 84
- Reinikainen T, Ruohonen L, Nevanen T, Laaksonen L, Kraulis P, Jones TA, Knowles JK, Teeri TT** (1992) Investigation of the function of mutated cellulose-binding domains of *Trichoderma reesei* cellobiohydrolase I. *Proteins* **14**: 475-482
- Reiter WD, Chapple C, Somerville CR** (1997) Mutants of *Arabidopsis thaliana* with altered cell wall polysaccharide composition. *Plant J* **12**: 335-345
- Rennie EA, Scheller HV** (2014) Xylan biosynthesis. *Current Opinion in Biotechnology* **26**: 100-107

- Roudier F, Fernandez AG, Fujita M, Himmelspach R, Borner GH, Schindelman G, Song S, Baskin TI, Dupree P, Wasteneys GO, Benfey PN** (2005) COBRA, an Arabidopsis extracellular glycosyl-phosphatidyl inositol-anchored protein, specifically controls highly anisotropic expansion through its involvement in cellulose microfibril orientation. *Plant Cell* **17**: 1749-1763
- Roudier F, Schindelman G, DeSalle R, Benfey PN** (2002) The COBRA family of putative GPI-anchored proteins in Arabidopsis. A new fellowship in expansion. *Plant Physiol* **130**: 538-548
- Sato S, Kato T, Kakegawa K, Ishii T, Liu YG, Awano T, Takabe K, Nishiyama Y, Kuga S, Sato S, Nakamura Y, Tabata S, Shibata D** (2001) Role of the putative membrane-bound endo-1,4-beta-glucanase KORRIGAN in cell elongation and cellulose synthesis in Arabidopsis thaliana. *Plant Cell Physiol* **42**: 251-263
- Somerville C** (2006) Cellulose synthesis in higher plants. *Annu Rev Cell Dev Biol* **22**: 53-78
- Somerville C** (2007) Biofuels. *Curr Biol* **17**: R115-119
- Szabo L, Jamal S, Xie H, Charnock SJ, Bolam DN, Gilbert HJ, Davies GJ** (2001) Structure of a family 15 carbohydrate-binding module in complex with xylopentaose. Evidence that xylan binds in an approximate 3-fold helical conformation. *J Biol Chem* **276**: 49061-49065
- Szyjanowicz PM, McKinnon I, Taylor NG, Gardiner J, Jarvis MC, Turner SR** (2004) The irregular xylem 2 mutant is an allele of korrrigan that affects the secondary cell wall of Arabidopsis thaliana. *Plant J* **37**: 730-740
- Takahashi J, Rudsander UJ, Hedenstrom M, Banasiak A, Harholt J, Amelot N, Immerzeel P, Ryden P, Endo S, Ibatullin FM, Brumer H, del Campillo E, Master ER, Scheller**

- HV, Sundberg B, Teeri TT, Mellerowicz EJ** (2009) KORRIGAN1 and its aspen homolog PttCel9A1 decrease cellulose crystallinity in Arabidopsis stems. *Plant Cell Physiol* **50**: 1099-1115
- Tan L, Eberhard S, Pattathil S, Warder C, Glushka J, Yuan C, Hao Z, Zhu X, Avcı U, Miller JS, Baldwin D, Pham C, Orlando R, Darvill A, Hahn MG, Kieliszewski MJ, Mohnen D** (2013) An Arabidopsis Cell Wall Proteoglycan Consists of Pectin and Arabinoxylan Covalently Linked to an Arabinogalactan Protein. *The Plant Cell Online* **25**: 270-287
- Taylor NG, Laurie S, Turner SR** (2000) Multiple Cellulose Synthase Catalytic Subunits Are Required for Cellulose Synthesis in Arabidopsis. *The Plant Cell Online* **12**: 2529-2539
- Timmers J, Vernhettes S, Desprez T, Vincken JP, Visser RG, Trindade LM** (2009) Interactions between membrane-bound cellulose synthases involved in the synthesis of the secondary cell wall. *FEBS Lett* **583**: 978-982
- Tomme P, Creagh AL, Kilburn DG, Haynes CA** (1996) Interaction of polysaccharides with the N-terminal cellulose-binding domain of *Cellulomonas fimi* CenC. 1. Binding specificity and calorimetric analysis. *Biochemistry* **35**: 13885-13894
- Tormo J, Lamed R, Chirino AJ, Morag E, Bayer EA, Shoham Y, Steitz TA** (1996) Crystal structure of a bacterial family-III cellulose-binding domain: a general mechanism for attachment to cellulose. *Embo j* **15**: 5739-5751
- Turner SR, Somerville CR** (1997) Collapsed xylem phenotype of Arabidopsis identifies mutants deficient in cellulose deposition in the secondary cell wall. *Plant Cell* **9**: 689-701
- Urbanowicz BR, Peña MJ, Moniz HA, Moremen KW, York WS** (2014) Two Arabidopsis proteins synthesize acetylated xylan in vitro. *The Plant Journal* **80**: 197-206

- Urbanowicz BR, Pena MJ, Ratnaparkhe S, Avci U, Backe J, Steet HF, Foston M, Li H, O'Neill MA, Ragauskas AJ, Darvill AG, Wyman C, Gilbert HJ, York WS** (2012) 4-O-methylation of glucuronic acid in Arabidopsis glucuronoxylan is catalyzed by a domain of unknown function family 579 protein. *Proc Natl Acad Sci U S A* **109**: 14253-14258
- von Schantz L, Gullfot F, Scheer S, Filonova L, Cicortas Gunnarsson L, Flint JE, Daniel G, Nordberg-Karlsson E, Brumer H, Ohlin M** (2009) Affinity maturation generates greatly improved xyloglucan-specific carbohydrate binding modules. *BMC Biotechnol* **9**: 92
- Wu AM, Rihouey C, Seveno M, Hornblad E, Singh SK, Matsunaga T, Ishii T, Lerouge P, Marchant A** (2009) The Arabidopsis IRX10 and IRX10-LIKE glycosyltransferases are critical for glucuronoxylan biosynthesis during secondary cell wall formation. *Plant J* **57**: 718-731
- York WS, O'Neill MA** (2008) Biochemical control of xylan biosynthesis - which end is up? *Curr Opin Plant Biol* **11**: 258-265
- Zabackis E, Huang J, Muller B, Darvill AG, Albersheim P** (1995) Characterization of the cell-wall polysaccharides of Arabidopsis thaliana leaves. *Plant Physiol* **107**: 1129-1138
- Zabotina OA** (2012) Xyloglucan and its biosynthesis. *Front Plant Sci* **3**: 134
- Zabotina OA, Avci U, Cavalier D, Pattathil S, Chou YH, Eberhard S, Danhof L, Keegstra K, Hahn MG** (2012) Mutations in multiple XXT genes of Arabidopsis reveal the complexity of xyloglucan biosynthesis. *Plant Physiol* **159**: 1367-1384

- Zabotina OA, van de Ven WT, Freshour G, Drakakaki G, Cavalier D, Mouille G, Hahn MG, Keegstra K, Raikhel NV** (2008) Arabidopsis XXT5 gene encodes a putative alpha-1,6-xylosyltransferase that is involved in xyloglucan biosynthesis. *Plant J* **56**: 101-115
- Zhang X, Rogowski A, Zhao L, Hahn MG, Avci U, Knox JP, Gilbert HJ** (2014) Understanding How the Complex Molecular Architecture of Mannan-degrading Hydrolases Contributes to Plant Cell Wall Degradation. *Journal of Biological Chemistry* **289**: 2002-2012
- Zhong R, Pena MJ, Zhou GK, Nairn CJ, Wood-Jones A, Richardson EA, Morrison WH, 3rd, Darvill AG, York WS, Ye ZH** (2005) Arabidopsis fragile fiber8, which encodes a putative glucuronyltransferase, is essential for normal secondary wall synthesis. *Plant Cell* **17**: 3390-3408
- Zuo J, Niu QW, Nishizawa N, Wu Y, Kost B, Chua NH** (2000) KORRIGAN, an Arabidopsis endo-1,4-beta-glucanase, localizes to the cell plate by polarized targeting and is essential for cytokinesis. *Plant Cell* **12**: 1137-1152

## CHAPTER 2

### CHARACTERIZATION OF THE BINDING SPECIFICITIES OF FLUORESCENT PROTEIN TAGGED CBMS

#### **Abstract**

Carbohydrate-Binding Modules (CBMs) are a diverse set of non-catalytic protein domains that are present in diverse microbial glycoside hydrolases. CBMs are particularly attractive as cell wall probes because of their individual, intrinsic specificities toward polysaccharides, ease of heterologous expression, and convenience of modification with peptide and small molecule detection tags. We have developed fluorescent protein tagged CBMs and expressed those constructs in Arabidopsis. Before transferring the fluorescent protein tagged CBMs to Arabidopsis, the binding specificities of the fluorescent CBM fusion proteins were examined by ELISA against cell wall glycans and labeling of fixed Arabidopsis stem sections. The variations in CBM specificity depend on the target configuration of cell wall polymers, and points to the utility of these modules in further studies.

#### **Introduction**

Glycoside hydrolases deployed by microbes that degrade plant cell walls have multi-modular structures in which one or more catalytic modules are appended to non-catalytic carbohydrate-binding modules (CBMs). CBMs promote binding to polysaccharides and recently have been developed as probes for *in vitro* cell wall analysis. Compared to antibodies, CBMs have advantages in that the gene/protein sequences and protein structures are often known,

reducing the difficulties for the generation of probes (Bertani, 1951; McCann and Knox, 2010). These features of CBMs generate opportunities for engineering of fluorescent protein-tagged CBMs and further expression of these fusion proteins in *Arabidopsis* to allow the tagged CBMs to interact with their glycan ligands *in vivo*.

Three groups of CBMs were selected for our study, based on their binding specificities, listed in Table 2.1, that display specificity for cellulose, xylan or xyloglucan. The capacities of these CBMs to bind to plant cell walls had been assessed by using an indirect triple labeling immunofluorescence procedure (His-tagged CBM, anti-His mouse-Ig, anti-mouse Ig fluorescein isothiocyanate) in sections of tobacco stems and tamarind seeds (Blake et al., 2006; McCartney et al., 2006; von Schantz et al., 2009). CBM2a and CBM3a, which bind to cellulose, are effective binders to both primary and secondary cell walls (Blake et al., 2006). CBM2b-1-2, which binds to xylans, targets the secondary cell walls of specific cell types such as xylem vessels and interfascicular fibres (McCartney et al., 2006). CBM35 displays no binding to arabinoxylan or methylglucuronoxylan, exhibiting a preference for an unsubstituted form of xylan (McCartney et al., 2006). In tobacco, CBM35 does not bind to all secondary cell walls of xylem vessels (McCartney et al., 2006). Xyloglucan-binding CBMXG34/1-X and CBM34/2-VI were created by CBM engineering, which modified xylan-directed CBM proteins through random mutagenesis in combination with phage display technology (Gunnarsson et al., 2006; von Schantz et al., 2009). CBMXG34/1-X and CBMXG34/2-VI bind specifically to the endosperm of tamarind seed sections, which is rich in non-fucosylated xyloglucan (von Schantz et al., 2009). Before undertaking experiments to transfer the fluorescent protein-tagged CBMs to *Arabidopsis*, the binding specificities of the tagged fluorescent CBM fusion proteins were

analyzed by binding of fluorescent protein-tagged CBMs to a diverse panel of 55 plant polysaccharides.

**Table 2.1. List of CBMs in this project**

<b>Group</b>	<b>Protein</b>	<b>Source enzymes</b>	<b>Organism</b>	<b>Binding Ligand</b>	<b>Reference</b>
A. Cellulose-Binding group	CBM2a	Xylanase 10A	<i>C. japonicas</i>	Glucose resides of cellulose chains	(Blake et al., 2006)
	CBM3a	Scaffoldin	<i>C. thermocellum</i>	Glucose resides of cellulose chains	(Blake et al., 2006)
B. Xylan-Binding group	CBM2b-1-2	Xylanase 11A	<i>C. fimi</i>	Xylose residues in the xylan backbone	(McCartney et al., 2006)
	CBM35	Arabino-furanosidase 62A	<i>C. japonicas</i>	Undecorated xylose residues in the xylan backbone	(McCartney et al., 2006)
C. Non-fucosylated Xyloglucan-Binding group	CBMXG3 4/1-X	Modified Xylanase 10A	<i>R. marinus</i>	Xylose residues in xyloglucan	(von Schantz et al., 2009)
	CBMXG3 4/2-VI	Modified Xylanase 10A	<i>R. marinus</i>	Xylose residues in xyloglucan	(von Schantz et al., 2009)

## Materials and Methods

### Preparation of Fluorescent Protein-tagged CBMs

The fluorescent protein tagged CBM:mCherry probes were produced as His-tagged recombinant proteins using the T7 expression-system consisting of the pET22b vector (Novagen, Madison, WI) harbored in *Escherichia coli* BL21(DE3). The *CBM* genes were inserted into the

vector using PCR. Digestion of purified PCR products and pET22b with NotI and XhoI (Thermo Scientific Inc) enabled cloning of the genes between NdeI/XhoI sites in the vector resulting in constructs encoding recombinant proteins containing a hexahistidine tag. The bacteria were routinely cultured at 37 °C in Luria broth (Bertani, 1951; Sambrook et al., 1989), and expression of the recombinant proteins was induced with 100 µM isopropyl-β-D-thiogalactopyranoside at 16 °C overnight. The fluorescent protein/His tagged CBM:mCherry fusion proteins, which were produced in soluble form in the cytoplasm of *E. coli*, were purified by immobilized metal ion affinity chromatography (Sigma) using Talon™ Buffer (10 mM Tris/HCl pH 8.0 containing 300 mM NaCl) as the column matrix. The concentrations of purified CBM:mCherry fusion proteins were determined spectrophotometrically from absorbance measurements at 280nm.

### **Preparation of Polysaccharides**

Polysaccharides from various plant sources were obtained from commercial sources (Megazyme, Sigma, and Sunkist) and our lab stocks. Detailed information about these polysaccharides is given in Supplemental Table S2.1. Stock solutions were prepared by dissolving the polysaccharides at 1mg mL<sup>-1</sup> in deionized water and solutions were stored at -20 °C.

### **Enzyme-Linked Immunosorbent Assay (ELISA)**

Polysaccharides were applied (50 µl of 10 µg mL<sup>-1</sup> in deionized water per well) to 96-well plates and were dried to the well surfaces by evaporation overnight at 37 °C. Control wells were coated with deionized water. The plates were blocked with 200 µl of 1% (w/v) instant nonfat dry milk in Tris-buffered saline (50 mM Tris-HCl, pH 7.6, containing 100 mM sodium chloride) for 1 h. All subsequent aspiration and wash steps were performed using an ELx405 microplate

washer (Bio-Tek Instruments). Blocking agent was removed by aspiration. First, 50  $\mu$ l of fluorescent protein tagged CBM proteins (100  $\mu$ M) were added to each well and incubated for 1 h. Then wells were washed three times with 300  $\mu$ l of 0.1% (w/v) instant nonfat dry milk in Tris-buffered saline (wash buffer) and peroxidase-conjugated mouse anti-his antibodies (Sigma-Aldrich) were diluted 1:5000 in wash buffer and 50  $\mu$ l were added to each well and incubated for another 1 h. Finally, wells were washed five times with 300  $\mu$ l of wash buffer. Substrate solution (3,3',5,5'-Tetramethylbenzidine) (Vector Laboratories) was freshly prepared according to the manufacturer's instructions, and 50  $\mu$ l were added to each well. After 20 min, the reaction was stopped by adding 50  $\mu$ l of 0.5 N sulfuric acid to each well. The OD of each well was read as the difference in A450 and A655 using a model 680 microplate reader (Bio-Rad). The reading from each test well was subtracted from that of a control well on the same plate that contained the fluorescent protein tagged CBM and antibodies but no immobilized polysaccharide.

### **Cellulose Pull-Down Assay**

Avicel® microcrystalline cellulose (10 mg) that was purified from fibrous plants (Sigma-Aldrich, Ireland) was mixed with 50  $\mu$ g fluorescent protein tagged CBM fusion proteins and incubated at 30 °C for 1 hour with 80 rpm rotation speed (about 50-200  $\mu$ l). Loosely bound proteins were removed by washing with 5 volumes of Talon Buffer (about 1 ml) (Clontech). The cellulose-binding proteins were eluted with 50  $\mu$ l 10% (w/v) SDS Talon Buffer and boiled. The eluate was collected as the cellulose-binding fraction and separated by 12% SDS-PAGE and stained with Coomassie blue G-250 (Bio-Rad Laboratories, Hercules, CA).

### **Tissue Fixation**

Two-month-old *Arabidopsis* inflorescence stems were fixed for 2.5 h in 1.6% (w/v) paraformaldehyde and 0.2% (w/v) glutaraldehyde in 25 mM sodium phosphate buffer, pH 7.1.

Tissue was washed with buffer twice for 15 min, and dehydrated through a graded ethanol series [35%, 50%, 75%, 95% (v/v), 100%, 100%, and 100% ethanol] for 30 min for each step. The dehydrated tissue was moved to 4 °C and gradually infiltrated with cold LR White embedding resin (Ted Pella) using 33% (v/v) and 66% (v/v) resin in 100% ethanol for 24 h each, followed by 100% resin for three times of 24 h infiltration. The infiltrated tissue was transferred to gelatin capsules containing 100% resin for embedding, and resin was polymerized by exposing the capsules to 365-nm UV light at 4 °C for 48 h.

### **Direct fluorescence labeling by fluorescent protein tagged CBMs**

Semi-thin sections (250 nm) were cut using a Leica EM UC6 ultramicrotome (Leica Microsystems) and mounted on glass slides (colorfrost/plus; Fisher Scientific). Labeling was performed at room temperature as follows. Sections were blocked with 3% (w/v) nonfat dry milk in KPBS (0.01 M potassium phosphate, pH 7.1, containing 0.5 M NaCl) for 20 min and then washed with KPBS for 5 min. 15 µl fluorescent protein-tagged CBM proteins (1-2 mg/ml) were applied and incubated for 1 h. Sections were washed with KPBS three times for 5 min and distilled water for 5 min. Prior to applying a coverslip, Citifluor antifade mounting medium AF1 (Electron Microscopy Sciences) was applied to the sections.

## **Results**

### **Fluorescent protein tagged CBM construction and production**

Fluorescent protein-tagged CBMs were constructed by joining fluorescent protein (mCherry or YFP or GFP) to the C-terminus of CBMs via a 15-residue proline-threonine (PT) linker. Fluorescent protein mCherry tagged CBMs were produced as His-tagged recombinant proteins expressed in *E. coli* BL21(DE3) and purified by immobilized metal ion affinity chromatography. The molecular weight of these six mCherry tagged CBMs is between 40 KDa

and 55 KDa (Table 2.2) based on their amino acid sequences. The purified fluorescent protein tagged CBMs were examined to confirm whether they were homogenous by SDS-PAGE (Fig.2.1). The purified proteins electrophoresed as single bands with the expected sizes under typical SDS-PAGE conditions. The binding of these six CBM fusion proteins to cell wall polysaccharides was explored in more detail as follows.

**Table 2.2. Size of the fluorescent protein mCherry tagged CBMs used in this study**

Protein	Size (KDa)
CBM2a:mCherry	41.8
CBM3a:mCherry	46.3
CBM2b-1-2:mCherry	50.4
CBM35:mCherry	47.5
CBMXG34/1-X:mCherry	48.6
CBMXG34/2-VI:mCherry	48.6

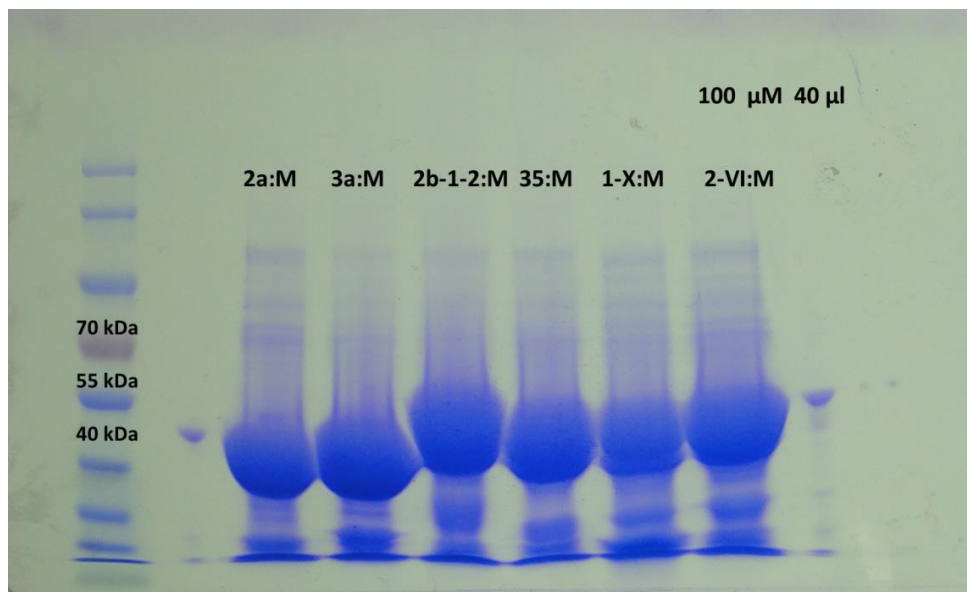


**Figure 2.1. Expression of mCherry fluorescent protein tagged CBMs** SDS-PAGE of immobilized metal ion affinity chromatography purified total soluble protein isolated from *E. coli* cell expressing mCherry fluorescent protein tagged CBMs.

## **Binding of fluorescent protein tagged CBMs to a diverse panel of 55 plant polysaccharides**

*In vitro* binding characteristics of these six fluorescent protein mCherry tagged CBMs towards 55 diverse plant polysaccharide preparations, whose detailed chemical compositions were previously known (Pattathil et al., 2010), were screened by ELISA. The 55 plant polysaccharide preparations were divided into groups of Xyloglucans, Xylans, Mannans,  $\beta$ -Glucans, Galactans, Arabinogalactans, Rhamnogalacturonans, Mucilages, Homogalacturonans (See detail information in Supplemental Table S2.1). Due to the high insolubility, cellulose cannot be dissolved in deionized water and in turn applied to 96-well plate for ELISA screens. Thus, cellulose is not included in this screening.

### *Cellulose-binding Group*

The ELISA results with the fluorescent protein mCherry tagged CBM2a and CBM3a were in agreement with known specificities of CBM2a and CBM3a for crystalline cellulose. That is, the ELISA screen revealed that neither CBM2a:mCherry nor CBM3a:mCherry effectively recognized most samples of hemicellulose and pectin tested in this screen. However, CBM2a:mCherry displayed some binding capacity to tamarind seed xyloglucan, Sinapus seed mucilage and seed xyloglucan of *Hymenea courbaril* (Figure 2.2). Mucilage is extruded from the seed coat of epidermal cells and is typically composed primarily of pectin and cellulose. It has been suggested that within the cellulose-binding CBM group, CBMs exhibit both similarities and differences in cell wall specificity that are plant- and tissue-specific (Blake et al., 2006). In our studies, CBM2a:mCherry showed some binding to xyloglucan from tamarind seed, jatoba seed and mucilage from sinapus seed, while CBM3a:mCherry did not bind to these hemicellulose and pectin samples (Figure 2.3), implicating variations between these two CBMs towards plant-specific cell wall components.

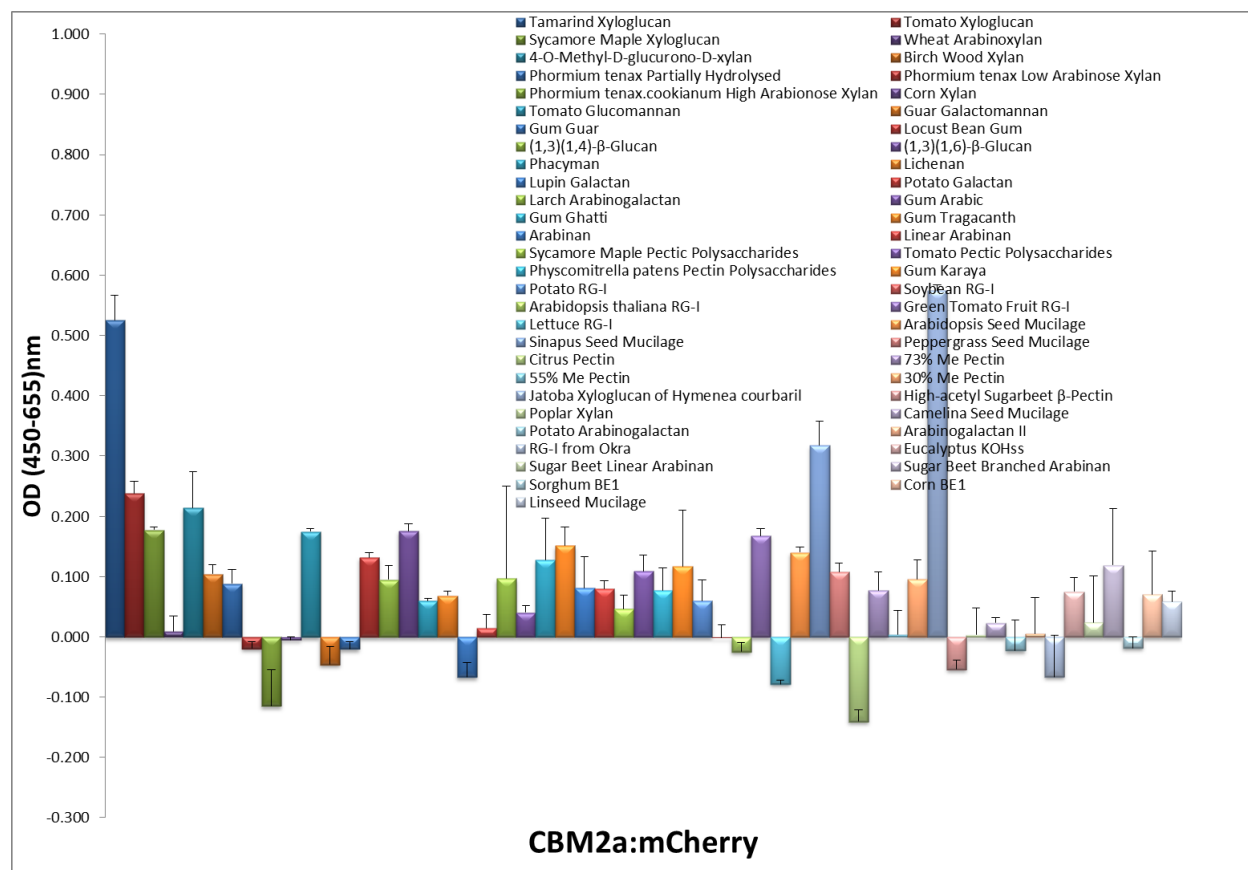


**Figure 2.2. Binding specificity of CBM2a:mCherry towards 55 plant polysaccharides**

The specificity of CBM2a:mCherry is illustrated by its polysaccharide recognition pattern based on ELISA responses. Each column reflects the binding pattern of CBM2a:mCherry against an immobilized polysaccharide on the plate. The negative optical density (OD) value is due to the subtraction of a control well on the same plate that contained CBM2a:mCherry and peroxidase-conjugated mouse anti-his antibodies but no immobilized polysaccharide. The error bars represent the standard deviation of experiments performed in triplicate.

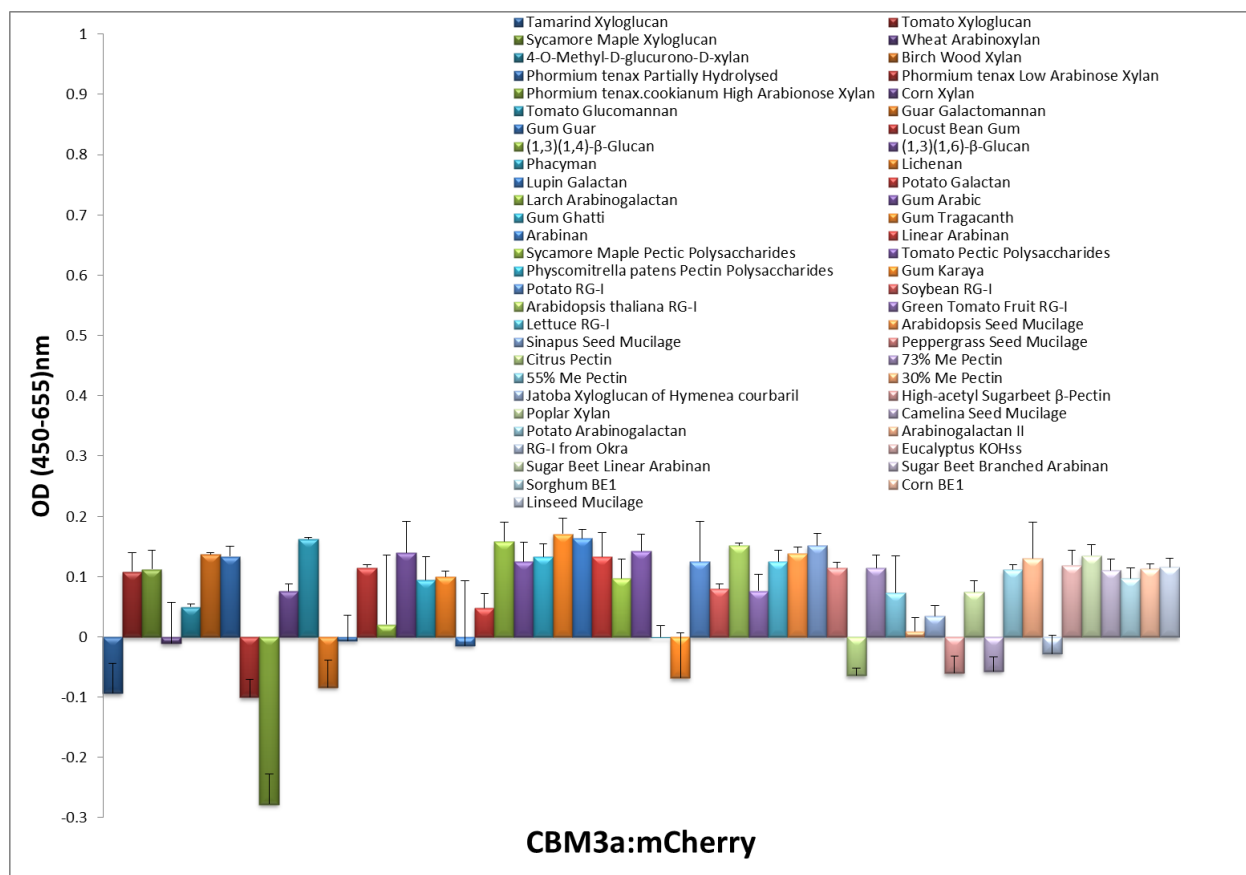


**Figure 2.3. Binding specificity of CBM3a:mCherry towards 55 plant polysaccharides**

The specificity of CBM3a:mCherry is illustrated by its polysaccharide recognition pattern based on ELISA responses. Each column reflects the binding pattern of CBM3a:mCherry against an immobilized polysaccharide on the plate. The negative optical density (OD) value is due to the subtraction of a control well on the same plate that contained CBM3a:mCherry and peroxidase-conjugated mouse anti-his antibodies but no immobilized polysaccharide. The error bars represent the standard deviation of experiments performed in triplicate.

### *Xylan-binding group*

Previous studies of ligand specificities have shown that CBM2b-1-2 and CBM35 displayed significant variation (McCartney et al., 2006). CBM35 exhibited more restricted ligand specificity against purified xylans (McCartney et al., 2006). The ELISA screens revealed that both CBM2b-1-2:mCherry and CBM35:mCherry bound effectively to xylan preparations including wheat Arabinoxylan, 4-O-Methyl-D-glucurono-D-xylan, Birch Wood xylan, Poplar xylan and Eucalyptus KOH extract (which is largely xylan). However, these mCherry-tagged CBMs did not recognize most of the monocot xylans included among these 55 polysaccharides including *Phormium tenax* partially hydrolysed xylan, *Phormium tenax* low arabinose xylan, *Phormium cookianum* high arabinose xylan and corn xylan. The inability of xylan-binding CBMs to recognize xylans isolated from some monocot species most probably reflects variations in the structures of these different xylans. Compared to dicots, cell walls of monocots are distinctive in that they typically contain a heavily substituted glucuronoarabinoxylan (GAX) (Carpita, 1996). Our results suggest that these two CBMs do not bind to such heavily substituted GAXs *in vitro*.

In addition to xylan, CBM2b-1-2:mCherry and CBM35:mCherry produced different patterns of binding to RG-I and seed mucilage from different species. Both CBM2b-1-2:mCherry and CBM35:mCherry showed significant capacity to bind to Sycamore Maple Pectic Polysaccharide (which is mostly RG-I) (Figures 2.4 and 2.5). However, neither CBM2b-1-2:mCherry nor CBM35:mCherry bound effectively to Arabidopsis RG-I. The structure of the RG-I side chain can vary greatly among plants (Harholt et al., 2010). Therefore, the binding pattern of Sycamore Maple Pectic Polysaccharide RG-I was distinctive from the binding pattern of Arabidopsis RG-I. Compared to CBM35:mCherry, CBM2b-1-2:mCherry showed notably

stronger binding to Green Tomato Fruit RG-I, Camelina Seed mucilage (Xylose sugar composition 2.2 Mol %), Peppergrass seed mucilage (Xylose sugar composition 9.8 Mol %) and Arabidopsis Seed mucilage (Xylose sugar composition 1.5 Mol %) (Pattathil et al., 2010) (Figure 2.4).

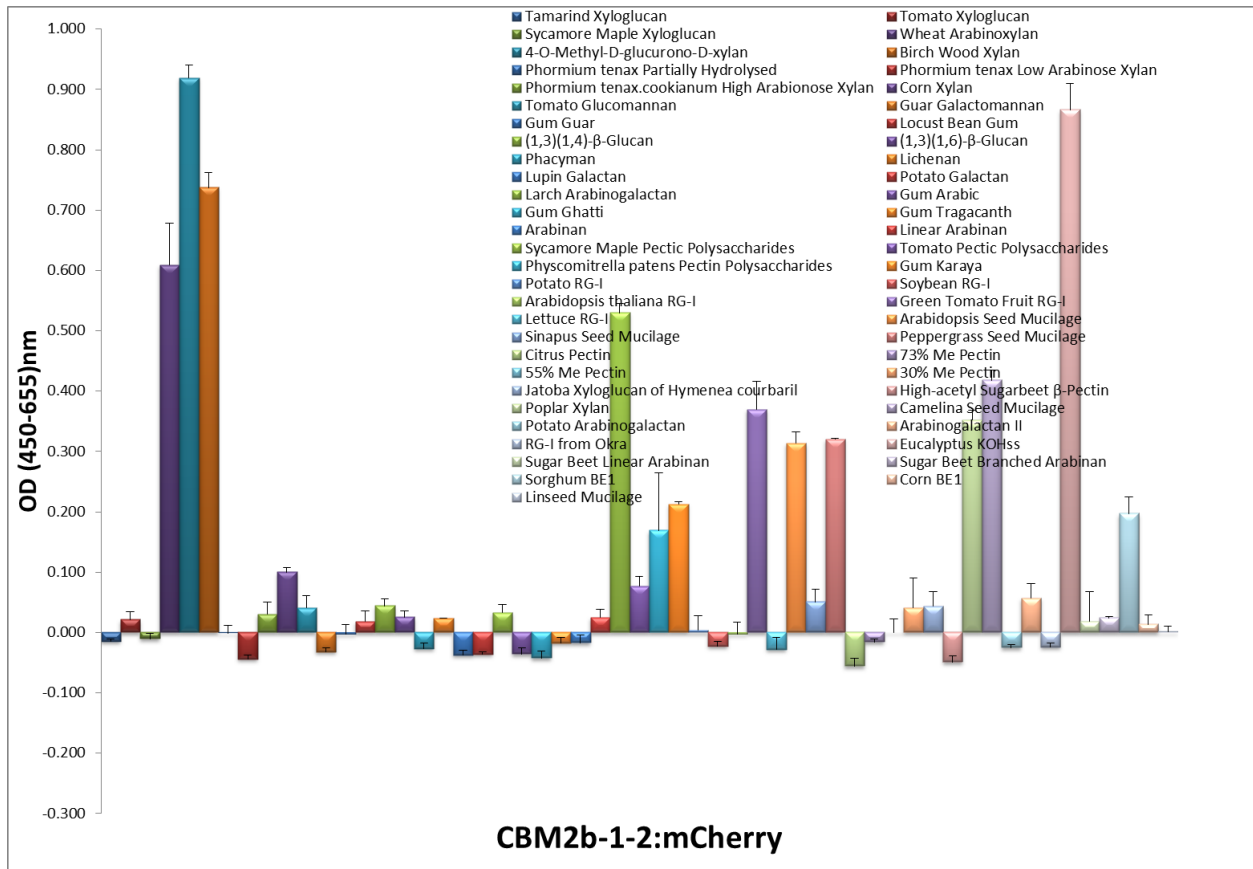


**Figure 2.4. Binding specificity of CBM2b-1-2:mCherry towards 55 plant polysaccharides**

The specificity of CBM2b-1-2:mCherry is illustrated by its polysaccharide recognition pattern based on ELISA responses. Each column reflects the binding pattern of CBM2b-1-2:mCherry against an immobilized polysaccharide on the plate. The negative optical density (OD) value are due to the subtraction of a control well on the same plate that contained CBM2b-1-2:mCherry and peroxidase-conjugated mouse anti-his antibodies but no immobilized polysaccharide. The error bars represent the standard deviation of experiments performed in triplicate.

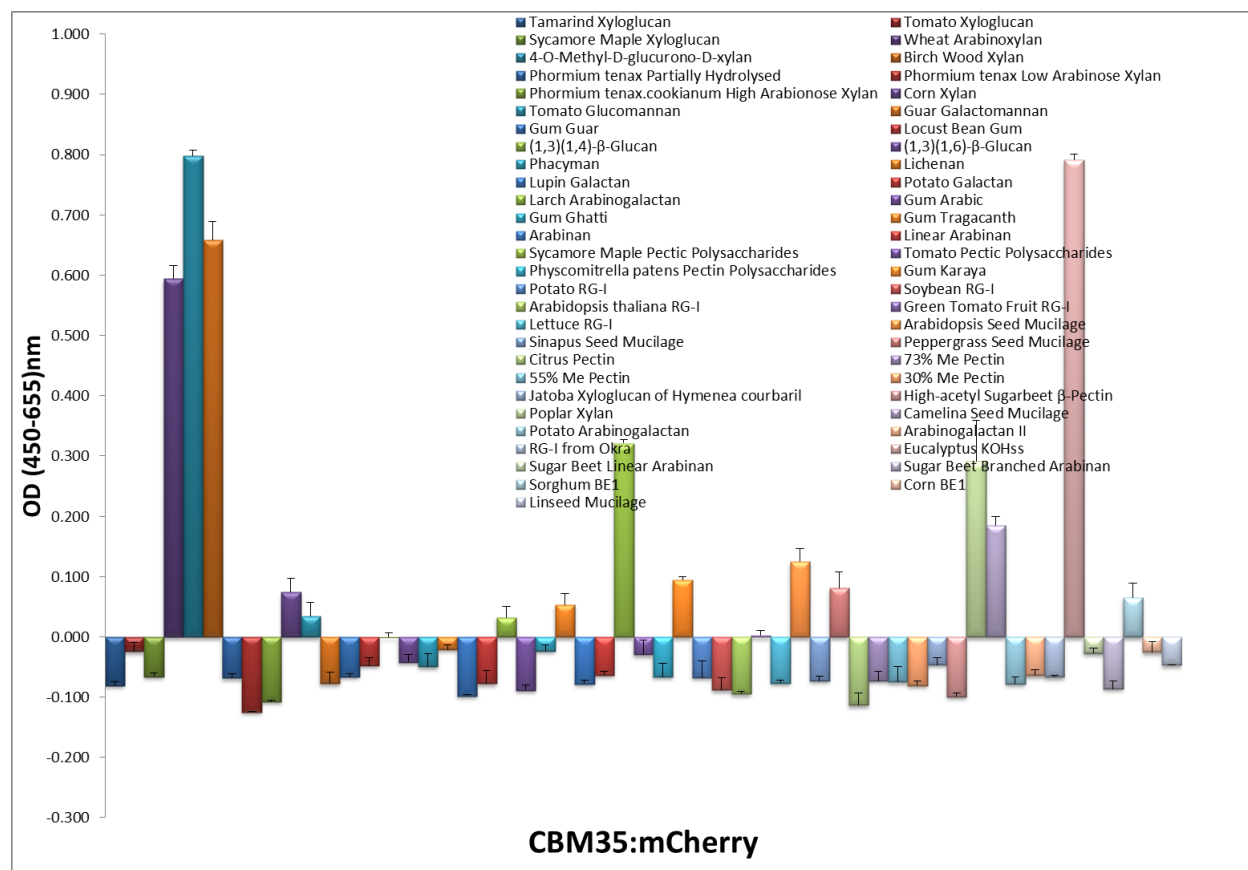


**Figure 2.5. Binding specificity of CBM35:mCherry towards 55 plant polysaccharides**

The specificity of CBM35:mCherry is illustrated by its polysaccharide recognition pattern based on ELISA responses. Each column reflects the binding pattern of CBM35:mCherry against an immobilized polysaccharide on the plate. The negative optical density (OD) values are due to the subtraction of a control well on the same plate that contained CBM35:mCherry and peroxidase-conjugated mouse anti-his antibodies but no immobilized polysaccharide. The error bars represent standard deviation of experiments performed in triplicate.

### *Xyloglucan-binding group*

CBMXG34/1-X and CBMXG34/2-VI are two modified proteins with greatly improved affinity for non-fucosylated xyloglucan (von Schantz et al., 2009). Xyloglucan consists of a

cellulose-like  $\beta$ -1-4 glucan backbone that may be substituted up to 75% with xylose units. The xyloses in turn can be decorated with galactose and fucose units. Some xyloglucans occur without any fucose on side chains and are collectively referred as non-fucosylated xyloglucan. CBMXG34/1-X:mCherry and CBMXG34/2-VI:mCherry exhibited strong specificity and binding capacity to xyloglucans, especially to Tamarind seed xyloglucan and seed xyloglucan of *Hymenea courbail*, which are rich in non-fucosylated xyloglucans (Buckeridge, 2010). CBMXG34/1-X:mCherry and CBMXG34/2-VI:mCherry discriminated non-fucosylated xyloglucan from fucosylated xyloglucan as shown by their notably weaker ability to bind to fucosylated Sycamore Maple xyloglucan.

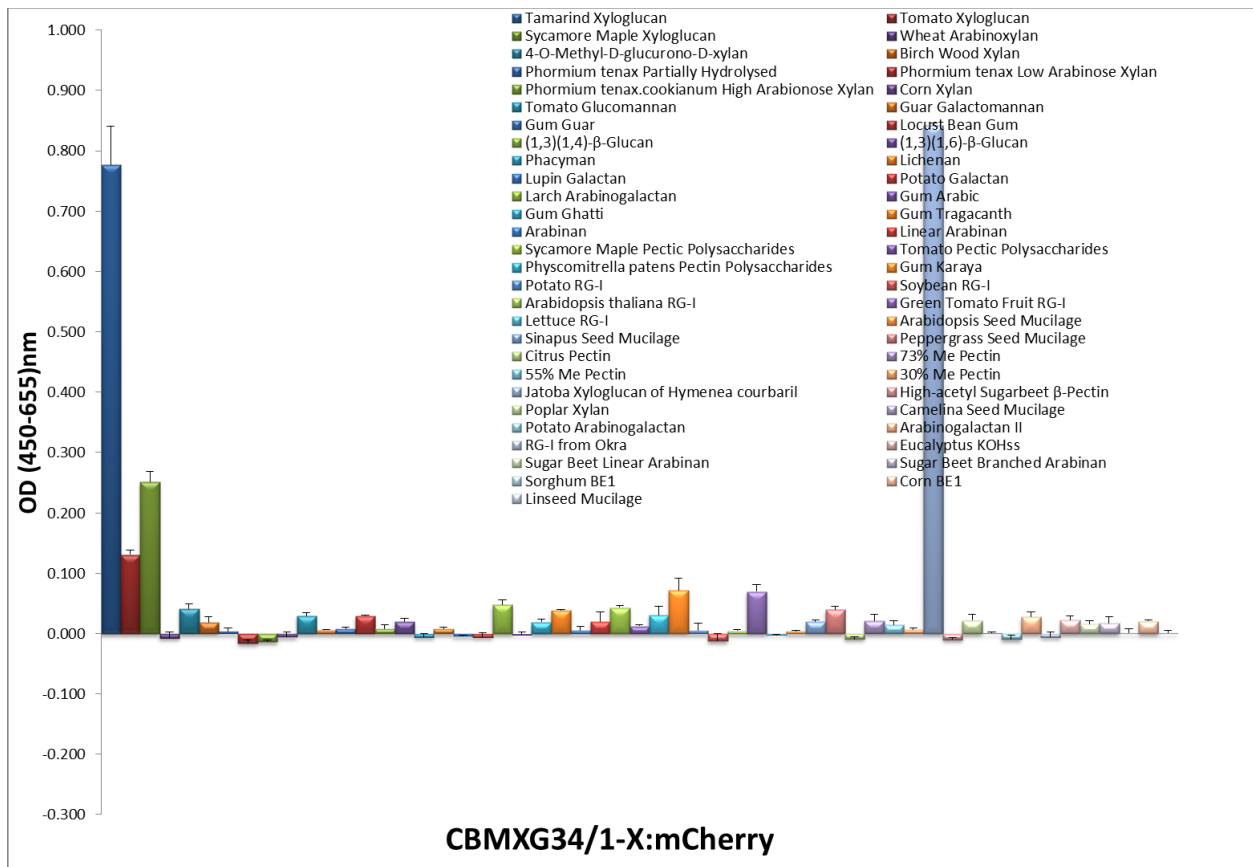


**Figure 2.6. Binding specificity of CBMXG34/1-X:mCherry towards 55 plant polysaccharides**

The specificity of CBMXG34/1-X:mCherry is illustrated by its polysaccharide recognition pattern based on ELISA responses. Each column reflects the binding pattern of CBM35:mCherry against an immobilized polysaccharide on the plate. The negative optical density (OD) values are due to the subtraction of a control well on the same plate that contained CBMXG34/1-X:mCherry and peroxidase-conjugated mouse anti-his antibodies but no immobilized polysaccharide. The error bars represent the standard deviation of experiments performed in triplicate.

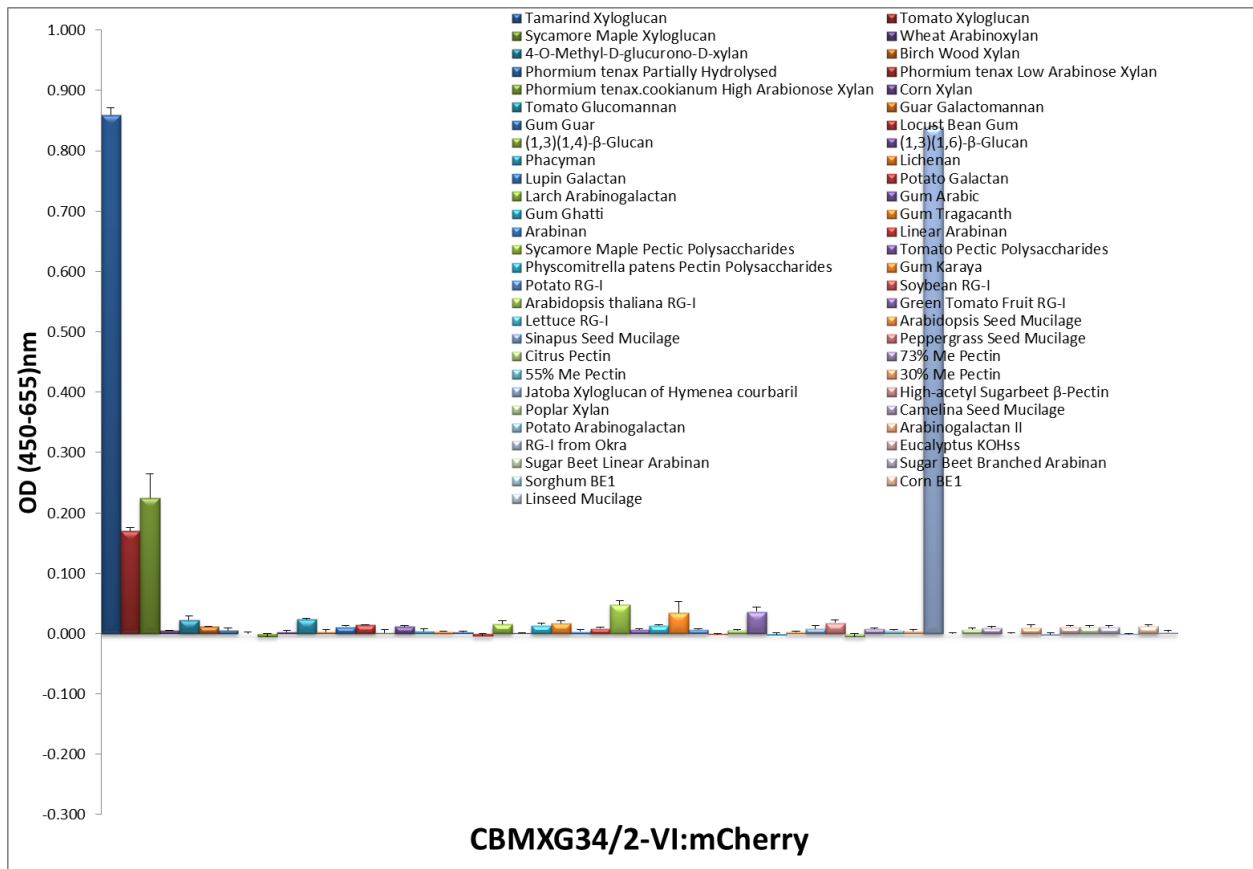


## **Figure 2.7. Binding specificity of CBMXG34/1-X:mCherry towards 55 plant polysaccharides**

The specificity of CBMXG34/2-VI:mCherry is illustrated by its polysaccharide recognition pattern based on ELISA responses. Each column reflects the binding pattern of CBM35:mCherry against an immobilized polysaccharide on the plate. The negative optical density (OD) values are due to the subtraction of a control well on the same plate that contained CBMXG34/2-VI:mCherry and peroxidase-conjugated mouse anti-his antibodies but no immobilized polysaccharide. The error bars represent the standard deviation of experiments performed in triplicate.

## **Binding capacity of mCherry tagged cellulose-binding CBMs towards cellulose *in vitro***

The *in vitro* binding capacity of the CBM2a:mCherry and CBM3a:mCherry fusion proteins towards cellulose was confirmed by Cellulose Pull-Down assays. In this experiment, Avicel (insoluble substrate) were used as bait and CBM fusion proteins were tested as prey. Xylan-binding CBM2b-1-2:mCherry and CBM35:mCherry, as expected, did not bind to Avicel (Figure 2.8). The xyloglucan-binding CBMXG34/1-X:mCherry and CBMXG34/2-VI:mCherry did not bind to Avicel also (data not shown). In contrast, CBM2a:mCherry and CBM3a:mCherry were pulled down by Avicel. Thus, the CBM2a:mCherry and CBM3a:mCherry fusion proteins functioned as cellulose-binding modules.

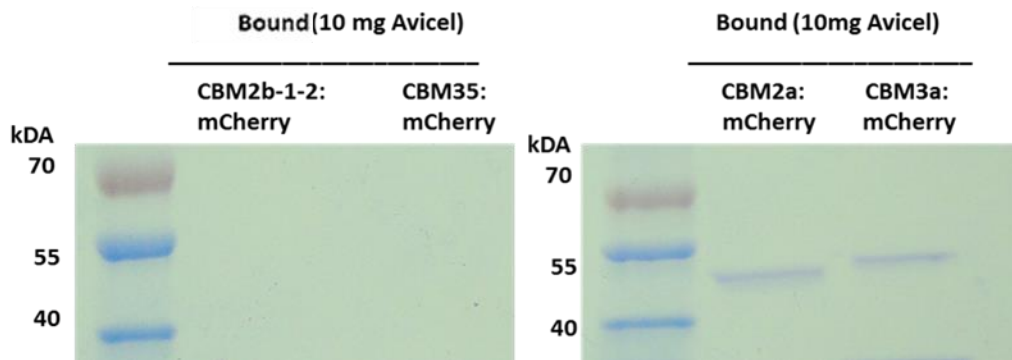


**Figure 2.8. Cellulose Pull-Down Assay of mCherry tagged CBMs**

Left: xylan-binding CBM2b-1-2:mCherry and CBM35:mCherry were not pulled down by Avicel;  
 Right: cellulose-binding CBM2a:mCherry and CBM3a:mCherry were pulled down by Avicel.

### **Direct and indirect labeling of fixed Arabidopsis stem sections using tagged CBMs**

The binding capacity of these six fluorescent protein-tagged CBMs to Arabidopsis cell walls was initially assessed by direct labeling of stem sections with His-tagged CBM:mCherry fusion proteins, and also by indirect labeling of stem sections with His-tagged CBM:mCherry fusion proteins and Alexa Fluor® 488 attached to an anti-His monoclonal antibody. As shown in Figure 2.8, the two cellulose-binding CBMs, CBM2a:mCherry and CBM3a:mCherry, displayed different patterns on Arabidopsis stems (Figure 2.8 A1, B1). CBM3a:mCherry recognized the walls of every tissue in the Arabidopsis stem including epidermis, cortex, phloem, interfascicular fibres, vascular xylem and pith. CBM2a:mCherry displayed binding mainly to cellulose within cell walls of xylem vessels and interfascicular fibres. Both xylan-binding CBM2b-1-2:mCherry and CBM35:mCherry showed labeling to secondary cell walls of xylem vessels and interfascicular fibres. However, CBM35:mCherry weakly labeled secondary walls of some vascular xylem cells (indicated by stars in Figure 2.8 D1). The xyloglucan-binding CBMXG34/1-X:mCherry and CBM34/2-VI:mCherry did not bind to Arabidopsis stem sections

(Data not shown). Thus, results from labeling of fixed Arabidopsis stem sections with CBM:mCherry fusion proteins confirmed that cellulose-binding and xylan-binding CBMs can recognize Arabidopsis cell walls when applied to tissue sections *in vitro*.

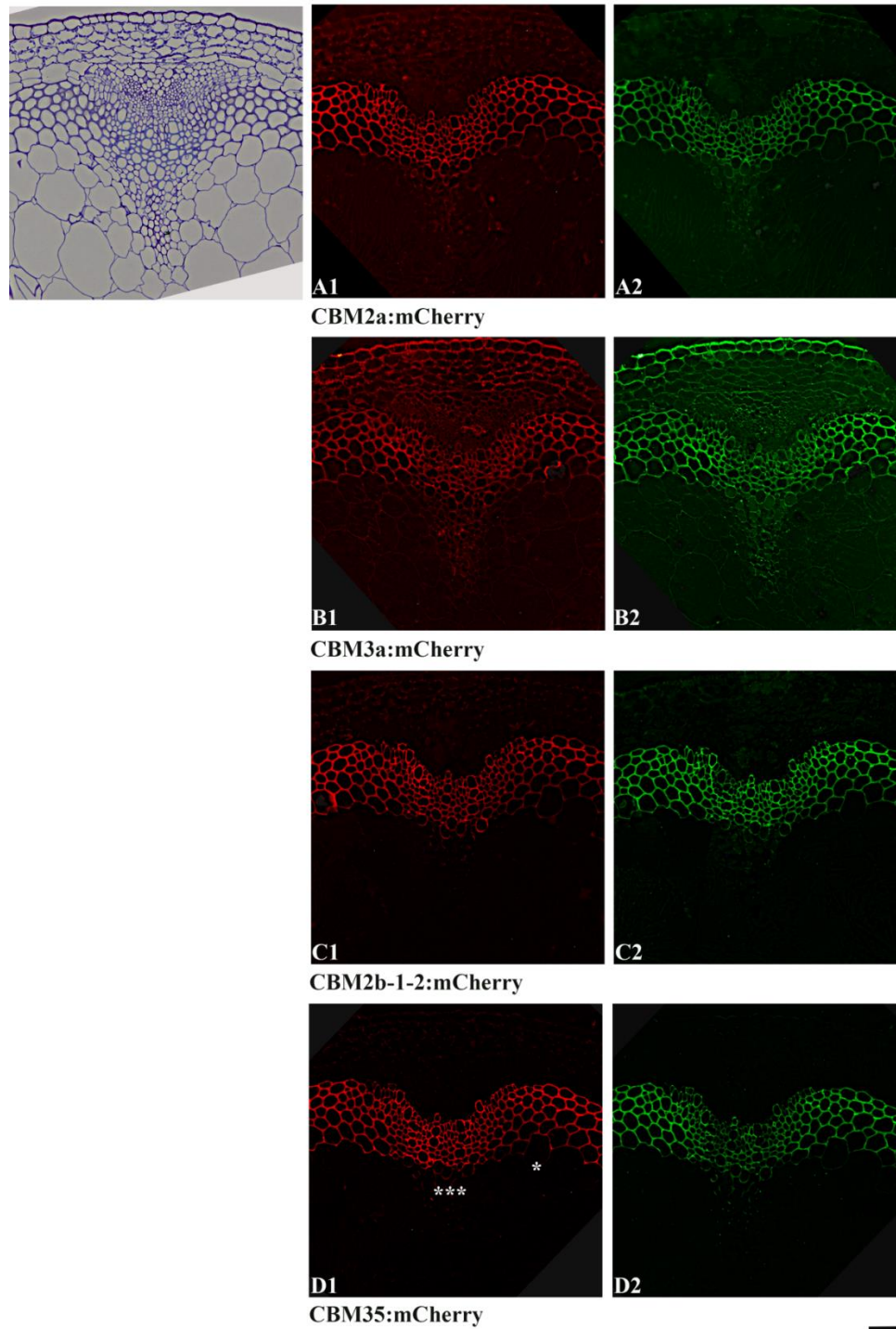


**Figure 2.9. Labeling of Arabidopsis stem sections *in vitro* with tagged CBM fusion proteins.**

**Left (A1, B1, C1, D1):** Direct labeling of transverse section of WT Arabidopsis basal stem by His-tagged fluorescent protein CBM fusion proteins. **Right (A2, B2, C2, D2):** Immunolabeling of transverse sections of WT Arabidopsis basal stem with His-tagged fluorescent protein CBM fusion proteins and Alexa Fluor® 488 attached to an anti-His monoclonal antibody. Tissues were taken from the base of 6-week-old *Col-0* (WT) stems, fixed and embedded in LR White resin, and 250 nm thick transverse sections were cut by microtome. Scale bar = 50  $\mu\text{m}$ .

**Binding of Xyloglucan-Binding CBMs to Arabidopsis cell wall KOH extracts**

Since xyloglucan-binding CBMXG34/1-X:mCherry and CBMXG34/2-VI:mCherry did not exhibit labeling capacity on fixed Arabidopsis stem sections, the binding capacities of these xyloglucan-binding CBMs was explored in more detail by ELISA with Arabidopsis cell wall extracts from both leaves and stems. Arabidopsis cell walls were sequentially extracted with increasingly harsh solvents to release cell wall components. Cell walls were treated with 1M KOH and 4M KOH to solubilize primarily hemicelluloses, mainly xylan and xyloglucan (Zablackis et al., 1995). In this experiment, CCRC-M1, which recognizes terminal  $\alpha$ -1,2-linked fucosyl residues in fucosylated xyloglucans, and CCRC-M87, which recognizes non-fucosylated xyloglucan epitope, were used as controls. Both CCRC-M1 and CCRC-M87 exhibited significant binding capacity to 4M KOH Arabidopsis cell wall extracts and moderate binding capacity to 1M KOH extracts. These results are consistent with results obtained by others in the Hahn lab. In contrast, CBMXG34/1-X:mCherry and CBMXG34/2-VI:mCherry bound poorly to Arabidopsis cell wall KOH extracts, though they bound strongly to tamarind xyloglucan, which is a non-fucosylated xyloglucan. Therefore, the xyloglucan structure(s) recognized by

CBMXG34/1-X:mCherry and CBMXG34/2-VI:mCherry appear to be poorly represented in the xyloglucans present in Arabidopsis cell walls.

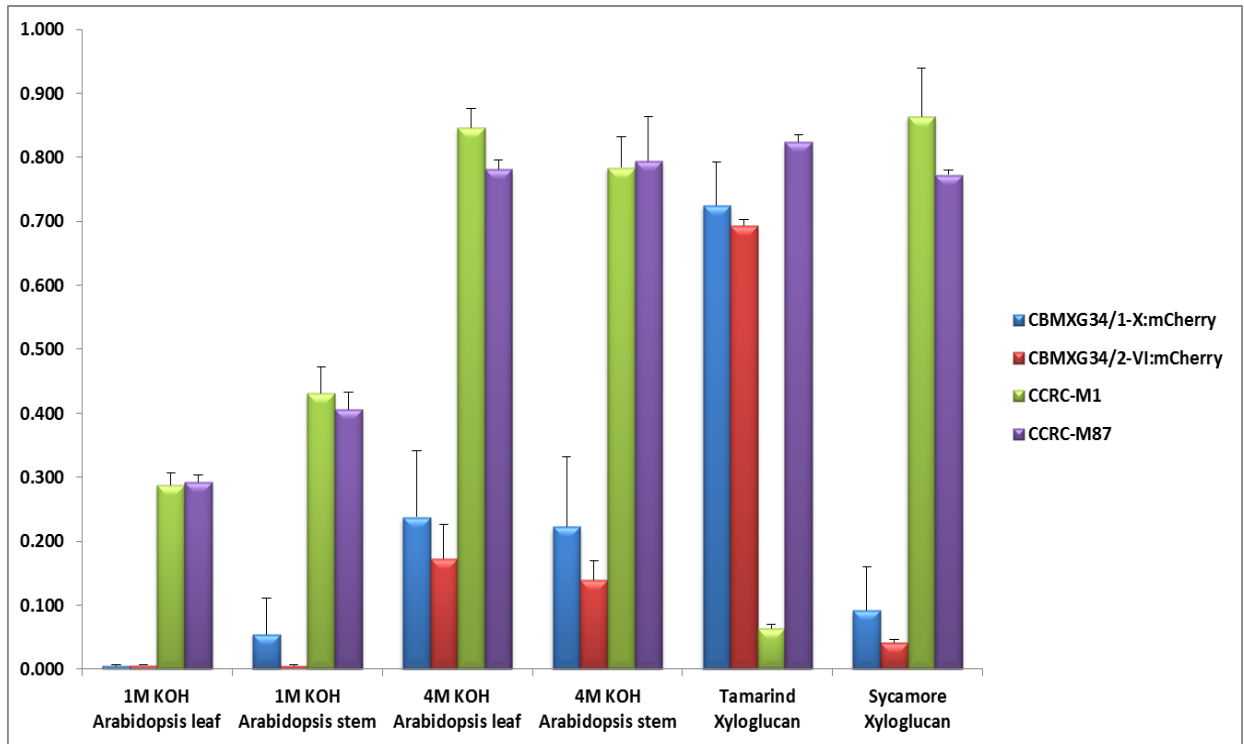


**Figure 2.10. Binding studies of fluorescent protein tagged CBMs on Arabidopsis cell wall extracts.** ELISAs of xyloglucan-Binding CBMXG34/1-X:mCherry and CBMXG34/2-VI:mCherry were performed using plates coated with 1M KOH and 4M KOH cell wall extracts from Arabidopsis stem and leaf cell wall preparations. Wells coated with a fucosylated xyloglucan from sycamore or a non-fucosylated xyloglucan from tamarind seed were included as positive controls. Xyloglucan-directed antibodies CCRC-M1 and CCRC-M87 were also included as controls. The error bars represent the standard deviation of experiments performed in triplicate.

## Discussion

We have investigated the binding specificities of several tagged CBMs that bind to different plant cell wall polysaccharides. Within the cellulose-binding group, CBM3a:mCherry bound evenly to primary and secondary cell walls, whereas CBM2a:mCherry displayed a preference for secondary cell walls of interfascicular fibres and vascular xylem in labeling of fixed *Arabidopsis* stem sections. CBM3a is a module in the cellulosome, a multi-enzyme plant cell wall-degrading complex produced by the anaerobic bacterium *Clostridium thermocellum* (Bayer et al., 2004). Thus, there will be a strong selective pressure for CBM3a to display broad specificity for cellulose microfibrils present in a range of cell walls in order for CBM3a to target the cellulosome to the array of crystalline cellulosic material that is likely to exist in the *C. thermocellum* environment (Blake et al., 2006). CBM2a is the carbohydrate-binding module in Xylanase 10A. It is possible that CBM2a is used to target the enzyme preferentially to cellulose within secondary cell walls, where cellulose is in intimate contact with xylan. In ELISAs, CBM2a:mCherry showed binding capacity to non-fucosylated xyloglucan, whereas CBM3a:mCherry did not exhibit any cross-reactivity with these xyloglucan samples. Cellulose and xyloglucan are not covalently linked to each other as far as is known. These two polysaccharides share common structural features (xyloglucan has a cellulose-like  $\beta$ 1-4 glucan backbone which may be substituted up to 75% with xylose units). Cellulose-binding CBMs appear to make few significant hydrogen bonds with the microfibril cellulose structures (Blake et al., 2006). It has been suggested that the binding face of the cellulose-binding CBMs may interact with other polysaccharides that are in intimate contact with the cellulose (Blake et al., 2006). Therefore, it is possible for CBM2a:mCherry to also have binding capacity to xyloglucans, though this still requires additional experimental verification.

In dicots, glucuronoxylan (GX) and methylglucuronoxylan (MGX) are abundant in the secondary cell walls of specific cell types such as xylem vessels and interfascicular fibers; primary cell walls have low levels of xylans that are of the GX type (Darvill et al., 1980; O'Neill and York, 2003). Within the xylan-binding group, CBM2b-1-2 binds to the backbone of linear and substituted xylans, whereas CBM35 binds to GX, but not to MGX (McCartney et al., 2006). Consistent with a recent study (Urbanowicz et al., 2012), CBM2b-1-2:mCherry extensively labeled the secondary walls of interfascicular fibers and vascular bundles in Arabidopsis stem section. CBM35:mCherry weakly labeled secondary cell walls of some vascular xylem cells in Arabidopsis stem section, indicating that the xylans in the cell walls of these cells are highly methylated. In ELISAs, CBM2b-1-2:mCherry and CBM35:mCherry exhibited notable recognition of some RG-I preparations. Xylan and pectin structure were not thought to be interdependent wall polysaccharides until the recent identification of ARABINOXYLAN PECTIN ARABINO GALACTAN PROTEIN1 (APAP1), which was found to carry both pectin (RGI/homogalacturonan) and xylan structures linked to the same arabinogalactan (Tan et al., 2013). Thus, these observed cross-reactivities of the xylan-directed CBMs might be explained by the presence of APAP1 or APAP1-like molecules in those RG-I preparations.

CBMs exhibit plant- and tissue-specific differences in cell wall recognition, providing insights into the complex molecular architecture of plant cell wall (Knox, 2008). Previous studies revealed that xyloglucan-binding CBMXG34/1-X and CBMXG34/2-VI bound selectively to non-fucosylated xyloglucan of tamarind seed (von Schantz et al., 2009). ELISA screens of mCherry fluorescent protein CBMXG34/1-X:mCherry and CBMXG34/2-VI:mCherry fusion proteins demonstrated their ability to bind to tamarind seed xyloglucan. However, these two xyloglucan-binding CBMs did not exhibit strong binding capacity to Arabidopsis cell walls,

even though *Arabidopsis* stem cell walls are known to contain non-fucosylated xyloglucan structural features as shown by binding of monoclonal antibodies directed against these epitopes (Cavalier et al., 2008; Zabolina et al., 2008; Zabolina et al., 2012). Therefore, CBMXG34/1-X and CBMXG34/2-VI appear to bind to non-fucosylated xyloglucan structural features that are not abundant in *Arabidopsis* cell walls. Thus, these two CBMs are not suitable for our further studies which focus on *Arabidopsis* cell walls.

## References

- Bayer EA, Belaich JP, Shoham Y, Lamed R** (2004) The cellulosomes: multienzyme machines for degradation of plant cell wall polysaccharides. *Annu Rev Microbiol* **58**: 521-554
- Bertani G** (1951) STUDIES ON LYSOGENESIS I.: The Mode of Phage Liberation by Lysogenic *Escherichia coli*. *Journal of Bacteriology* **62**: 293-300
- Blake AW, McCartney L, Flint JE, Bolam DN, Boraston AB, Gilbert HJ, Knox JP** (2006) Understanding the biological rationale for the diversity of cellulose-directed carbohydrate-binding modules in prokaryotic enzymes. *J Biol Chem* **281**: 29321-29329
- Buckeridge MS** (2010) Seed Cell Wall Storage Polysaccharides: Models to Understand Cell Wall Biosynthesis and Degradation. *Plant Physiology* **154**: 1017-1023
- Carpita NC** (1996) STRUCTURE AND BIOGENESIS OF THE CELL WALLS OF GRASSES. *Annu Rev Plant Physiol Plant Mol Biol* **47**: 445-476
- Cavalier DM, Lerouxel O, Neumetzler L, Yamauchi K, Reinecke A, Freshour G, Zabolina OA, Hahn MG, Burgert I, Pauly M, Raikhel NV, Keegstra K** (2008) Disrupting Two *Arabidopsis thaliana* Xylosyltransferase Genes Results in Plants Deficient in Xyloglucan, a Major Primary Cell Wall Component. *The Plant Cell Online* **20**: 1519-1537
- Darvill JE, McNeil M, Darvill AG, Albersheim P** (1980) Structure of Plant Cell Walls: XI. GLUCURONOARABINOXYLAN, A SECOND HEMICELLULOSE IN THE PRIMARY CELL WALLS OF SUSPENSION-CULTURED SYCAMORE CELLS. *Plant Physiology* **66**: 1135-1139
- Gunnarsson LC, Zhou Q, Montanier C, Karlsson EN, Brumer H, 3rd, Ohlin M** (2006) Engineered xyloglucan specificity in a carbohydrate-binding module. *Glycobiology* **16**: 1171-1180

- Harholt J, Suttangkakul A, Vibe Scheller H** (2010) Biosynthesis of Pectin. *Plant Physiology* **153**: 384-395
- Knox JP** (2008) Revealing the structural and functional diversity of plant cell walls. *Current Opinion in Plant Biology* **11**: 308-313
- McCann MC, Knox JP** (2010) Plant Cell Wall Biology: Polysaccharides in Architectural and Developmental Contexts. *In Annual Plant Reviews*. Wiley-Blackwell, pp 343-366
- McCartney L, Blake AW, Flint J, Bolam DN, Boraston AB, Gilbert HJ, Knox JP** (2006) Differential recognition of plant cell walls by microbial xylan-specific carbohydrate-binding modules. *Proceedings of the National Academy of Sciences of the United States of America* **103**: 4765-4770
- O'Neill MA, York WS** (2003) The composition and structure of plant primary cell walls. *The plant cell wall*: 1-54
- Pattathil S, Avcı U, Baldwin D, Swennes AG, McGill JA, Popper Z, Bootten T, Albert A, Davis RH, Chennareddy C, Dong R, O'Shea B, Rossi R, Leoff C, Freshour G, Narra R, O'Neil M, York WS, Hahn MG** (2010) A Comprehensive Toolkit of Plant Cell Wall Glycan-Directed Monoclonal Antibodies. *Plant Physiology* **153**: 514-525
- Sambrook J, Fritsch EF, Maniatis T** (1989) *Molecular Cloning: A Laboratory Manual*, Ed 2nd. Cold Spring Harbor Laboratory Press, Plainview, N.Y
- Tan L, Eberhard S, Pattathil S, Warder C, Glushka J, Yuan C, Hao Z, Zhu X, Avcı U, Miller JS, Baldwin D, Pham C, Orlando R, Darvill A, Hahn MG, Kieliszewski MJ, Mohnen D** (2013) An Arabidopsis Cell Wall Proteoglycan Consists of Pectin and Arabinoxylan Covalently Linked to an Arabinogalactan Protein. *The Plant Cell Online* **25**: 270-287

- Urbanowicz BR, Pena MJ, Ratnaparkhe S, Avci U, Backe J, Steet HF, Foston M, Li H, O'Neill MA, Ragauskas AJ, Darvill AG, Wyman C, Gilbert HJ, York WS (2012)** 4-O-methylation of glucuronic acid in Arabidopsis glucuronoxylan is catalyzed by a domain of unknown function family 579 protein. *Proc Natl Acad Sci U S A* **109**: 14253-14258
- von Schantz L, Gullfot F, Scheer S, Filonova L, Cicortas Gunnarsson L, Flint JE, Daniel G, Nordberg-Karlsson E, Brumer H, Ohlin M (2009)** Affinity maturation generates greatly improved xyloglucan-specific carbohydrate binding modules. *BMC Biotechnol* **9**: 92
- Zabackis E, Huang J, Muller B, Darvill AG, Albersheim P (1995)** Characterization of the Cell-Wall Polysaccharides of Arabidopsis thaliana Leaves. *Plant Physiology* **107**: 1129-1138
- Zabotina OA, Avci U, Cavalier D, Pattathil S, Chou YH, Eberhard S, Danhof L, Keegstra K, Hahn MG (2012)** Mutations in multiple XXT genes of Arabidopsis reveal the complexity of xyloglucan biosynthesis. *Plant Physiol* **159**: 1367-1384
- Zabotina OA, van de Ven WT, Freshour G, Drakakaki G, Cavalier D, Mouille G, Hahn MG, Keegstra K, Raikhel NV (2008)** Arabidopsis XXT5 gene encodes a putative alpha-1,6-xylosyltransferase that is involved in xyloglucan biosynthesis. *Plant J* **56**: 101-115

**Supplementary Table S2.1 List of 55 plant polysaccharides**

	<b>Antigens Name</b>	<b>Heat Map Name</b>	<b>Group</b>	<b>Source and Reference(s)/Website for Structural Studies</b>	<b>Sugar Composition (Mol %)</b>
A01	Tamarind Xyloglucan	Tam XG	Xyloglucans	CCRC, UGA; (York et al., 1993); Hahn lab data (Pattathil et al., 2010)	Glc (43), Xyl (37), Gal (17) and Ara (3)
A02	Tomato Xyloglucan	Tom XG	Xyloglucans	CCRC, UGA; (Jia et al., 2003); Hahn lab data (Pattathil et al., 2010)	Glc (44), Xyl (32), Gal (14) and Ara (10)
A03	Sycamore Maple Xyloglucan	Syc XG	Xyloglucans	CCRC, UGA; (Stevenson et al., 1986); Hahn lab data (Pattathil et al., 2010)	Glc (42), Xyl (31), Gal (10), Man (9), Fuc (4) and Ara (4)
A04	Wheat Arabinoxylan	Wh Araxyl	Xylans	Megazyme, Bray, Ireland; Hahn lab data (Pattathil et al., 2010), <a href="http://secure.megazyme.com/Arabinoxylan-Wheat-Flour-Insoluble">http://secure.megazyme.com/Arabinoxylan-Wheat-Flour-Insoluble</a>	Ara (37), Xyl (61) and traces of other sugars
A05	4-O-Methyl-D-glucurono-D-xylan	MeGLA Xy	Xylans	Sigma-Aldrich, St. Louis, MO; Hahn lab data (Pattathil et al., 2010)	Xyl (82.8) and Methyl GlcA (17.2)
A06	Birch Wood Xylan	BW Xyl	Xylans	Sigma-Aldrich, St. Louis, MO; Hahn lab data (Pattathil et al., 2010)	Xyl (100)
A07	<i>Phormium tenax</i> Partially Hydrolysed	PT Xyl PH	Xylans	IRL, New Zealand; Hahn lab data (Pattathil et al., 2010)	Xyl (94) and Gluc (6)
A08	<i>Phormium tenax</i> Low Arabinose Xylan	PT Xyl LA	Xylans	IRL, New Zealand; Hahn lab data (Pattathil et al., 2010)	Xyl (87), Ara (8) and Glc (5)
A09	<i>Phormium tenax</i> cookianum High Arabinose Xylan	PC Xyl	Xylans	IRL, New Zealand; Hahn lab data (Pattathil et al., 2010)	Xyl (70), Ara (27) and Glc (3)
A10	Corn Xylan	Corn Xyl	Xylans	National Renewable Energy Lab, Golden, CO; Hahn lab data (Pattathil et al., 2010)	Xyl (100)
A11	Tomato Glucomannan	Tom GlucM	Mannans	CCRC, UGA; Hahn lab data (Pattathil et al., 2010)	Glc (61) and Man (39)
B01	Guar Galactomannan	Guar GalM	Mannans	Megazyme, Bray, Ireland; Hahn lab data (Pattathil et al., 2010), <a href="http://secure.megazyme.com/Galactomannan-Guar-Medium-Viscosity">http://secure.megazyme.com/Galactomannan-Guar-Medium-Viscosity</a>	Man (62) and Gal (38)
B02	Gum Guar	Gum Guar	Mannans	Sigma-Aldrich, St. Louis, MO; Hahn lab data (Pattathil et al., 2010)	Man (63), Gal (36) and Ara (1)
B03	Locust Bean Gum	Loc Bean G	Mannans	Sigma-Aldrich, St. Louis, MO; Hahn lab data (Pattathil et al., 2010)	Man (81) and Gal (19)
B04	(1,3)(1,4)- $\beta$ -Glucan	1314 Gluc	$\beta$ -Glucans	Megazyme, Bray, Ireland; Hahn lab data (Pattathil et al., 2010)	Glc (97), Man (2) and Ara (1)

B05	(1,3)(1,6)- $\beta$ -Glucan	1315 Gluc	$\beta$ -Glucans	CCRC, UGA; (Hahn et al., 1992); Hahn lab data (Pattathil et al., 2010)	Glc (91), Man (7) and Ara (2)
B06	Pachyman	Pachyman	$\beta$ -Glucans	Megazyme, Bray, Ireland; Hahn lab data (Pattathil et al., 2010), <a href="http://secure.megazyme.com/Pachyman">http://secure.megazyme.com/Pachyman</a>	D-glucose essentially all of which is 1,3- $\beta$ -linked (>98)
B07	Lichenan	Lichenan	$\beta$ -Glucans	Megazyme, Bray, Ireland; Hahn lab data (Pattathil et al., 2010), <a href="http://secure.megazyme.com/Lichenan-Icelandic-Moss">http://secure.megazyme.com/Lichenan-Icelandic-Moss</a>	Glc (98) and Ara (2)
B08	Lupin Galactan	Lup Gal	Galactans	Megazyme, Bray, Ireland; Hahn lab data (Pattathil et al., 2010), <a href="http://secure.megazyme.com/Galactan-Lupin">http://secure.megazyme.com/Galactan-Lupin</a>	Gal (83), GalA (5), Rha (5), Ara (3), Xyl (2) and traces of Glc
B09	Potato Galactan	Pot Gal	Galactans	Megazyme, Bray, Ireland; Hahn lab data (Pattathil et al., 2010), <a href="http://secure.megazyme.com/Galactan-Potato">http://secure.megazyme.com/Galactan-Potato</a>	Gal (88), GalA (6), Ara (3) and Rha (3)
B10	Larch Arabinogalactan	Lar Ara Gal	Arabinogalactans	Megazyme, Bray, Ireland; Hahn lab data (Pattathil et al., 2010), <a href="http://secure.megazyme.com/Arabinogalactan-Larch-Wood">http://secure.megazyme.com/Arabinogalactan-Larch-Wood</a>	Gal (81), Ara (14) and traces of other sugars
B11	Gum Arabic	Gum Arabic	Arabinogalactans	Sigma-Aldrich, St. Louis, MO; (Stephen, Phillips, and Williams, 2006); Hahn lab data (Pattathil et al., 2010)	Ara (37), Gal (40), Rha (20) and traces of Glc
C01	Gum Ghatti	Gum Ghatti	Arabinogalactans	Sigma-Aldrich, St. Louis, MO; (Stephen, Phillips, and Williams, 2006); Hahn lab data (Pattathil et al., 2010)	Ara (49), Gal (31), Man (10), GlcA (8) and Xyl (2)
C02	Gum Tragacanth	Gum Trag	Arabinogalactans	Sigma-Aldrich, St. Louis, MO; (Stephen, Phillips, and Williams, 2006); Hahn lab data (Pattathil et al., 2010)	Gal (32.3), Ara (31.7), Xyl (12), Glc (12.3), Fuc (8.4) and Rha (3.3)
C03	Arabinan	Arabinan	Arabinogalactans	Megazyme, Bray, Ireland; Hahn lab data (Pattathil et al., 2010), <a href="http://secure.megazyme.com/Arabinan-Sugar-Beet">http://secure.megazyme.com/Arabinan-Sugar-Beet</a>	Ara (88), Gal (3), Rha (2) and GalA (7)
C04	Linear Arabinan	Linear Arabinan	Arabinogalactans	Megazyme, Bray, Ireland; Hahn lab data (Pattathil et al., 2010), <a href="http://secure.megazyme.com/Linear-1-5-alpha-L-Arabinan-Sugar-Beet">http://secure.megazyme.com/Linear-1-5-alpha-L-Arabinan-Sugar-Beet</a>	Ara (97.5), GalA (2), Gal (0.4) and Rha (0.1)
C05	Sycamore Maple Pectic Polysaccharides	Syc PecP	RG-I	CCRC, UGA; (Stevenson et al., 1986); Hahn lab data (Pattathil et al., 2010)	Gal (52.4), GlcA (15), GalA (11), Xyl (7.9), Ara (7.5), Glc (2.6), Rha (2), Man (1.3) and traces of Fuc

C06	Tomato Pectic Polysaccharides	Tom PecP	RG-I	CCRC, UGA; (Jia et al., 2003); Hahn lab data (Pattathil et al., 2010)	Gal (57.4), Ara (25.2), GalA (6.5), Rha (4.4), Xyl (4.3) and Fuc (2.2)
C07	<i>Physcomitrella patens</i> Pectin Polysaccharides	PhyscPe cP	RG-I	CCRC, UGA; (Peña et al., 2008); Hahn lab data (Pattathil et al., 2010)	GalA (46.7), Rha (24), Gal(17.4), Ara (8.1), Glc (2.3) and Xyl (1.5)
C08	Gum Karaya	Gum Karaya	RG-I	Sigma-Aldrich, St. Louis, MO; Hahn lab data (Pattathil et al., 2010)	GalA (57), GlcA (8), Gal (17), Rha (16) and traces of Glc
C09	Potato RG-I	Pot RG-I	RG-I	Megazyme, Bray, Ireland; Hahn lab data (Pattathil et al., 2010), <a href="http://secure.megazyme.com/Rhamnogalacturonan-I-Potato">http://secure.megazyme.com/Rhamnogalacturonan-I-Potato</a>	GalA (51), Rha (28.6), Gal (14), Ara (5.4) and Xyl (1)
C10	Soybean RG-I	Soy RG-I	RG-I	Megazyme, Bray, Ireland; Hahn lab data (Pattathil et al., 2010), <a href="http://secure.megazyme.com/Rhamnogalacturonan-Soy-Bean">http://secure.megazyme.com/Rhamnogalacturonan-Soy-Bean</a>	GalA (51), Xyl (13), Gal (11), Rha (10), Fuc (9) and Ara (6)
C11	<i>Arabidopsis thaliana</i> RG-I	At RG-I	RG-I	CCRC, UGA; (Zablackis et al., 1995); Hahn lab data (Pattathil et al., 2010)	GalA (34), Rha (27), Gal (17), Ara (14), Xyl (5), Fuc (1), GlcA (1) and GalA (1)
D01	Green Tomato Fruit RG-I	GrTomFrR	RG-I	CCRC, UGA; Hahn lab data (Pattathil et al., 2010)	GalA (49.5), Gal (43.8), Rha (4.7), GlcA (1), Ara (0.5) and traces of Xyl and Glc
D02	Lettuce RG-I	Let RG-I	RG-I	CCRC, UGA; Hahn lab data (Pattathil et al., 2010)	Gal (54.9), GalA (23.4), Rha (6.9), GlcA (5.7), Ara (4.9) and Xyl (4.2)
D03	<i>Arabidopsis Seed</i> Mucilage	At Seed Mu	Mucilages	CCRC, UGA; Hahn lab data (Pattathil et al., 2010)	Rha (69), GalA (27.7), Gal (1.8) and Xyl (1.5)
D04	Sinapis Seed Mucilage	Sin Seed Mu	Mucilages	CCRC, UGA; Hahn lab data (Pattathil et al., 2010)	GalA (57), Gal (19), Rha (12), GlcA (10) and traces of Man and Glc
D05	Peppergrass Seed Mucilage	Pep Gr S Mu	Mucilages	CCRC, UGA; (Deng et al., 2009); Hahn lab data (Pattathil et al., 2010)	GlcA (22.2), GalA (22.1), Gal (18.9), Xyl (9.8), Rha (8), Glc (7), Fuc (5.2), Ara (5) and Man (1.8)
D06	Citrus Pectin	Citrus Pectin	HG	Hercules, Wilmington, DE; Hahn lab data (Pattathil et al., 2010)	GalA (85), Rha (13) and Gal (2)
D07	73% Me Pectin	73% MePec	HG	Hercules, Wilmington, DE; Hahn lab data (Pattathil et al., 2010)	GalA (81), Gal (7), Rha (6.5), Ara (4.6) and Glc (0.9)
D08	55% Me Pectin	55% MePec	HG	Hercules, Wilmington, DE; Hahn lab data (Pattathil et al., 2010)	GalA (81), Gal (10), Rha (9)
D09	33% Me Pectin	33% Me Pec	HG	Hercules, Wilmington, DE; Hahn lab data (Pattathil et al., 2010)	GalA (89), Gal (7), Rha (4)
D10	Jatoba Xyloglucan of <i>Hymenaea courbaril</i>	Znone	Xyloglucans	CCRC, UGA; Hahn lab data (unpublished)	

D11	High-acetyl Sugarbeet $\beta$ -Pectin	HAcSB Pec	HG	Hercules, Wilmington, DE; Hahn lab data (Pattathil et al., 2010)	GalA (56.2), Rha (21.3), Gal (15) and Ara (7.5)
E01	Poplar Xylan	Pop Xyl	Xylans	National Renewable Energy Lab, Golden, CO; Hahn lab data (Pattathil et al., 2010)	Xyl (94), GalA (4) and Rha (2)
E02	Camelina Seed Mucilage	Cam Seed	Mucilages	CCRC, UGA; Hahn lab data (Pattathil et al., 2010)	Rha (57.1), GalA (24.4), Gal (13.3), Xyl (2.2), Ara (2.3) and Man (0.8)
E03	Potato Arabinogalactan	Pot Ara Gal	Arabinogalactans	Dr. Henk Schols, Laboratory of Food Chemistry, Wageningen, The Netherlands; personal communication	Gal (63), Ara (20) and UA (17)
E04	Arabinogalactan II	Ara Gal II	Arabinogalactans	Dr. Henk Schols, Laboratory of Food Chemistry, Wageningen, The Netherlands; personal communication	Gal (84) and Gal (16)
E05	RG-I from Okra	Okra RG-I	RG-I	Dr. Henk Schols, Laboratory of Food Chemistry, Wageningen, The Netherlands; personal communication	Gal (53), GalA (26), Rha (14), GlcA (4), Glc (2.5) Ara (1) and Man (1)
E06	Eucalyptus KOHs	Eucal KOH	Xylans	Dr. Henk Schols, Laboratory of Food Chemistry, Wageningen, The Netherlands; personal communication	Xyl (81), UA (13), Gal (3), Rha (2), Ara (1), Glc (1) and Man (1)
E07	Sugar Beet Linear Arabinan	SB Lin Ara	Arabinogalactans	Dr. Henk Schols, Laboratory of Food Chemistry, Wageningen, The Netherlands; personal communication	Ara (74), UA (14) and Gal (12)
E08	Sugar Beet Branched Arabinan	SB Branch	Arabinogalactans	Dr. Henk Schols, Laboratory of Food Chemistry, Wageningen, The Netherlands; personal communication	Ara (>80)
E09	Sorghum BE1	Sorg BE1	Xylans	Dr. Henk Schols, Laboratory of Food Chemistry, Wageningen, The Netherlands; personal communication	Ara (45.8), Xyl (40.9), UA (9.8), Gal (1.8), Glc (1.7) and Man (0.2)
E10	Corn BE1	Corn BE1	Xylans	Dr. Henk Schols, Laboratory of Food Chemistry, Wageningen, The Netherlands; personal communication	Ara (38.4), Xyl (48.3), UA (8.3), Gal (4.3), Glc (0.7) and Man (0.1)
E11	Linseed Mucilage	Lin Seed Mu	Mucilages	CCRC, UGA; Hahn lab data (Pattathil et al., 2010)	Rha (44.2), GalA (18.5), Xyl (15.8), Gal (11.1), Fuc (3), Ara (4.6) and Glc (2.9)

## Supplemental References

**Deng C, O'Neill MA, Hahn MG, York WS** (2009) Improved procedures for the selective chemical fragmentation of rhamnogalacturonans. *Carbohydr Res* **344**: 1852-1857

**Hahn MG, Darvill A, Albersheim P, Bergmann C, Cheong J-J, Koller A, Lò V-M** (1992) Preparation and characterization of oligosaccharide elicitors of phytoalexin accumulation. In S Gurr, M McPherson, DJ Bowles, eds, *Molecular Plant Pathology (Volume II): A Practical Approach*, Oxford University Press, Oxford, UK, pp 103-147

**Jia ZH, Qin Q, Darvill AG, York WS** (2003) Structure of the xyloglucan produced by suspension-cultured tomato cells. *Carbohydr Res* **338**: 1197-1208

**Pattathil S, Avci U, Baldwin D, Swennes AG, McGill JA, Popper Z, Bootten T, Albert A, Davis RH, Chennareddy C, Dong R, O'Shea B, Rossi R, Leoff C, Freshour G, Narra R, O'Neil M, York WS, Hahn MG** (2010) A Comprehensive Toolkit of Plant Cell Wall Glycan-Directed Monoclonal Antibodies. *Plant Physiology* **153**: 514-525

**Peña MJ, Darvill AG, Eberhard S, York WS, O'Neill MA** (2008) Moss and liverwort xyloglucans contain galacturonic acid and are structurally distinct from the xyloglucans synthesized by hornworts and vascular plants. *Glycobiology* **18**: 891-904

**Stevenson TT, McNeil M, Darvill AG, Albersheim P** (1986) Structure of plant cell walls XVIII. An analysis of the extracellular polysaccharides of suspension-cultured sycamore cells. *Plant Physiol* **80**: 1012-1019

**Stephen AM, Phillips GO, Williams PA** eds, (2006) *Food Polysaccharides and Their Applications*. CRC Press, Boca Raton, FL, pp 1-733

**York WS, Harvey LK, Guillen R, Albersheim P, Darvill AG** (1993) Structural analysis of tamarind seed xyloglucan oligosaccharides using  $\beta$ -galactosidase digestion and spectroscopic methods. *Carbohydr Res* **248**: 285-301

**Zabackis E, Huang J, Müller B, Darvill AG, Albersheim P** (1995) Characterization of the cell wall polysaccharides of *Arabidopsis thaliana* leaves. *Plant Physiol* **107**: 1129-1138

**CHAPTER 3**  
***IN VIVO* VISUALIZATION OF XYLAN IN WILD-TYPE AND MUTANT PLANTS**  
**USING CBM2B-1-2**

**Abstract**

Carbohydrate Binding Modules (CBMs) are carbohydrate-binding protein domains commonly found attached to glycosyl hydrolases produced by diverse bacteria and fungi, especially those that attack plant biomass. The binding specificities of a number of CBMs have been fully elucidated biochemically and, in some cases, using crystallographic data. Knowledge of the binding specificities of CBMs has led to their increased use as probes to localize specific glycan structures in plant cell walls. CBM2b-1-2 from *Cellulomonas fimi* xylanase 11A is a xylan-binding CBM that binds specifically to secondary plant cell walls in *Arabidopsis thaliana*. Heterologous expression of fluorescent protein (mCherry/GFP)-tagged CBM2b-1-2 has no noticeable deleterious effect on *Arabidopsis* morphology or development. The heterologously expressed fluorescent protein-tagged CBM2b-1-2 selectively labels cell walls that contain xylan, including those of xylem vessels and interfascicular fibers associated with phloem in wild-type plants. As a functional *in vivo* visualization tool, we were interested in testing whether fluorescent protein-tagged CBM2b-1-2 would allow us to observe effects that arise from mutations in genes that affect the synthesis and deposition of xylan *in vivo*. Toward this end, the stable CBM2b-1-2:mCherry expression line was crossed with a plant line carrying a mutation in a *WRKY* transcription factor gene that causes ectopic xylan deposition in pith cells of *Arabidopsis*. Examination of F2 plants resulting from this cross demonstrated that the ectopic deposition of xylan can be observed simply and conveniently via hand sectioning. These results

suggest that the fluorescent protein-tagged xylan-binding CBM2b-1-2 is a functional *in vivo* visualization tool to follow xylan dynamics during plant development.

## **Introduction**

Xylan is a polymer of  $\beta$ -(1,4)-linked xylose with various additional substitutions commonly found in monocot grasses and in dicot secondary cell walls. As a major hemicellulose in the dicot plant cell wall, particularly in vascular tissues, xylan provides structure and protection for plant cells and is essential for plant growth and development. Xylan is also as a major constituent of lignocellulosic biomass for biofuel production (Carroll and Somerville, 2009) and animal feed (Bedford and Partridge, 2010). Synthesis of xylan requires the coordinated action and regulation of a number of proteins including biosynthetic enzymes, transporters, and transcription factors (Rennie and Scheller, 2014). Until recently, the genes that encode these proteins have been identified using genetic and biochemical techniques. However, the biochemical activities of the majority of these proteins have been difficult to demonstrate (Hao and Mohnen, 2014) and several enzymes that have been shown to affect xylan synthesis have not yet been assigned biosynthetic roles (Rennie and Scheller, 2014), indicating that there is still much to be elucidated. At the same time, relating to the identification and annotation of genes involved in xylan biosynthesis, a better understanding of the occurrence of xylan during development demands novel tools that would facilitate the genetic, biochemical, and cellular analyses of xylan synthesis and function in the cell wall.

The traditional way to visualize cell wall polysaccharides is by immunolabeling of fixed, sectioned tissues. The activity and distribution of cell wall polysaccharides during the dynamics of plant development as cells grow, divide and differentiate cannot be observed in these “dead” tissues. Live cell imaging of plant cells was ushered in just over a decade ago (Haseloff et al.,

1997) and has become a powerful approach towards yielding new information about enzymes involved in cell wall biosynthesis (Paredes et al., 2006). *In vivo* imaging of polysaccharides is severely limited since, unlike protein or nucleic acid synthesis where sequences are directly encoded by or related to gene sequences, the biosynthesis of plant polysaccharides occurs indirectly from the combined action of specific enzymes that include not only those involved in the biosynthesis of the polymer, but also enzymes that function in polymer degradation and modification (Fry, 2010). The biosynthesis of plant polysaccharides also depends on the availability of the required precursor substrates and whether the availability of these precursors may confine the biosynthetic reaction in specific cells, cellular locations, compartments or tissues (Stone et al., 2010). More recently, localization of a plant polysaccharide has been achieved by incorporating fluorescent dye/fluorescence-tagged probes metabolically into living plant cells (Anderson et al., 2010; Tobimatsu et al., 2013). However, these methods suffer from several disadvantages such as dye effects on plant growth, difficulties in achieving dye uptake by plant cells, sample preparation times, and artifacts for probe incorporation.

Non-catalytic carbohydrate-binding modules (CBMs) from microbial cell wall polysaccharide hydrolases play critical roles in the recognition of plant cell wall polymers and potentiating the activity of these degradative enzymes (Gilbert et al., 2013). CBMs have been developed as probes for *in vitro* cell wall analysis and have advantages over antibodies in that the gene/protein sequences are readily obtained and at least some protein structural information is already known (Knox, 2008). These features of CBMs generate opportunities for creating fluorescent protein-tagged CBMs, which can be utilized as live imaging tools to study the complex temporal and developmental relationships among cell wall polysaccharides. Analysis of xylan-binding CBM2b-1-2 modules indicated that CBM2b-1-2 has a very shallow xylan

binding site, which allows this CBM to bind effectively to all dicot secondary cell walls (McCartney et al., 2006). In this study, we exploited the ability to generate fluorescent protein-tagged CBM2b-1-2 and evaluated the tagged CBM for its potential to allow *in vivo* imaging of xylan distribution patterns in the walls of Arabidopsis cells by fluorescent microscopy.

## **Materials and Methods**

### **Plant Material and Growth Conditions**

Both Arabidopsis wild type and transgenic plant lines generated were in the ecotype Columbia (Col-0) background. A homozygous plant line of *atwrky12-1* (At2g44745) was obtained from Dr. Richard A. Dixon (Noble Research Foundation, Ardmore, OK). Seeds of Arabidopsis were sterilized, cold treated at 4 °C for 48 h, and germinated on one-half-strength Murashige and Skoog medium (Sigma) in an environmental chamber under a 16-h-light/8-h-dark cycle at 19 °C during the light period and 15 °C during the dark period. The light intensity was 120  $\mu\text{mol m}^{-2} \text{s}^{-1}$ , and the relative humidity was maintained at 70%. One-week-old seedlings were transferred to soil and grown in growth chambers under the same conditions.

### **Gene Constructs and Plant Transformation**

The coding sequence of the *AtExpansin10* signal peptide (At1g26770) (Cho and Cosgrove, 2000) was amplified by AtSP-F and AtSP-R primers (containing KpnI and XbaI restriction enzyme sites) with Platinum Tag High Fidelity DNA Polymerase (Invitrogen 12574-030) (all the primers designed for gene constructs are listed in Supplemental Table S3.1). A proline-threonine (PT) linker coding sequence was amplified from a modified pET22b vector (obtained from Dr. Gilbert, Newcastle University, UK) using PT linker Forward Primer (containing the XmaI restriction enzyme site) and PT linker Reverse Primer (containing the AgeI

restriction enzyme site). The *mCherry* gene was amplified from the pmCherry vector (Clontech PT3973-5) using mCherry Forward Primer (containing the AgeI restriction enzyme site) and mCherry Reverse Primer (containing the AgeI restriction enzyme site). The *CBM2b-1-2* gene was amplified from a *Cellulomonas fimi* strain harboring the *CBM2b-1-2* gene (obtained from Dr. Gilbert, Newcastle University, UK) using CBM2b-1-2 Forward primer (containing the XmaI restriction enzyme site) and CBM2b-1-2 Reverse primer (containing the XhoI restriction enzyme site). PCR products were cleaved by the appropriate restriction enzymes (Thermo) and ligated into the pBI121 vector (Clontech). All constructs were confirmed by sequencing (Macrogen, USA) and individually transformed into *Agrobacterium tumefaciens* GV3101 competent cells by electroporation. Transformation of Arabidopsis was conducted by floral dipping (Clough and Bent, 1998).

### **Screening of Homozygous Plants with T-DNA Insertion**

To identify homozygous plants with T-DNA insertions in the *WRKY12* gene among the F1 generation of crosses, genomic DNA was extracted by GeneJET Genomic DNA Purification Kit (Thermo). T-DNA insertions were identified using the flanking primers (LP and RP) generated by the T-DNA verification primer design website (<http://signal.salk.edu/tdnaprimers.html>) and primers are listed in Supplemental Table S3.2.

### **RNA Isolation and Reverse Transcript (RT)-PCR Analysis**

Plant stems to be used for RNA isolation were frozen immediately in liquid nitrogen and stored at  $-80^{\circ}\text{C}$  until use. RNA was isolated using RNeasy plant mini kit (Qiagen) and treated with RNase-free DNase (Qiagen) to remove contaminating genomic DNA. Total RNA (500 ng) was reverse-transcribed using Superscript<sup>®</sup> III Reverse Transcriptase (Invitrogen). RT-PCR was performed in 20  $\mu\text{l}$  of reaction mixture, composed of 2  $\mu\text{l}$  of a given cDNA, 0.4  $\mu\text{l}$  dNTP

(10mM), 0.2  $\mu$ l DreamTaq DNA Polymerase (5 U/ $\mu$ l) (Thermo), 2  $\mu$ l 10X DreamTaq DNA Polymerase Buffer, and 14.6  $\mu$ l Nuclease-free water. Amplifications were performed using a Tetrad 2 DNA Engine PCR machine (Bio-Rad) under the following conditions: initial polymerase activation: 95  $^{\circ}$ C, 3 min; then 35 cycles of 30 s at 95 $^{\circ}$ C and 30 s at 55 $^{\circ}$ C. *Actin2* (At3g18780) was used as reference gene. Gene-specific primers are listed in Supplemental Table S3.3.

### **Fluorescent Microscopy**

Live plants expressing CBM2b-1-2:mCherry fusion proteins (hand-sectioned 5-week-old and 9-week-old stems, 3-day-old roots) were examined by fluorescence microscopy on an Eclipse 80i microscope (Nikon) equipped with epifluorescence optics. Images were captured with a Nikon DS-Ri1 camera head using NIS-Element Basic Research software, and images were assembled using Adobe Photoshop (Adobe Systems).

### **Tissue Fixation**

Five-week-old and 9-week-old *Arabidopsis* inflorescence stem pieces were fixed for 2.5 h in 1.6% (w/v) paraformaldehyde and 0.2% (w/v) glutaraldehyde in 25 mM sodium phosphate buffer, pH 7.1. Tissue was washed with buffer twice for 15 min, and dehydrated through a graded ethanol series [35%, 50%, 75%, 95% (v/v), 100%, 100%, and 100% ethanol] for 30 min for each step. The dehydrated tissue was moved to 4  $^{\circ}$ C and then gradually infiltrated with cold LR White embedding resin (Ted Pella) using 33% (v/v) and 66% (v/v) resin in 100% ethanol for 24 h each, followed by 100% resin for 24 h three times. The infiltrated tissue was transferred to gelatin capsules containing 100% resin for embedding, and resin was polymerized by exposing the capsules to 365-nm UV light at 4  $^{\circ}$ C for 48 h.

## **Direct *in vitro* Fluorescence Labeling of Tissue Sections by Fluorescent Protein Tagged CBMs and Immunolabeling**

Semi-thin sections (250 nm) were cut with a Leica EM UC6 ultramicrotome (Leica Microsystems) and mounted on glass slides (Colorfrost/plus; Fisher Scientific). Labeling was performed at room temperature as follows. Sections were blocked with 3% (w/v) nonfat dry milk in KPBS (0.01 M potassium phosphate, pH 7.1, containing 0.5 M NaCl) for 20 min and were washed with KPBS for 5 min. 15  $\mu$ l (1-2 mg/ml) of fluorescent protein-tagged CBM proteins were applied and incubated for 1 h. For immunolabeling, undiluted hybridoma supernatant of the mAb under study was applied and incubated for 1 h, sections were washed with KPBS three times for 5 min each, and goat anti-mouse IgG or goat anti-rat IgG conjugated to Alexa-fluor488 (Invitrogen) diluted 1:100 in KPBS was applied and incubated for 1 h. All sections (CBM and antibody) were washed with KPBS three times for 5 min and distilled water for 5 min. Prior to applying a coverslip, Citifluor antifade mounting medium AF1 (Electron Microscopy Sciences) was applied.

## **Results**

### **Heterologous Expression of Microbial CBM2b-1-2:mCherry in Arabidopsis**

The experimental design for the heterologous expression of fluorescent protein-tagged CBMs in Arabidopsis is outlined in Figure 3.1. In the pBI121 vector (Clontech), a fluorescent protein-tagged form of the xylan-binding CBM2b-1-2 was generated by fusing the gene encoding the red fluorescent protein, mCherry (Shaner et al., 2005), in frame to the 3'-terminal of the *CBM2b-1-2* gene isolated from *Cellulomonas fimi* (McCartney et al., 2006) via a proline-threonine (PT) linker. The full-length *CBM2b-1-2:mCherry* gene was fused in frame with the *AtExpansin10* signal peptide (SP) coding sequence (Cho and Cosgrove, 2000) at the 5'-end in

order to target the translated fusion protein to the cell wall through the secretory pathway in Arabidopsis. The empty vector containing the *AtExpansin10* signal peptide coding sequence directly fused with *mCherry* via the same PT linker was produced as a negative control to verify that expression of the mCherry protein itself does not bind to or affect the plant cell wall. After transformation, kanamycin antibiotic-resistant transgenic plants were selected and the expression of introduced genes was confirmed by Reverse Transcript (RT)-PCR analysis using total RNA harvested from stems. Fluorescent localization of CBM2b-1-2:mCherry/SP:mCherry was carefully examined in these transgenic plants in the T1 generation. For each construct, three independent lines were isolated and selfed. T2 generations of these transgenic plants were screened for kanamycin resistance and examined by RT-PCR and fluorescence microscopy. Among the T2 plants, the introduced *CBM2b-1-2:mCherry/SP:mCherry* genes were stably inherited and CBM2b-1-2:mCherry/SP:mCherry proteins were expressed in an active (fluorescent) form. In our imaging analysis, transgenic plants were grown from seeds of one line of each transgenic plant expressing CBM2b-1-2:mCherry/SP:mCherry.

Xylan is abundant in the secondary cell walls of specific cell types such as xylem vessels and interfascicular fibers (McCartney et al., 2006). The plant cell starts producing the secondary cell wall after the primary cell wall is complete and the cell has stopped expanding (Carpita, 2000). Thus, the secondary cell wall is located between the primary cell wall and the plasma membrane. In relation to plant development, xylan synthesis and deposition increases with increasing stem maturity. To observe the *in vivo* xylan deposition during plant development, transgenic CBM2b-1-2:mCherry plants were examined by hand-sectioning the basal, middle, and top parts of 5-week-old and 9-week-old stems in comparison with WT and SP:mCherry controls. In addition, direct labeling and immunolabeling studies were carried out on the basal parts of the

same stems used for *in vivo* observation to obtain independent *in vitro* verification of xylan distribution patterns to compare with results from *in vivo* observation of CBM2b-1-2:mCherry localization. These *in vitro* studies were done using CBM2b-1-2:mCherry protein expressed in *Escherichia coli* and xylan-directed mAbs (CCRC-M138, CCRC-M147, CCRC-M149, CCRC-M153 and LM11) on these fixed stem sections.

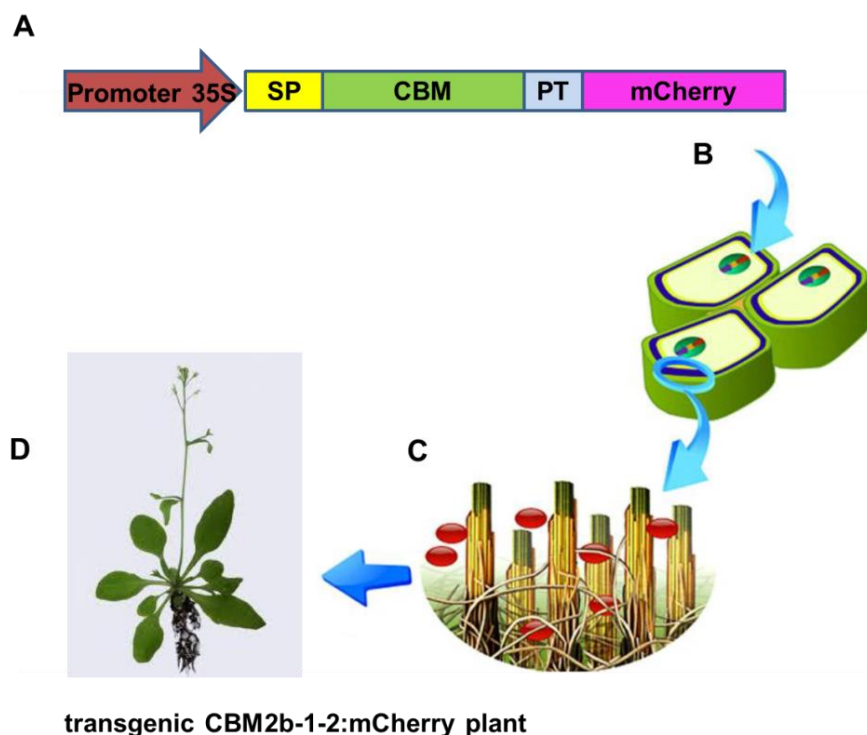


**Figure 3.1. Outline of heterologous expression of CBM2b-1-2:mCherry in transgenic plants.**

[Figure is modified from Figure 1 of (Abramson et al., 2010)]

- (A) Gene constructs consisting of a constitutive promoter (Cauliflower Mosaic Virus 35S promoter (red)), a cell wall targeting signal peptide (yellow), *CBM2b-1-2* gene (green), proline and threonine (PT) linker (blue) and mCherry fluorescent protein (cherry-pink).
- (B) Transformation of *CBM2b-1-2:mCherry* gene into the plant genome.

- (C) CBM2b-1-2:mCherry protein is then expressed and secreted into the cell wall: (green strands - crystalline cellulose; yellow strands - amorphous cellulose; brown strands - hemicellulose).
- (D) Transgenic CBM2b-1-2:mCherry plant is generated and expression of CBM2b-1-2:mCherry protein is examined.

### **Expression of SP:mCherry in Arabidopsis**

In this study, mCherry was chosen to avoid issues arising from autofluorescence of lignin in secondary cell walls, which occurs in the green part of the spectrum where GFP fluorescence is observed. This autofluorescence is not typically observed in fixed and embedded material (Utku Avcı, personal communication), but was observed in fresh hand-cut sections (Supplemental Figure S3.1). Observation of WT stem (Figure 3.2A-B) revealed that autofluorescence under microscopy conditions used for mCherry observation was almost absent in secondary cell walls of xylem vessels and interfascicular fibers in both 5-week-old and 9-week-old stages. This result confirmed the advantage of red fluorescent mCherry for *in vivo* plant cell wall visualization by circumventing possible interference from autofluorescence of secondary cell walls.

In 5-week-old basal stems of transgenic SP:mCherry plants, strong mCherry fluorescent signal was detected in epidermis, cortex, xylem vessels and interfascicular fibers and weak fluorescent signal was detected in pith cells (Figure 3.3A). Higher magnification of fiber cells from the middle section of SP:mCherry stems revealed that the SP:mCherry protein was localized in the intercellular spaces (Supplemental Figure S3.2). In particular, the empty triangle-shaped region at tri-cellular junctions of fiber cells was occupied by SP:mCherry

proteins. In 9-week-old basal stems, strong fluorescence of SP:mCherry was detected throughout the entire stem without a clear cell wall pattern (Figure 3.3B), indicating that the SP:mCherry fusion protein accumulates in the vacuoles and cytosol in addition to the apoplastic space (including the cell walls). It is possible that with only the signal peptide, the mCherry protein cannot be secreted to the plant cell wall and the mCherry protein accumulates either in the intercellular spaces or in the vacuoles. The observed distribution pattern of SP:mCherry is consistent with previous observations of the expression of a tobacco extensin signal peptide:EGFP fusion (Est évez et al., 2006). In that study, the signal peptide:EGFP was also found mostly soluble in the cytosol (Est évez et al., 2006).

### **Heterologous Expression of CBM2b-1-2:mCherry Permits the Visualization of Xylan *in vivo***

In contrast to SP:mCherry, transgenically expressed CBM2b-1-2:mCherry yielded fluorescent signal *in vivo* only in the cell walls of xylan-containing tissues such as xylem vessels and interfascicular fibers, and not in tissues known to be xylan-deficient such as pith and cortex (Figure 3.4 A,B). These results support the hypothesis that heterologously expressed CBM2b-1-2:mCherry protein binds only to cell walls where xylan occurs. At the 5-week-old stage, the fluorescent signal of CBM2b-1-2:mCherry was detected in basal stem and middle stem, but not in top stem sections (Figure 3.4 A), indicating that xylan was not being formed in CBM2b-1-2:mCherry stem tissues at this developmental stage. At the 9-week-old stage, the mCherry fluorescent signal was observed in all parts of the stem of transgenic CBM2b-1-2 plants examined, but only in those cell types that make xylan. *In vitro* direct labeling of fixed 5-week-old and 9-week-old basal stems of transgenic CBM2b-1-2:mCherry plants using CBM2b-1-2:mCherry protein expressed in *E. coli* (Figure 3.4C) and immunolabeling using xylan-directed

antibodies (Figure 3.4D) independently verified the presence of xylan in the cell walls of cells labeled by *in vivo* expression of CBM2b-1-2:mCherry fluorescent protein.

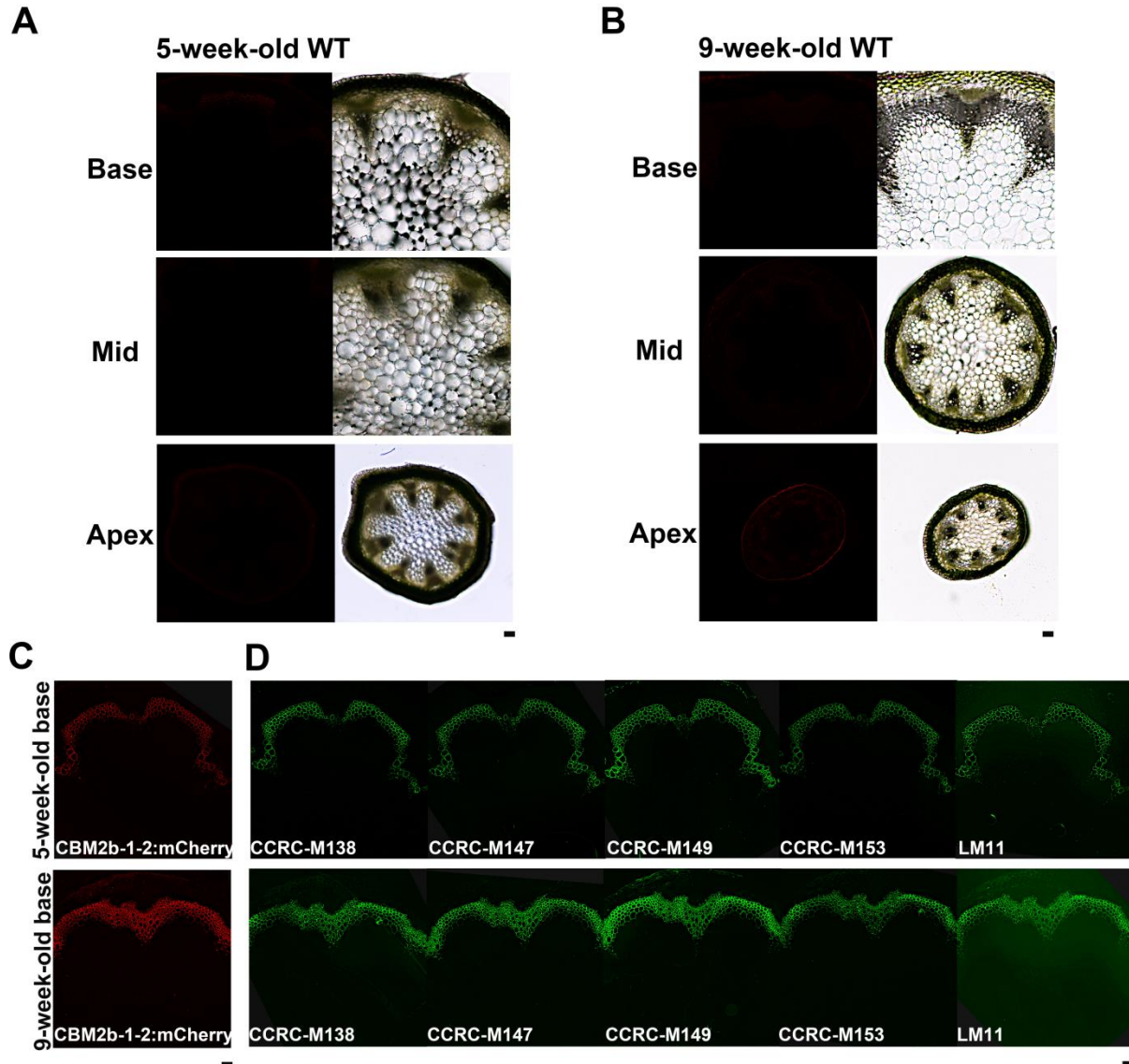


**Figure 3.2. Observation of WT plants *in vivo* and *in vitro*.** Hand-sectioned basal, middle and top parts of stems of (A) 5-week-old WT and (B) 9-week-old WT plants were visualized under identical imaging conditions (left panels, excitation = 528-553 nm, emission = 590-650 nm) and white light (right panels). (C) Direct labeling in fixed stem sections using CBM2b-1-2:mCherry

protein expressed in and purified from *E. coli* and (D) immunolabelling using xylan-directed mAbs (CCRC-M138, CCRC-M147, CCRC-M149, CCRC-M153 and LM11) on 5-week-old and 9-week-old basal stems of WT plants. Scale bar = 50  $\mu$ m.

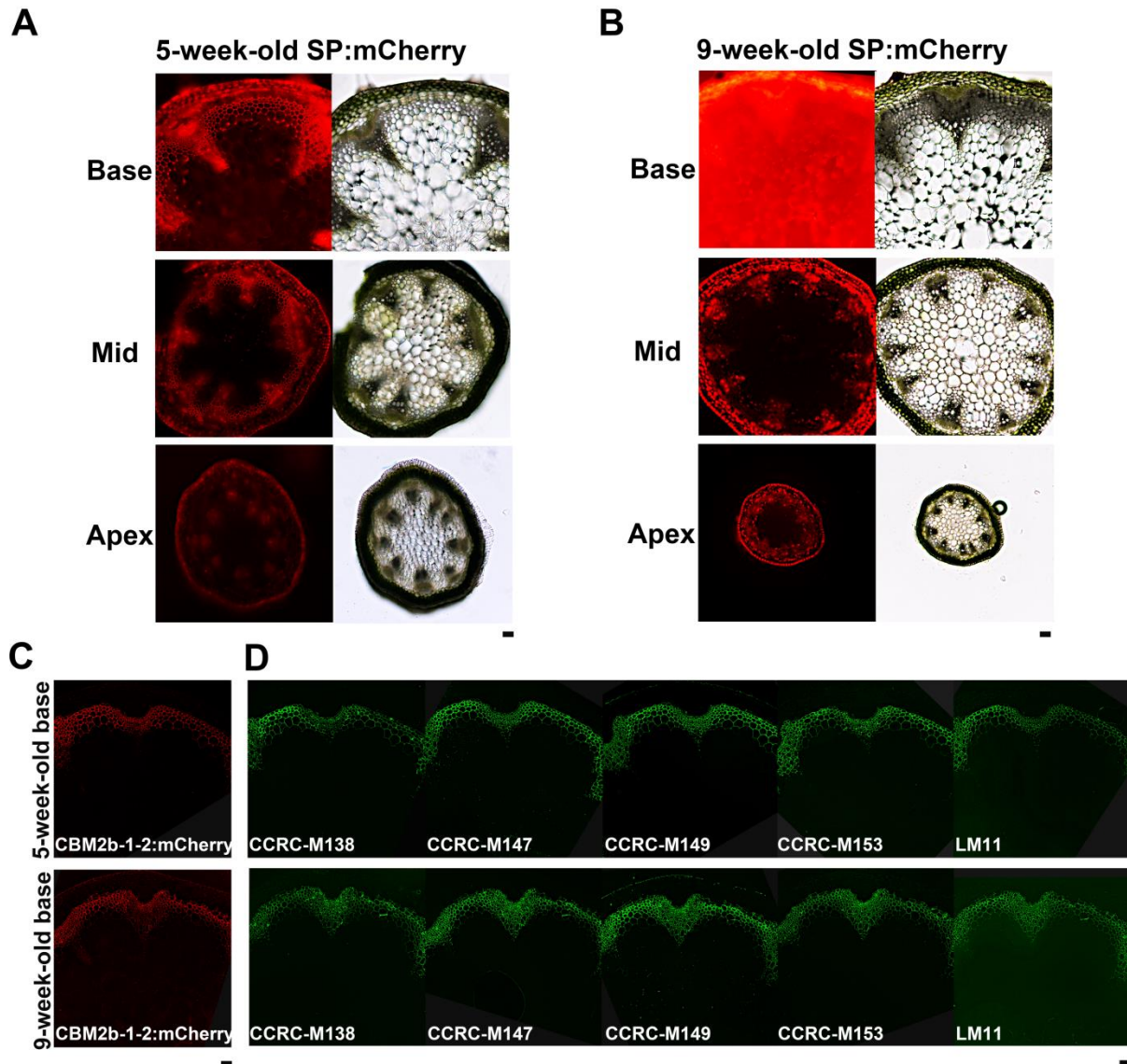


**Figure 3.3.** Observation of transgenic SP:mCherry plants *in vivo* and *in vitro*. Hand-sectioned basal, middle and top parts of stems of (A) 5-week-old and (B) 9-week-old SP:mCherry plants were visualized under identical imaging conditions (left panels, excitation =

528-553 nm, emission = 590-650 nm) and white light (right panels). (C) Direct labeling in fixed stem sections using CBM2b-1-2:mCherry protein expressed in and purified from *E. coli* and (D) immunolabelling using xylan-directed mAbs (CCRC-M138, CCRC-M147, CCRC-M149, CCRC-M153 and LM11) on 5-week-old and 9-week-old basal stems of transgenic SP:mCherry plants. Scale bar = 50  $\mu$ m.

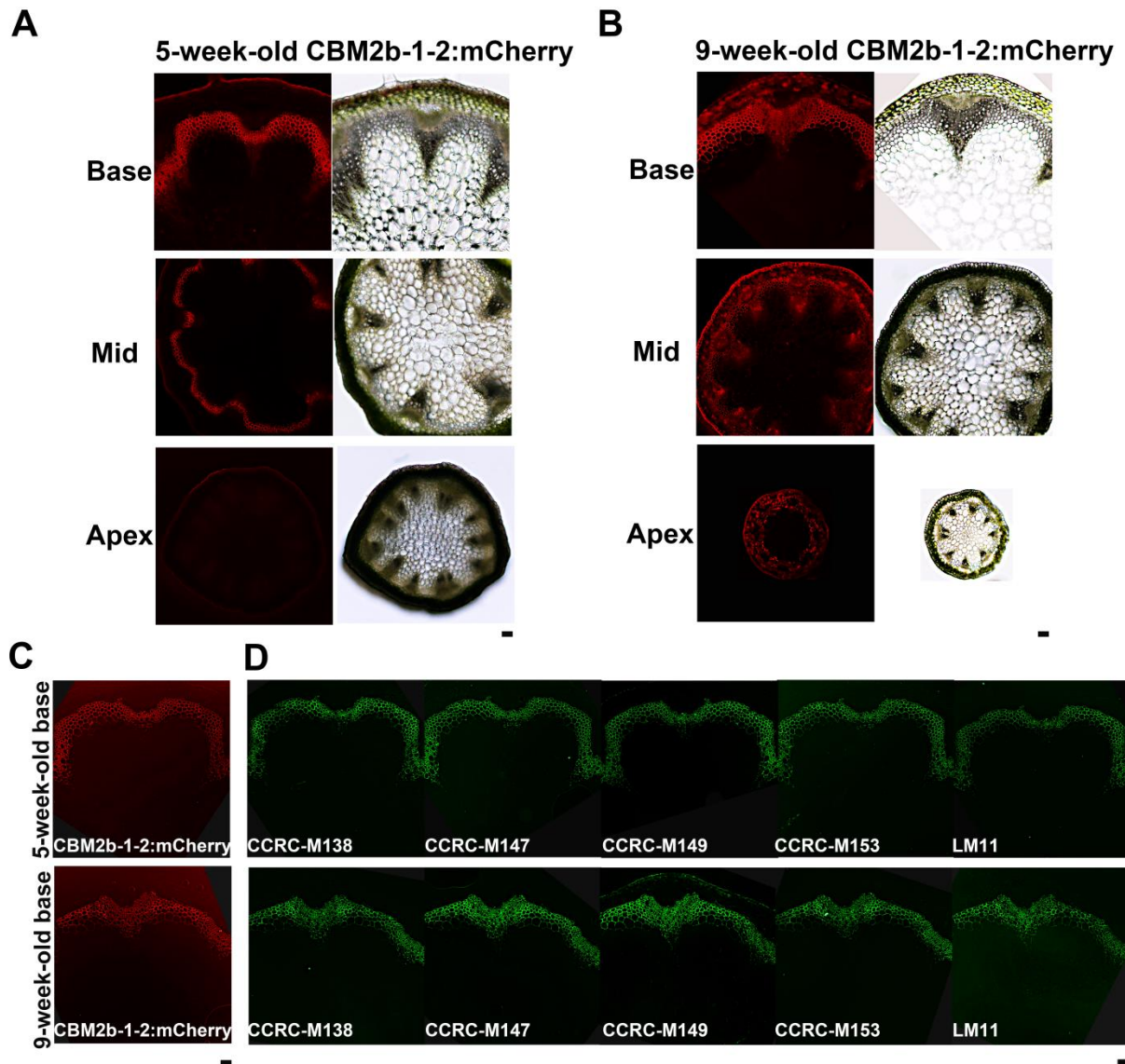


**Figure 3.4. Observation of transgenic CBM2b-1-2:mCherry plants *in vivo* and *in vitro*.** Hand-sectioned basal, middle and top parts of stems of (A) 5-week-old and (B) 9-week-old CBM2b-1-2:mCherry plants were visualized under identical imaging conditions (left panels, excitation = 528-553 nm, emission = 590-650 nm) and white light (right panels). (C) Direct labeling in fixed stem sections using CBM2b-1-2:mCherry protein expressed in and purified from *E. coli* and (D) immunolabelling using xylan-directed mAbs (CCRC-M138, CCRC-M147, CCRC-M149, CCRC-M153 and LM11) on 5-week-old and 9-week-old basal stems of transgenic CBM2b-1-2:mCherry plants. Scale bar = 50  $\mu\text{m}$ .

### ***In vivo* Localization of CBM2b-1-2:mCherry Reveals Altered Patterns of Xylan Deposition in the *wrky* Cell Wall Mutant**

We tested the effectiveness of the CBM2b-1-2:mCherry protein as a functional *in vivo* visualization tool by examining what happens to the fluorescence labeling pattern when the distribution of xylan is altered by mutagenesis. Toward this end, we chose to work with the *wrky12* mutant in *Arabidopsis* (Wang et al., 2010). Pith cells of *Arabidopsis* normally do not undergo secondary wall thickening, nor do they deposit xylans in their walls. However, a mutant plant line carrying a transfer (T)-DNA insertion in the *AtWRKY12* transcription factor gene exhibits secondary thickening in pith cell walls together with ectopic xylan deposition (Wang et al., 2010). Mutations in the *AtWRKY12* gene have little impact on overall plant growth and development (Wang et al., 2010). Thus, we crossed the stable transgenic CBM2b-1-2:mCherry plant with the *wrky12-1* plant and observed the labeling pattern in progeny carrying a homozygous T-DNA insertion at the *AtWRKY12* locus. The outline of this experiment was: F1 progeny of the cross were selfed to generate homozygous plants for the *wrky12* mutation. The

genotype of the F2 generation was examined, and PCR was used to identify lines that harbored T-DNA insertions in both *WRKY* alleles (Figure 3.5A). Homozygous *wrky12-1* plants showed the reduced transcript abundance of *AtWRKY12* (Figure 3.5B). Development of CBM2b-1-2:mCherry X *wrky12-1*, CBM2b-1-2:mCherry, *wrky12-1*, and SP:mCherry plants grown side by side with wild type plants was observed, and no visible differences were detected at the whole plant level (Figure 3.5C-D).

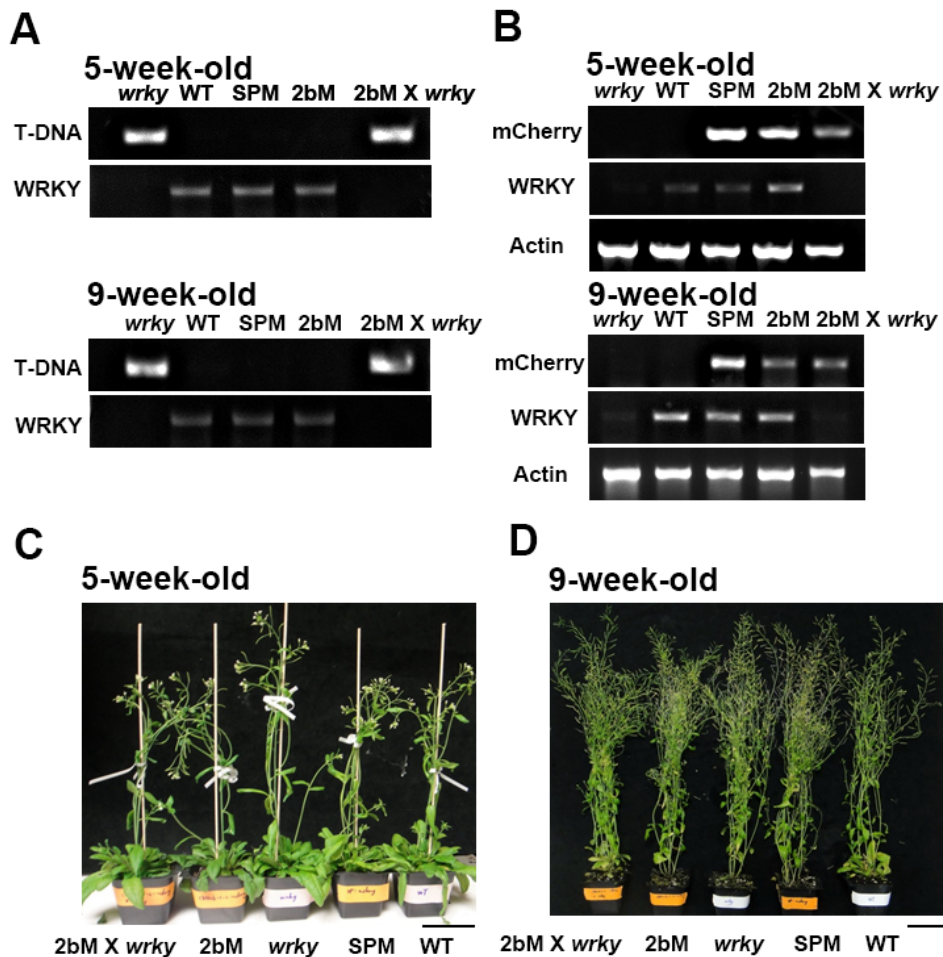


**Figure 3.5. Identification and phenotypic characterization of CBM2b-1-2:mCherry X *wrky12-1*, CBM2b-1-2:mCherry and SP:mCherry plants.** (A) PCR identification of homozygotes of the T-DNA insertion lines: WT, SP:mCherry and CBM2b-1-2:mCherry only

have a *wrky* gene-specific band, whereas the insertion lines *wrky12-1* and CBM2b-1-2:mCherry X *wrky12-1* have only a T-DNA-specific band. (B) RT-PCR analyses. *mCherry* and *WRKY* expression was examined using primers covering the full length of the cDNAs. *ACTIN* expression was used as the control. (C-D) From left to right: growth of CBM2b-1-2:mCherry X *wrky12-1*, CBM2b-1-2:mCherry, *wrky12-1*, SP:mCherry and WT plants at 5-weeks (C) and 9-weeks (D). Note that expression of CBM2b-1-2:mCherry and SP:mCherry have no visible impact on overall plant growth and development. Scale bar = 5cm.

At the 5-week-old developmental stage, the *in vivo* localization pattern of CBM2b-1-2:mCherry protein in the CBM2b-1-2 X *wrky12-1* plant was similar to that observed in the CBM2b-1-2:mCherry plant. The CBM2b-1-2:mCherry protein was localized in the xylem vessels and interfascicular fibers of basal and middle stems, but not in the top stems (Figure 3.6A). At the 9-week-old developmental stage, fluorescent signal from CBM2b-1-2:mCherry was detected in some pith cell walls and the intensity appeared to be indistinguishable from the signal detected in the secondary cell walls of adjacent xylem cells in basal stem (Figure 3.4A). This result suggested that these pith cells in CBM2b-1-2:mCherry X *wrky12-1* contained ectopic deposition of xylan in the 9-week-old basal stem. In contrast, the pattern of CBM2b-1-2:mCherry fluorescence at the middle and top of CBM2b-1-2:mCherry X *wrky12* stems (Figure 3.6B) was essentially identical to that observed at the middle and top of CBM2b-1-2:mCherry stems (Figure 3.4B).

*In vitro* direct labeling with exogenous CBM2b-1-2:mCherry and immunolabeling studies with xylan-directed mAbs confirmed there was no ectopic xylan in pith cells in basal stems of CBM2b-1-2:mCherry X *wrky12-1* and *wrky12-1* at the 5-week-old stage (Figure 3.6C-

D; Figure 3.7C-D). These results demonstrate that pith cells in the *wrky* background did not initiate secondary wall thickening at the 5-week-old stage. At the 9-week-old stage, xylan-binding CBM2b-1-2:mCherry protein and xylan-directed mAbs labeled walls of xylem vessels, interfascicular fibers and some pith cells in basal stems of both CBM2b-1-2:mCherry X *wrky12* and *wrky12*, displaying the same xylan distribution pattern as *in vivo* localization of CBM2b-1-2:mCherry fluorescent protein. Taken together, the *in vivo* and *in vitro* localization data indicate that in the *wrky* mutant, xylan is first deposited into the xylem vessels and interfascicular fibers, and is then ectopically deposited into pith cells with increasing stem maturity.

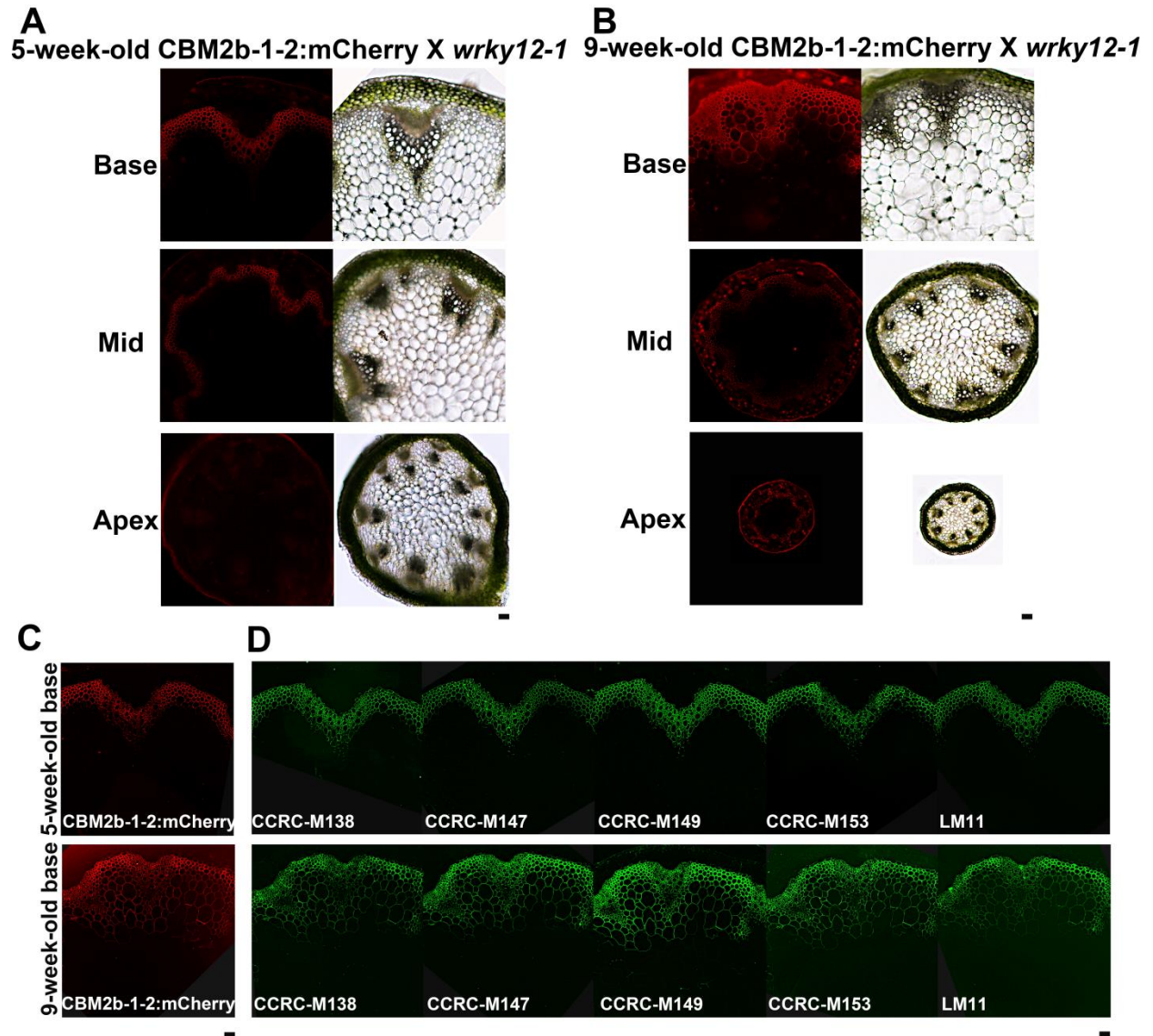


**Figure 3.6. Observation of CBM2b-1-2:mCherry X *wrky12-1* plants *in vivo* and *in vitro*.** Hand-sectioned basal, middle and top part stems of (A) 5-week-old and (B) 9-week-old plants were visualized by CBM2b-1-2:mCherry X *wrky12-1* under identical imaging conditions (left panels, excitation = 528-553 nm, emission = 590-650 nm) and white light (right panels). (C) Direct labeling using CBM2b-1-2:mCherry protein expressed in and purified from *E. coli* and (D) immunolabelling using xylan-directed mAbs (CCRC-M138, CCRC-M147, CCRC-M149, CCRC-

M153 and LM11) on 5-week-old and 9-week-old basal stems of CBM2b-1-2:mCherry X *wrky12-1* plants. Scale bar = 50  $\mu$ m.

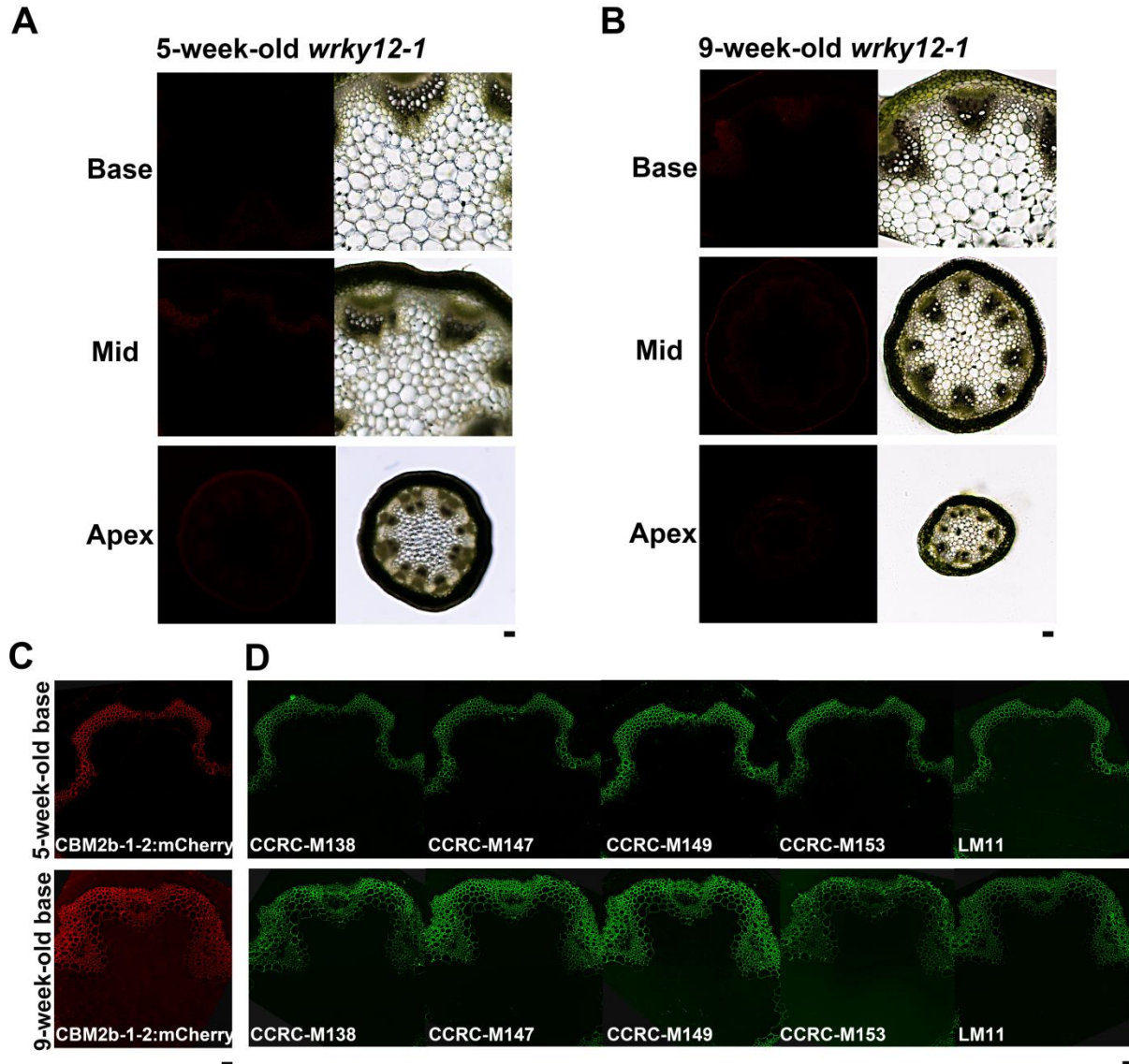


**Figure 3.7. Observation of *wrky12-1* plants *in vivo* and *in vitro*.** Hand-sectioned basal, middle and top part stems of (A) 5-week-old and (B) 9-week-old *wrky12-1* plants were visualized under identical imaging conditions (left panels, excitation = 528-553 nm, emission = 590-650 nm) and white light (right panels). (C) Direct labeling using CBM2b-1-2:mCherry protein expressed in

and purified from *E. coli* and (D) immunolabelling using xylan-directed mAbs (CCRC-M138, CCRC-M147, CCRC-M149, CCRC-M153 and LM11) on 5-week-old and 9-week-old basal stems of CBM2b-1-2:mCherry X *wrky12-1* plants. Scale bar = 50  $\mu$ m.

### ***In vivo* Localization of CBM2b-1-2:mCherry Reveals the Architecture of Xylan Deposition in Roots**

We also examined the maturation zone of roots of 3-day-old CBM2b-1-2:mCherry X *wrky*, CBM2b-1-2:mCherry, *wrky*, SP:mCherry and WT seedlings by fluorescent microscopy to test if the transgenically expressed CBM2b-1-2:mCherry would label xylan-containing walls in this organ. The intact (unsectioned) roots of SP:mCherry seedlings exhibited robust mCherry fluorescence throughout the root tissues, clearly showing SP:mCherry accumulation in all cells of the root. In contrast, no fluorescence was observed in intact WT and *wrky* seedlings (Figure 3.8). There was not much difference in the distribution patterns of CBM2b-1-2:mCherry between the intact CBM2b-1-2:mCherry root and the intact CBM2b-1-2:mCherry X *wrky12-1* root. In both CBM2b-1-2:mCherry X *wrky12-1* and CBM2b-1-2:mCherry roots, mCherry fluorescence was primarily observed in the cell walls of the central cylinder of the root, suggesting that xylan is already deposited into the cell walls of particular cells at the 3-day-old stage. The specific cell types whose cell walls are labeled by CBM2b-1-2:mCherry could not be delimited under the microscopic conditions used.

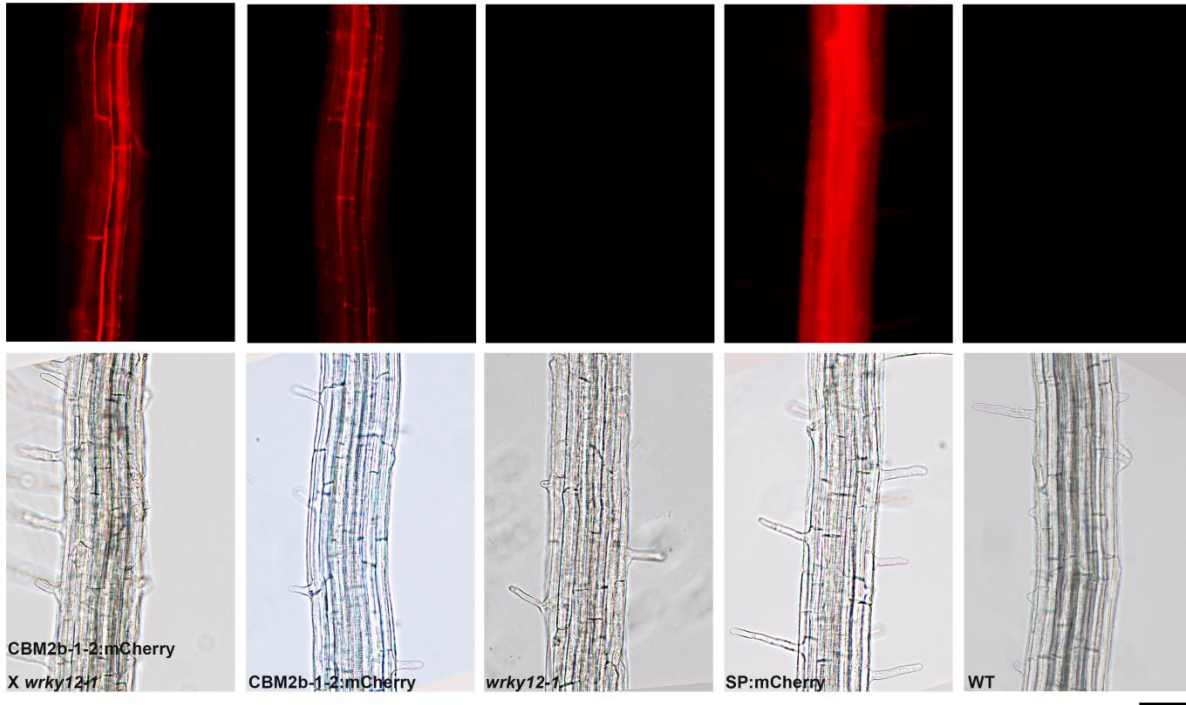


**Figure 3.8.** *In vivo* localization of CBM2b-1-2:mCherry/SP:mCherry proteins in maturation zone of intact 3-day-old CBM2b-1-2:mCherry x *wrky12-1*, CBM2b-1-2:mCherry, *wrky12-1*, SP:mCherry and WT plants. Intact roots were directly imaged under identical exposure conditions (upper panels, excitation = 528-553 nm, emission = 590-650 nm) and white light (lower panels). Scale bar = 50  $\mu$ m.

## Discussion

The complexity of the plant cell wall necessitates the development of *in vivo* tools in order to gain a deeper understanding of cell wall structure, function, and biology. Here, we have developed a transgenic Arabidopsis line that expresses fluorescent protein-tagged CBM2b-1-2 and have shown that this plant line can be used for *in vivo* imaging studies aimed at understanding xylan dynamics during plant development. Expression of CBM2b-1-2:mCherry in Arabidopsis does not appear to affect either plant morphology or development. More

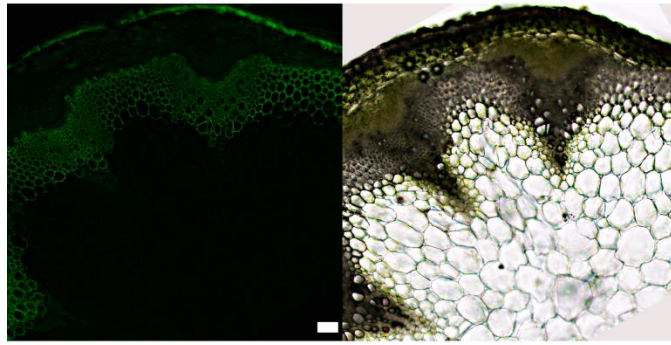
importantly, expression of CBM2b-1-2:mCherry and targeting this probe to the secretory pathway in Arabidopsis using the AtExpansin10 signal peptide leads to the selective labeling of xylans *in vivo* in both stems and roots. Incorporation of the CBM2b-1-2:mCherry specifically occurs in the secondary cell walls of stems and binds tightly to xylem vessels and interfascicular fibers where xylans are being produced and deposited. The resultant fluorescent protein-labeled xylan can be directly visualized by fluorescent microscopy. No labeling of cells that produce only primary cell walls, such as pith cells, was observed. Labeling of fixed embedded sections of Arabidopsis stems with diverse xylan-directed mAbs showed that the same cell walls were labeled *in vitro* as had been tagged *in vivo* with transgenically expressed CBM2b-1-2:mCherry. Thus, our results provide a proof of concept of the utility of transgenically expressed CBM2b-1-2:mCherry for *in vivo* imaging studies of xylans in plant cell walls without apparently disturbing plant physiology. Indeed, examination of the transgenic CBM2b-1-2:mCherry line using hand-cut sections documented the staged appearance of xylan in relation to plant development, showing that xylan deposition increases with increasing stem maturity without the need for extensive tissue preparation and manipulation. In fact, in root tissue it was possible to observe labeling of xylan in the intact organ, although confocal microscopy will be needed to provide cellular resolution of the xylan deposition patterns.

The utility of the transgenic CBM2b-1-2:mCherry for monitoring xylan deposition and dynamics was further illustrated by crossing this xylan tag into the *wrky* mutant of Arabidopsis. Mutation of the *WRKY12* gene had previously been shown to result in ectopic secondary wall formation and the ectopic deposition of xylan in pith cells, which normally do not express either character (Wang et al., 2010). The CBM2b-1-2:mCherry X *wrky* plant exhibited ectopic xylan labeling *in vivo* in pith cells adjacent to xylem vessels in basal stems, a pattern that was

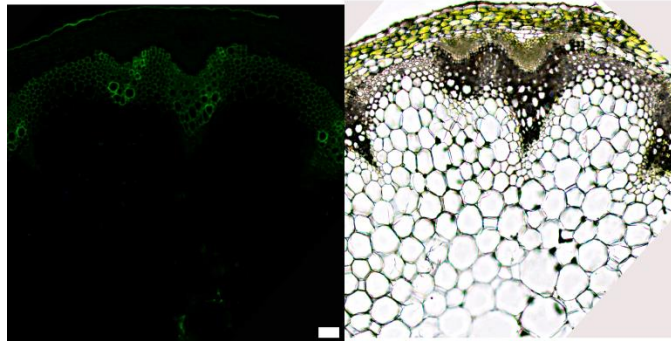
confirmed *in vitro* using xylan-directed mAbs to label sections taken from fixed embedded stems of these plants. This observation demonstrates that fluorescently tagged-CBMs allow one to monitor the effects of mutations on cell wall polysaccharide deposition *in vivo*. Indeed, our results document that the ectopic deposition of xylan in pith cell walls occurs after xylan deposition in the developing primary and secondary xylem, an observation that had not been made in the earlier study of the *wrky* mutant (Wang et al., 2010).

We are still at the stage of tool development in terms of documenting cell wall structure in relation to plant development, and to integrate this knowledge with an understanding of polysaccharide functions. Currently, immunohistochemical techniques carried out *in vitro* on fixed tissues are the main method to discern cell wall structures and to locate polysaccharides in plant cells, tissues and organs. However, substantial effort is required to demonstrate that *in vitro* measurements of polysaccharides precisely reflect the *in vivo* biochemical and structural complexity of polysaccharides. The methods and results described here create new opportunities to assay the effects of genetic, developmental, and environmental variation on xylan biosynthesis. To our knowledge, no other tool that can detect xylan *in vivo* is available now. Thus, heterologously expressed CBM2b-1-2:mCherry provides the plant research community the first *in vivo* xylan tracking tool. In the future, the use of this and similar tools is likely to expand our understanding of xylan synthesis and deposition, and bolster efforts to engineer xylan with improved properties for applications such as biofuel production.

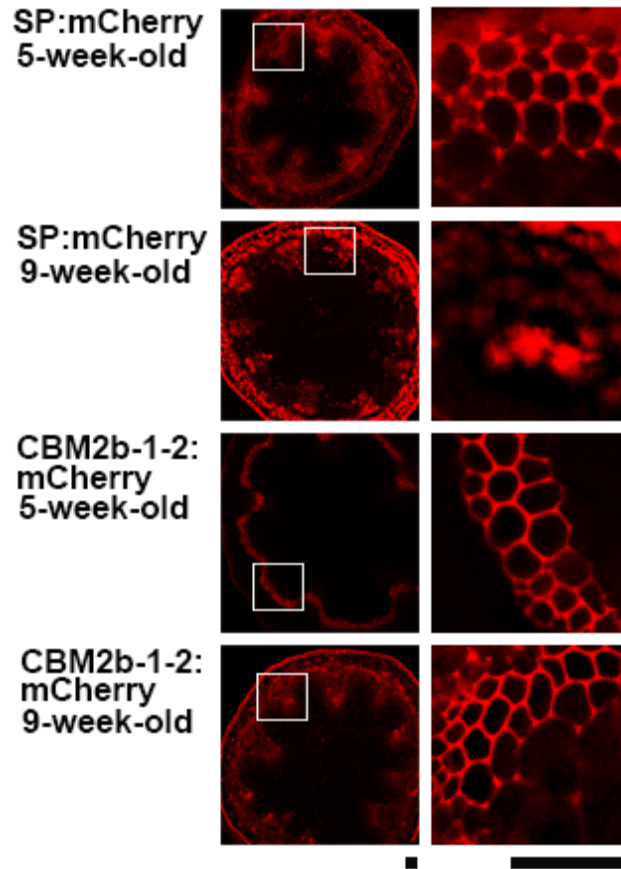
**CBM2b-1-2:GFP 9-week-old basal stem**



**WT 9-week-old basal stem**



**Supplemental Figure S3.1. Observation of transgenic CBM2b-1-2:GFP and WT plants *in vivo*.** Hand-sectioned basal part stems of 9-week-old transgenic CBM2b-1-2:GFP (upper) and WT (lower) plants were visualized by fluorescent microscopy (left panels) and white light (right panels). Scale bar = 50  $\mu\text{m}$ .



**Supplemental Figure S3.2. 10X magnification of interfascicular fiber cells from middle stems of 5-week-old and 9-week-old transgenic SP:mCherry and CBM2b-1-2:mCherry plants.** Squares in the left panel indicate the areas of high magnification views. Scale bar = 50  $\mu\text{m}$ .

**Supplemental Table S3.1 List of primer designed for gene constructs**

<b>Primer</b>	<b>Sequence</b>
AtSP-F	/5Phos/CTAGAATGGGTCATCTTGGGTTCTTAGTTATG ATTATGGTAGGAGTCATGGCTTCTTCTGTGAGCGGCT ACGGTG
AtSP-R	/5Phos/GATCCACCGTAGCCGCTCACAGAAGAAGCCA TGACTCCTACCATAATCATAACTAAGAACCCAAGAT GACCCATT
PT linker Forward	/5Phos/CCGTA <sup>CTCGAGGGCGGGC</sup> ACGGCGACCCC GACCCCCACGCCGACGCCGACGCCGGAATTCGAGCT CGTCGACGTA
PT linker Reverse	/5Phos/CCGGTACGTCGACGAGCTCGAATTCGGCGTC GGCGTCGGCGTGGGGGTCGGGGTCGCCGTGCCGCCG CCCTCGAGTA
mCherry Forward	5'-ACCGGTCGCCACCATGGTGAGCA-3'
mCherry Reverse	5'-ACCGGTCTTGTACAGCTCGTCC-3'
CBM2b-1-2 Forward	5'-CCCGGGTAATGGGATCCAGCACC-3'
CBM2b-1-2 Reverse	5'-CTCGAGGCCCGTGGCGCACGTAG-3'

**Supplemental Table S3.2 List of primers for Genotyping**

<b>Primer</b>	<b>Sequence</b>
LP	5'-TCATGCACCTCTAGGGTTTTC-3'
RP	5'-GCTCCACTCTCTTTTTTCACCC-3'
LBb1.3	5'- ATTTTGCCGATTTCGGAAC-3'

**Supplemental Table S3.3 List of primers for RT-PCR**

<b>Primer</b>	<b>Sequence</b>
RT- <i>mCherry</i> Forward	5'- CAAGGAGTTCATGCGCTTCAAGGT -3'
RT- <i>mCherry</i> Reverse	5'- TCTTGGCCTTGTAGGTGGTCTTGA
RT- <i>AtWRKY</i> Forward	5'-ATGGAAGGAGGAGGGAGAAGAG-3'
RT- <i>AtWRKY</i> Reverse	5'-TTAAAAGGAAGAGAGACAATCATGG-3'
Actin2-1	5'-ATCCTCCGTCTTGACCTTGC-3'
Actin2-2	5'-GACCTGCCTCATCATACTCG-3'.

## References

- Abramson M, Shoseyov O, Shani Z** (2010) Plant cell wall reconstruction toward improved lignocellulosic production and processability. *Plant Science* **178**: 61-72
- Anderson CT, Carroll A, Akhmetova L, Somerville C** (2010) Real-time imaging of cellulose reorientation during cell wall expansion in *Arabidopsis* roots. *Plant Physiol* **152**: 787-796
- Bedford MR, Partridge GG** (2010) *Enzymes in Farm Animal Nutrition*. CABI
- Carpita NM, M.** (2000) The cell wall. *In* WG B. Buchanan, and R. Jones, ed, *Biochemistry and Molecular Biology of Plants*. American Society of Plant Physiologists, Rockville, MD, pp 52-108
- Carroll A, Somerville C** (2009) Cellulosic biofuels. *Annu Rev Plant Biol* **60**: 165-182
- Cho H-T, Cosgrove DJ** (2000) Altered expression of expansin modulates leaf growth and pedicel abscission in *Arabidopsis thaliana*. *Proceedings of the National Academy of Sciences* **97**: 9783-9788
- Clough SJ, Bent AF** (1998) Floral dip: a simplified method for *Agrobacterium*-mediated transformation of *Arabidopsis thaliana*. *Plant J* **16**: 735-743
- Estévez JM, Kieliszewski MJ, Khitrov N, Somerville C** (2006) Characterization of Synthetic Hydroxyproline-Rich Proteoglycans with Arabinogalactan Protein and Extensin Motifs in *Arabidopsis*. *Plant Physiology* **142**: 458-470
- Fry SC** (2010) Cell Wall Polysaccharide Composition and Covalent Crosslinking. *In* *Annual Plant Reviews*. Wiley-Blackwell, pp 1-42
- Gilbert HJ, Knox JP, Boraston AB** (2013) Advances in understanding the molecular basis of plant cell wall polysaccharide recognition by carbohydrate-binding modules. *Current Opinion in Structural Biology* **23**: 669-677

- Hao Z, Mohnen D** (2014) A review of xylan and lignin biosynthesis: foundation for studying Arabidopsis irregular xylem mutants with pleiotropic phenotypes. *Crit Rev Biochem Mol Biol* **49**: 212-241
- Haseloff J, Siemerling KR, Prasher DC, Hodge S** (1997) Removal of a cryptic intron and subcellular localization of green fluorescent protein are required to mark transgenic Arabidopsis plants brightly. *Proc Natl Acad Sci U S A* **94**: 2122-2127
- Knox JP** (2008) Revealing the structural and functional diversity of plant cell walls. *Current Opinion in Plant Biology* **11**: 308-313
- McCartney L, Blake AW, Flint J, Bolam DN, Boraston AB, Gilbert HJ, Knox JP** (2006) Differential recognition of plant cell walls by microbial xylan-specific carbohydrate-binding modules. *Proceedings of the National Academy of Sciences of the United States of America* **103**: 4765-4770
- Paredes AR, Somerville CR, Ehrhardt DW** (2006) Visualization of Cellulose Synthase Demonstrates Functional Association with Microtubules. *Science* **312**: 1491-1495
- Rennie EA, Scheller HV** (2014) Xylan biosynthesis. *Current Opinion in Biotechnology* **26**: 100-107
- Shaner NC, Steinbach PA, Tsien RY** (2005) A guide to choosing fluorescent proteins. *Nat Methods* **2**: 905-909
- Stone BA, Jacobs AK, Hrmova M, Burton RA, Fincher GB** (2010) Biosynthesis of Plant Cell Wall and Related Polysaccharides by Enzymes of the GT2 and GT48 Families. *In Annual Plant Reviews*. Wiley-Blackwell, pp 109-165

**Tobimatsu Y, Wagner A, Donaldson L, Mitra P, Niculaes C, Dima O, Kim JI, Anderson N,**

**Loque D, Boerjan W, Chapple C, Ralph J** (2013) Visualization of plant cell wall lignification using fluorescence-tagged monolignols. *Plant J* **76**: 357-366

**Wang H, Avci U, Nakashima J, Hahn MG, Chen F, Dixon RA** (2010) Mutation of WRKY transcription factors initiates pith secondary wall formation and increases stem biomass in dicotyledonous plants. *Proc Natl Acad Sci U S A* **107**: 22338-22343

## CHAPTER 4

### HETEROLOGOUS EXPRESSION OF CRYSTALLINE CELLULOSE DIRECTED-CARBOHYDRATE BINDING MODULE 3A IN ARABIDOPSIS MODULATES PLANT CELL WALLS AND DEVELOPMENT

#### Abstract

The non-catalytic polysaccharide-recognizing modules within diverse microbial carbohydrate-active enzymes are defined as Carbohydrate-Binding Modules (CBMs). CBMs can bind to specific plant cell wall polysaccharides, such as cellulose, mannan or xylan. In this study, we have examined the effects of heterologous expression of crystalline cellulose binding-CBM3a fused with the mCherry fluorescent protein in Arabidopsis. Compared to wild type plants, transgenic CBM3a:mCherry plants displayed a dwarfed phenotype, had reduced cellulose and xylan content, and showed changes in glycan epitope extractability patterns. These results indicate that expression of a specific CBM in Arabidopsis may lead to changes in the composition and/or structure of the cell wall, which in turn, may have an impact on the development of the plant. Our results further suggest that creation of a set of Arabidopsis plants expressing diverse microbial CBMs and single-chain antibody fragments (ScFvs) may provide a toolset for manipulating plant cell wall structure to change or improve the properties of lingo-cellulosic biomass.

## **Introduction**

Growing plant cells are surrounded by a primary cell wall consisting predominantly of carbohydrate polymers. Cellulose is the most abundant biological macromolecule and is an extracellular, linear polymer of glucose molecules (Nishiyama et al., 2002). Cellulose exists as microfibrils composed of parallel  $\beta$ -1,4-linked glucan chains that are held together laterally by hydrogen bonds and vertically by hydrophobic stacking of the sugar rings. Cellulose is much more ordered than other components of the primary cell wall (Bootten et al., 2004), in keeping with its key role of providing strength and controlling growth. Xyloglucan was widely believed to act as a tether between cellulose fibers, limiting cell enlargement and regulating cell wall mechanical properties. However, recent studies suggest that only a minor xyloglucan component may be located in the limited regions of tight contact between cellulose fibers, playing an important role in wall mechanics (Cavalier et al., 2008; Zabolina et al., 2008; Dick-Perez et al., 2011; Park and Cosgrove, 2012; Zabolina et al., 2012). Pectin can form hydrated gels to facilitate slippage of cellulose microfibrils during cell growth. In relation to cell wall biology, the architecture of heterogeneous functional wall polysaccharides accommodates the dynamic processes of cell growth and differentiation.

Plant cell growth is precisely controlled by oriented expansion of the cell walls. The driving force for cell expansion is osmotic, but the rate and direction of expansion are controlled by the mechanical properties of the cell wall (Cho and Cosgrove, 2000). The stiffness of cell walls is greatest in the direction of cellulose microfibrils, expansion of the cell walls needs either widening the space (Marga et al., 2005) or facilitating slippage (Cosgrove, 2005) between cellulose microfibrils or both. In growing cell walls, when cellulose microfibrils are first laid down at the inner face of the primary cell wall, their orientation is normally transverse to the

direction of growth (Cosgrove, 2005). As the cell wall expands, cellulose microfibrils reorient toward the direction of growth (Anderson et al., 2010). Hemicellulose and pectin co-extensive with cellulose microfibrils resist these deformation (Zykwinska et al., 2007), and therefore help to control the rate of growth.

There is evidence that proteins, for example expansins, are involved in modifying cellulose-hemicellulose interactions and enhancing growth by mediating cell wall loosening (Choi et al., 2003). Carbohydrate-binding modules (CBMs) could also affect these interactions (Levy et al., 2002), leading to altered morphology or plant growth in transgenic plants (Safra-Dassa et al., 2006; Obembe et al., 2007). A CBM is defined as a contiguous amino acid sequence within a carbohydrate-active enzyme with a discreet fold having carbohydrate-binding activity (Boraston et al., 2004). CBMs are suggested to enhance the efficiency of enzymes by mediating prolonged and intimate contact between their cognate catalytic modules and their target substrates (Herve et al., 2010). CBMs have been grouped into 69 sequence-based families (<http://www.cazy.org/Carbohydrate-Binding-Modules.html>) and around half of these CBM families contain members that bind to an extensive range of plant cell wall polysaccharides (Knox, 2008), including cellulose (Blake et al., 2006), mannans (Filonova et al., 2007), xyloglucan (von Schantz et al., 2009) and xylan (McCartney et al., 2006). Recently, CBMs have been used as probes to assess and document the cell biological contexts of polysaccharides and cell wall diversity *in vitro* (Knox, 2008). Although CBMs do occur in plant enzymes, most CBMs being used as probes for cell wall polysaccharides are of microbial origin (McCann and Knox, 2010).

Cellulose microfibrils can exist in highly ordered crystalline, semi-ordered paracrystalline, and disordered noncrystalline (amorphous) states (Tomme et al., 1995). CBMs

located in family 3a bind to crystalline cellulose (Blake et al., 2006). A previous study has shown that recombinant His-tagged CBM3a from *Clostridium spp.* effectively binds to both primary and secondary cell walls in tobacco stem sections using an indirect triple labeling immunofluorescence procedure (His-tagged CBM, anti-His mouse-Ig, anti-mouse Ig fluorescein isothiocyanate) (Blake et al., 2006). We have shown previously that expression of a xylan-binding CBM can be used effectively as a tool for *in vivo* monitoring of xylan deposition (see Chapter 3 of this thesis). Since CBMs are the only cellulose-directed probes available, it was of interest to investigate the heterologous expression of CBM3a in the plant to determine if this CBM could be used as an *in vivo* probe for monitoring cellulose deposition and dynamics. Toward that end, we have expressed fluorescent protein mCherry-tagged CBM3a in Arabidopsis under the control of the 35S cauliflower mosaic virus (CaMV) promoter. We show here that transgenic expression of CBM3a:mCherry modulates plant cell wall structure and affects plant development.

## **Materials and Methods**

### **Plant Material and Growth Conditions**

Both Arabidopsis wild type and the transgenic plant CBM3a:mCherry lines are in the ecotype Columbia (Col-0) background. Seeds of Arabidopsis were sterilized, cold treated at 4 °C for 48 h, and germinated on one-half-strength Murashige and Skoog medium (Sigma) in a growth chamber under a 16-h-light/8-h-dark cycle at 19 °C during the light period and 15 °C during the dark period. The light intensity was 120  $\mu\text{mol m}^{-2} \text{s}^{-1}$ , and the relative humidity was maintained at 70%. One-week-old seedlings were transferred to soil and grown in growth chambers under the same conditions.

## **Gene Constructs and Plant Transformation**

The coding sequence of the AtExpansin10 signal peptide (At1g26770) (Cho and Cosgrove, 2000) was amplified by AtSP-F and AtSP-R primers (containing KpnI and XbaI restriction enzyme sites) with Platinum Tag High Fidelity DNA Polymerase (Invitrogen 12574-030) (all the primers designed for gene constructs are listed in Supplemental Table S4.1). A proline-threonine (PT) linker coding sequence was amplified from a modified pET22b vector (obtained from Dr. Gilbert, Newcastle University, UK) using PT linker Forward Primer (containing the XmaI restriction enzyme site) and PT linker Reverse Primer (containing the AgeI restriction enzyme site). Using mCherry Forward Primer (containing an AgeI restriction enzyme site) and mCherry Reverse Primer (containing an AgeI restriction enzyme site), the *mCherry* gene was amplified from the pmCherry vector (Clontech PT3973-5). Using CBM3a Forward primer (containing the BamHI restriction enzyme site) and CBM3a Reverse primer (containing the XhoI restriction enzyme site), the *CBM3a* gene was amplified from the scaffoldin of *Clostridium spp.* (obtained from Dr. Gilbert, New Castle University, UK). PCR products were cleaved by the appropriate restriction enzymes (Thermo Scientific Inc) and ligated into the pBI121 vector (Clontech). All constructs were confirmed by sequencing (Macrogen, USA) and individually transformed into *Agrobacterium tumefaciens* GV3101 competent cells by electroporation. Transformation of Arabidopsis was conducted by floral dipping (Clough and Bent, 1998).

## **RNA Isolation and Reverse Transcript (RT)-PCR Analysis**

Plant stems for RNA isolation were frozen in liquid nitrogen immediately after harvesting and stored at -80 °C until use. RNA was isolated using the RNeasy plant mini kit (Qiagen) and treated with RNase-free DNase (Qiagen) to remove contaminating genomic DNA. Total RNA

(500 ng) was reverse-transcribed using Superscript® III Reverse Transcriptase (Invitrogen). RT-PCR was performed in 20 µl of reaction mixture, composed of 2 µl of a given cDNA, 0.4 µl of each primer (10 µM), 0.4 µl dNTP (10mM), 0.2 µl DreamTaq DNA Polymerase (5 U/µl) (Thermo), 2 µl 10X DreamTaq DNA Polymerase Buffer, and 14.6 µl Nuclease-free water. Amplifications were performed using a Tetrad 2 DNA Engine PCR machine (Bio-Rad) under the following conditions: initial polymerase activation: 95 °C, 3 min; 35 cycles of 30 s at 95°C, and 30 s at 55°C. Actin2 (At3g18780) was used as reference gene. Gene-specific primers are listed in Supplemental Table S4.1.

### **Fluorescent Microscopy**

Live plants expressing CBM3a:mCherry fusion proteins (3-day-old roots and hand-sectioned 2-month-old stems) were examined by fluorescence microscopy on an Eclipse 80i (Nikon) microscope equipped with epifluorescence optics. Images were captured with a Nikon DS-Ri1 camera head using NIS-Element Basic Research software, and images were assembled using Adobe Photoshop (Adobe Systems).

### **Cellulose Content Analysis**

Fresh samples (stems) from each plant were collected and ground immediately under liquid nitrogen to a fine powder. Alcohol-insoluble residue (AIR) of each sample was prepared and destarched enzymatically as described (Foster et al., 2010). Roughly 60-70 mg AIR samples were subsequently hydrolyzed with 2 M trifluoroacetic acid (TFA) for 1 h at 120 °C. The pellet material remaining after TFA hydrolysis was used for cellulose content analysis as described (Foster et al., 2010).

## **TMS Methyl Glycoside Glycosyl Residue Composition Analysis by Gas Chromatography**

The AIR samples were aliquoted (1–3 mg) as acetone suspensions to individual tubes and allowed to air dry. Inositol (20 µg) was added to each tube and the samples were lyophilized and analyzed for glycosyl residue composition by combined gas chromatography–mass spectrometry (GC–MS) of the per-O-trimethylsilyl (TMS) derivatives of the monosaccharide methyl glycosides produced from the sample by acid methanolysis basically as described (York, 1985). The dry samples were hydrolyzed for 18 h at 80 °C in 1 M methanolic-HCl. The samples were cooled and evaporated under a stream of dry air and further dried two additional times with anhydrous methanol. The samples were derivatized with 200 µl of TriSil Reagent (Pierce-Endogen, Rockford, IL, USA) and heated to 80 °C for 20 min. The cooled samples were evaporated under a stream of dry air, re-suspended in 3 ml of hexane, and filtered through packed glass wool. The dried samples were re-suspended in 150 µl of hexane and 1 µl of sample was injected onto a fused silica capillary column in an Agilent gas chromatograph G1701EA. Monosaccharides were quantified based on standard curves obtained with monosaccharide standards.

## **Tissue Fixation**

Two-month-old Arabidopsis inflorescence stems were fixed for 2.5 h in 1.6% (w/v) paraformaldehyde and 0.2% (w/v) glutaraldehyde in 25 mM sodium phosphate buffer, pH 7.1. Tissue was then washed with buffer twice for 15 min, and dehydrated through a graded ethanol series [35%, 50%, 75%, 95% (v/v), 100%, 100%, and 100% ethanol] for 30 min for each step. The dehydrated tissue was moved to 4 °C and then gradually infiltrated with cold LR White embedding resin (Ted Pella) using 33% (v/v) and 66% (v/v) resin in 100% ethanol for 24 h each, followed by 100% resin for 24 h three times. The infiltrated tissue was transferred to gelatin

capsules containing 100% resin for embedding, and resin was polymerized by exposing the capsules to 365-nm UV light at 4 °C for 48 h.

### **Generation of Fluorescent CBM3a:mCherry protein in *Escherichia coli***

The fluorescent protein tagged CBM3a:mCherry was produced as a His-tagged recombinant protein using the T7 expression-system consisting of the pET22b vector (Novagen, Madison, WI) harbored in *Escherichia coli* BL21(DE3). The *CBM3a:mCherry* gene was inserted into the vector using PCR. Digestion of purified PCR products and pET22b with NotI and XhoI (Thermo Scientific Inc) enabled cloning of the gene between the NdeI/XhoI sites in the vector resulting in a construct encoding the recombinant protein containing a hexahistidine tag. The bacterium was routinely cultured at 37 °C in Luria broth (Bertani, 1951; Sambrook et al., 1989) and expression of the recombinant proteins was induced with 100 µM isopropyl-β-D-thiogalactopyranoside at 16 °C overnight. The fluorescent protein/His-tagged CBM3a:mCherry, which was produced in soluble form in the cytoplasm of *E. coli*, was purified by immobilized metal ion affinity chromatography (Sigma) using Talon™ Buffer (10 mM Tris/HCl pH 8.0 containing 300 mM NaCl) as the column matrix. The concentration of purified CBM3a:mCherry was determined spectrophotometrically from absorbance measurements at 280nm.

### **Direct *in vitro* Fluorescence Labeling of Tissue Sections by Fluorescent Protein-Tagged CBMs and Immunolabeling**

Semi-thin sections (250 nm) were cut from fixed, embedded plant tissues with a Leica EM UC6 ultramicrotome (Leica Microsystems) and mounted on glass slides (Colorfrost/plus; Fisher Scientific). Labeling was performed at room temperature as follows. Sections were blocked with 3% (w/v) nonfat dry milk in KPBS (0.01 M potassium phosphate, pH 7.1, containing 0.5 M NaCl) for 20 min and were washed with KPBS for 5 min. 15 µl (1-2 mg/ml)

fluorescent protein-tagged CBM3a:mCherry was applied and incubated for 1 h. For immunolabeling, undiluted hybridoma supernatant of the mAb under study was applied and incubated for 1 h, sections were washed with KPBS three times for 5 min each, and goat anti-mouse IgG conjugated to Alexa-fluor488 (Invitrogen) diluted 1:100 in KPBS was applied and incubated for 1 h. All sections were washed with KPBS three times for 5 min and distilled water for 5 min. Prior to applying a coverslip, Citifluor antifade mounting medium AF1 (Electron Microscopy Sciences) was applied.

### **Cell Wall Extraction for Glycome Profiling**

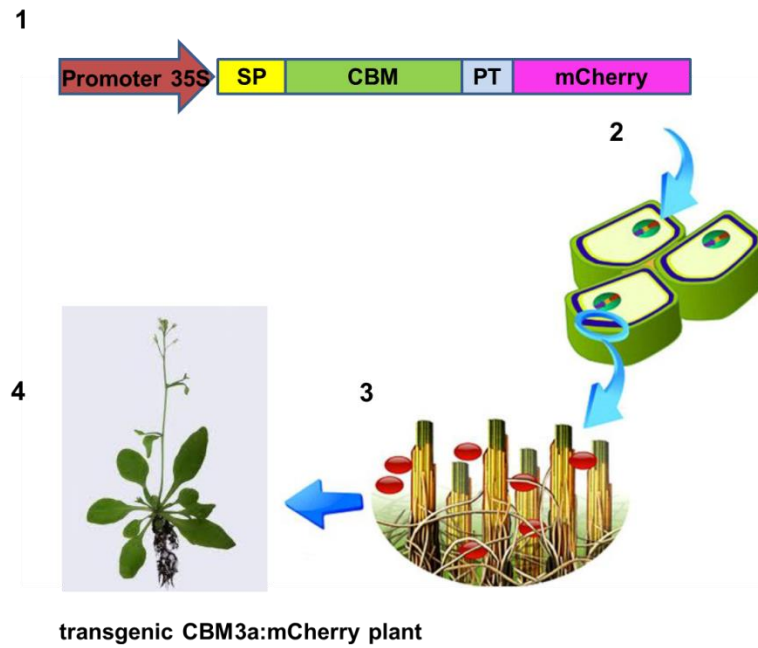
The AIR samples (200 mg) of cell walls was washed with increasingly harsh reagents in the following order: 50 mM ammonium oxalate (oxalate), 50 mM sodium carbonate with 0.5% (w/v) of sodium borohydride (carbonate), 1 M KOH with 1% (w/v) of sodium borohydride, 4 M KOH with 1% (w/v) of sodium borohydride, 100 mM sodium chlorite (Chlorite), and post-chlorite 4 M KOH with 1% (w/v) of sodium borohydride (4 M KOH PC) to isolate fractions enriched in cell wall components as previously described (Zhu et al., 2010). The 1 M KOH, 4 M KOH, and 4 M KOH PC fractions were neutralized using glacial acetic acid. All extracts were dialyzed against four changes of de-ionized water (sample:water~1:60) at room temperature for a total of 48 h and then lyophilized. Total sugars in the cell wall extracts were quantified using the phenol sulphuric acid method (Masuko et al., 2005), and ELISA analyses were done as previously described (Pattathil et al., 2012).

## Results

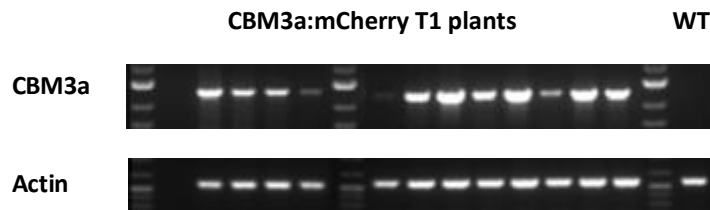
### Generation and Molecular Characterization of Transgenic CBM3a:mCherry Plants

A construct (Figure 4.1A) was created to heterologously express CBM3a:mCherry transgenically in Arabidopsis: the *CBM3a:mCherry* gene was inserted into a PBI121-derived vector containing a constitutive CaMV 35S promoter (red) and a cell wall secretory signal peptide (yellow) from *AtExpansin10* (Cho and Cosgrove, 2000). After Agrobacterium-mediated transformation, expression of the introduced *CBM3a:mCherry* gene in kanamycin antibiotic-resistant Arabidopsis was confirmed by Reverse-Transcript (RT) PCR analysis with total RNA. RT-PCR result revealed variations in the yield of *CBM3a* expression among individual T1 lines (Figure 4.1B). In total, 56 transgenic plants were obtained and all transgenic plants were grown side by side with wild-type Col-0 plants. Among these transgenic plants, 48% of the T1 transgenic CBM3a plants were not able to survive in the soil, 22% of the T1 transgenic CBM3a plants appeared normal as wild-type plants and 30% of the T1 transgenic CBM3a plants eventually developed into plants with reduced stem elongation. However, the expression level of *CBM3a:mCherry* does not correlate entirely positively with the severity of the phenotype. The seeds of dwarfed plants were collected, germinated and grown. This T2 generation inherited the stunted growth phenotype. One line of the T2 generation was chosen based on its dwarf phenotype and the relatively strong fluorescent signal of the CBM3a:mCherry fusion protein, and a further generation of this line (T3) was used for all subsequent analyses. RT-PCR showed that all T3 individuals had equivalent expression levels of CBM3a:mCherry compared to the actin controls (Figure 4.1C)

A



B



C

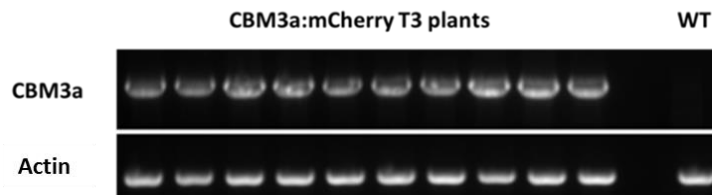


**Figure 4.1.** (A) Outline of the heterologous expression of CBM3a:mCherry in transgenic plants. [Figure is modified from Figure 1 of (Abramson et al., 2010)]: 1) Gene Construct consisting of a constitutive promoter, CaMV 35S (red), a cell wall targeting signal peptide (yellow), a CBM gene (green), proline and threonine (PT) linker (blue) and fluorescent marker (mCherry) (cherry-pink). 2) Transformation of the CBM gene into plant genome. 3) CBM protein is then

expressed and secreted into the cell wall (green strands - crystalline cellulose; yellow strands - amorphous cellulose; brown strands - hemicellulose). 4) Transgenic CBM-expressing plant is generated and expression level of CBM is examined.

**(B)** Agarose gels showing the presence and various expression levels of the *CBM3a* transgene by RT-PCR in T1 plants. Stems from 4-week-old plants were used to extract RNA. *Actin2* was amplified as the control.

**(C)** RT-PCR analysis confirming equal expression level of the *CBM3a* transgene in the T3 plants used in this study. Stems from 4-week-old plants were used to extract RNA. *Actin2* was amplified as the control.

### **Developmental Effects of Expressed CBM3a:mCherry in Transgenic Plants**

To observe the developmental effects of the expressed CBM3a:mCherry, weekly measurements of the growth of rosettes and inflorescence stems were conducted for transgenic CBM3a:mCherry plants, along with wild type plants. Heterologous expression of CBM3a:mCherry yielded phenotypes different than wild type in plant rosette size, plant height and plant developmental timing. Development in the transgenic plants was delayed by 2 to 3 weeks compared with development in wild type plants (Figure 4.2). At the rosette age (4-week-old), transgenic CBM3a:mCherry plants exhibited smaller leaves compared to wild type (Figure 4.2C). The rosette leaf eventually developed to a normal size at weeks 7 and 8 (Figure 4.2A). CBM3a:mCherry plants started bolting two weeks later than did wild type plants, and when they reached their final height at week 8, they averaged 29 cm tall, which was approximately 67% of the average height of wild type plants (Figures 4.2B and 4.2C).

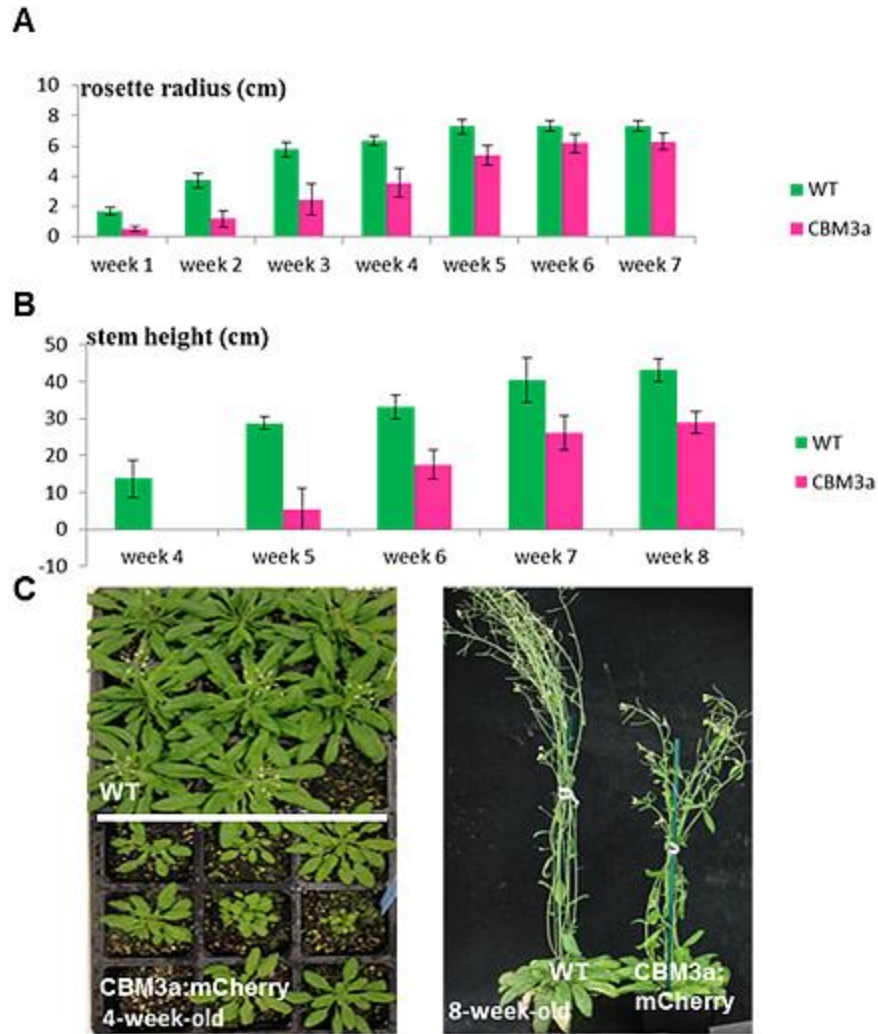


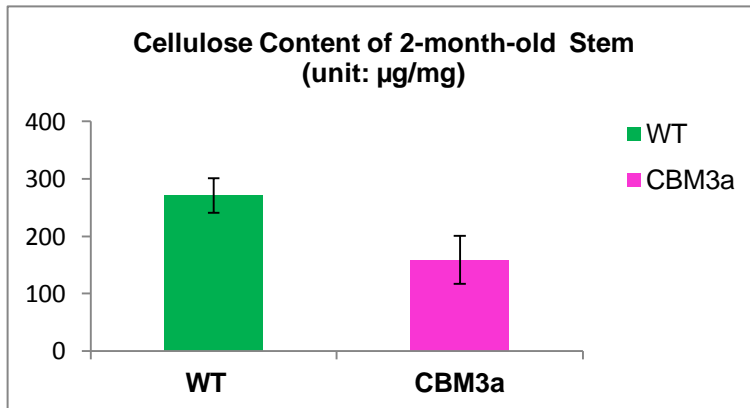
**Figure 4.2. Morphological phenotypes of transgenic CBM3a:mCherry plants**

- (A) Average radius of the rosettes  $\pm$  standard deviation (n=8 for wild type, n=10 for transgenic CBM3a:mCherry plants).
- (B) Average plant height  $\pm$  standard deviation (n=8 for wild type, n=8 for transgenic CBM3a:mCherry plants).
- (C) Four-week-old and 8-week-old transgenic CBM3a:mCherry plants along with wild type plants of the same ages.

## Analysis of Cell Wall Composition

To investigate whether the expressed CBM3a:mCherry affects the plant cell wall, cell wall composition analyses was performed on 2-month-old inflorescence stems from transgenic plants and wild type plants. Differences in cell wall composition were detected in stem crystalline cellulose content, as well as in stem matrix polysaccharide composition. Cellulose content was decreased by 41% in transgenic CBM3a:mCherry stems compared to wild type stems (Figure 4.3A). Furthermore, matrix cell wall monosaccharide analysis revealed a significant 20% reduction in xylose content compared to the wild type (Figure 4.4B). The observed increases for Arabinose, Rhamnose, Glucuronic Acid, Galacturonic Acid in CBM3a:mCherry stems could be attributable to the corresponding decrease in xylose. These results indicated that expression of CBM3a:mCherry affected stem cell wall composition.

A



**B**

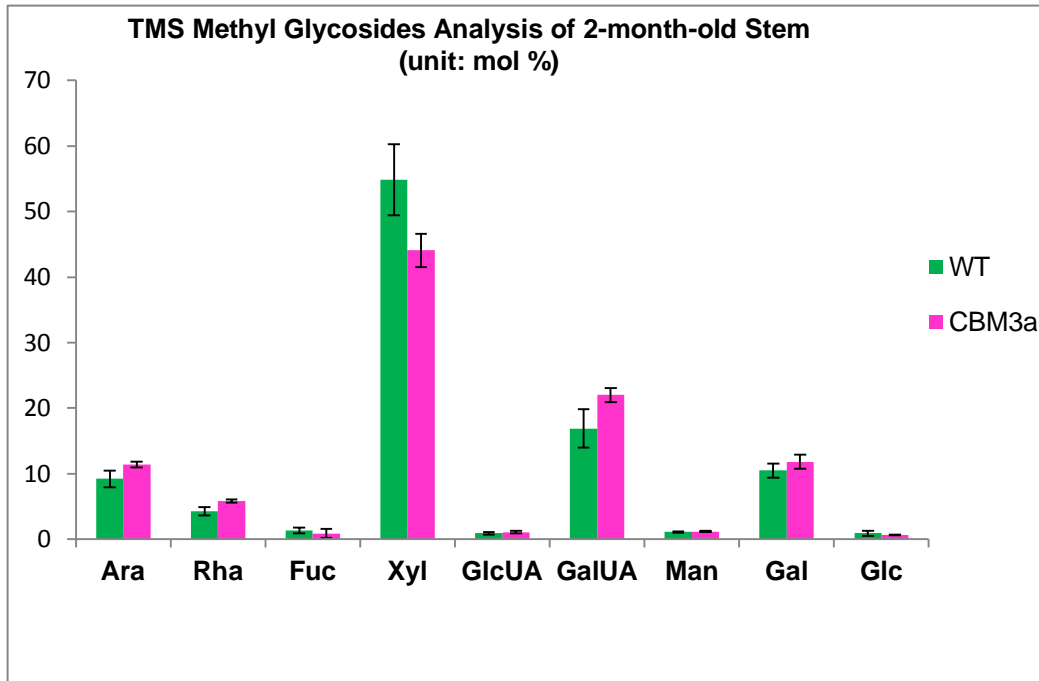


**Figure 4.3. Compositional analysis of cell walls from wild type and transgenic CBM3a:mCherry plants.** (A) Cellulose content in 2-month-old stems of wild type and transgenic CBM3a:mCherry plants. (B) The glycosyl residue composition of walls determined by GC of TMS derivatives was quantified from 2-month-old inflorescence stems of transgenic CBM3a:mCherry and wild type plants. Glycosyl residues are abbreviated as arabinose (Ara), rhamnose (Rha), fucose (Fuc), xylose (Xyl), glucuronic acid (GlcUA), galacturonic acid (GalUA), mannose (Man), galactose (Gal), and glucose (Glc). All data represent the average  $\pm$  standard deviation of n=3 biological replicates, each with three technical repetitions.

#### **Detection of Cellulose in CBM3a:mCherry Transgenic Plant Stem**

*In vitro* detection of crystalline cellulose using calcofluor staining and CBM3a:mCherry fusion protein generated from *E. coli* were carried out as independent controls for comparison

with the *in vivo* labeling patterns resulting from the heterologous expression of CBM3a:mCherry protein in transgenic plant stems. Calcofluor staining in transgenic CBM3a:mCherry plant stems showed less staining intensity in the walls of pith cells compared to wild type stem (Figure 4.4A & 4.4B). Direct labeling of stem sections with CBM3a:mCherry fusion protein revealed that CBM3a:mCherry binding was restricted to the epidermis and xylem cells in the CBM3a:mCherry plant stem (Figure 4.4C), whereas CBM3a:mCherry bound indiscriminately to the epidermis through the cortex and phloem to the vascular tissue in WT stem (Figure 4.5D). Since mCherry red fluorescent protein is not as bright as green fluorescent protein (GFP) (Shaner et al., 2005), indirect immunofluorescent localization using a His-tagged CBM3a:mCherry protein and Alexa Fluor® 488 attached anti-His antibody was used in an effort to get more information than could be obtained using direct labeling with CBM3a:mCherry. Using this *in vitro* method, it was shown that CBM3a bound to every tissue of wide type stem including pith parenchyma (Figure 4.4E). However, labeling was still weak in epidermis, phloem and pith of the transgenic CBM3a:mCherry plant stem (Figure 4.4F), suggesting decreased cellulose content in these tissues of the transgenic plant stem.

### **Expressed CBM3a:mCherry is Localized in Cell Walls**

The *in vivo* expression pattern of the CBM3a:mCherry fusion protein was determined in roots and stems of transgenic CBM3a:mCherry plants by fluorescent microscopy. The resulting images showed that fluorescence of CBM3a:mCherry fusion proteins was located in the cell walls of epidermis, cortex and endodermis in transgenic plant roots (Figure 4.5A2). In the stem, distribution of CBM3a:mCherry protein showed a cell-type specific pattern; the fluorescent signal of CBM3a:mCherry was specifically localized in xylem vessels and interfascicular fibres, whereas no mCherry fluorescence was observed in pith parenchyma cells (Figure 4.5C2). The *in*

*in vivo* distribution pattern of CBM3a:mCherry fusion protein in stem is consistent with *in vitro* detection of cellulose in fixed stem sections of 2-month-old CBM3a:mCherry using exogenous CBM3a:mCherry protein (Figure 4.4D) and CBM3a protein (Figure 4.4F), reflecting reduced cellulose content mainly in primary walls of epidermis, cortex, phloem and pith.

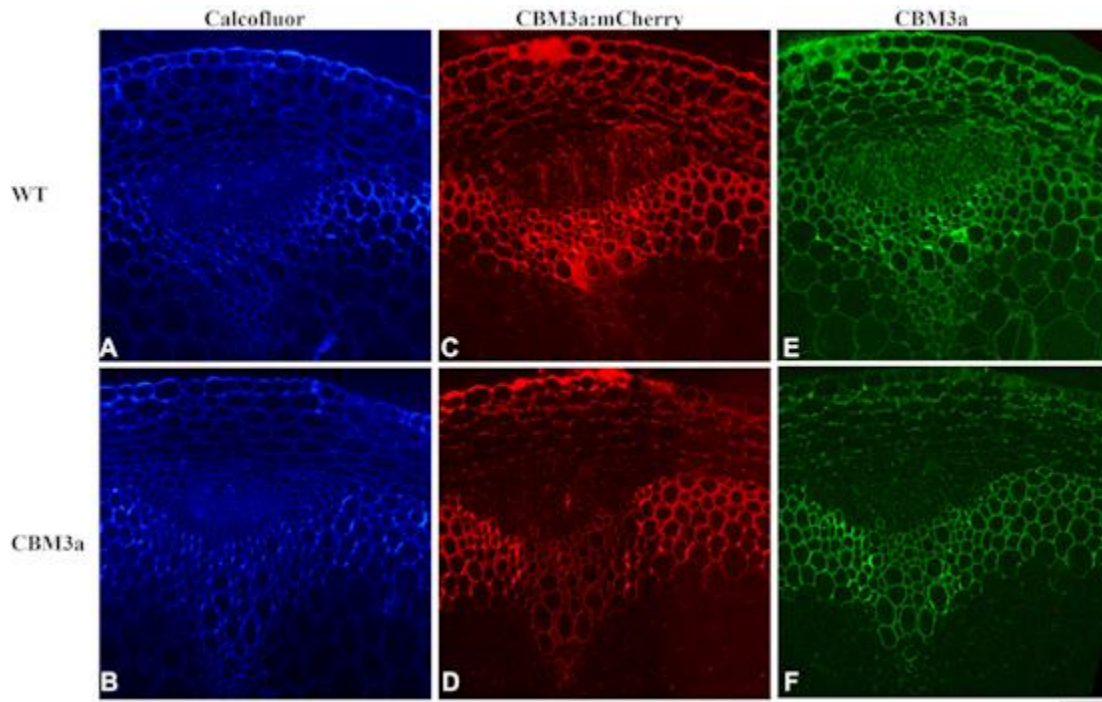


**Figure 4.4.** *In vitro* detection of cellulose in stem sections of 2-month-old WT plant (Upper) and transgenic CBM3a:mCherry plant (Lower). (A) (B) Calcofluor staining; (C) (D) Direct labeling with CBM3a:mCherry protein; (E) (F) Immunohistochemistry using CBM3a:mCherry protein and Alexa Fluor® 488 attached anti-his monoclonal antibody. Scale bar = 50  $\mu$ m.

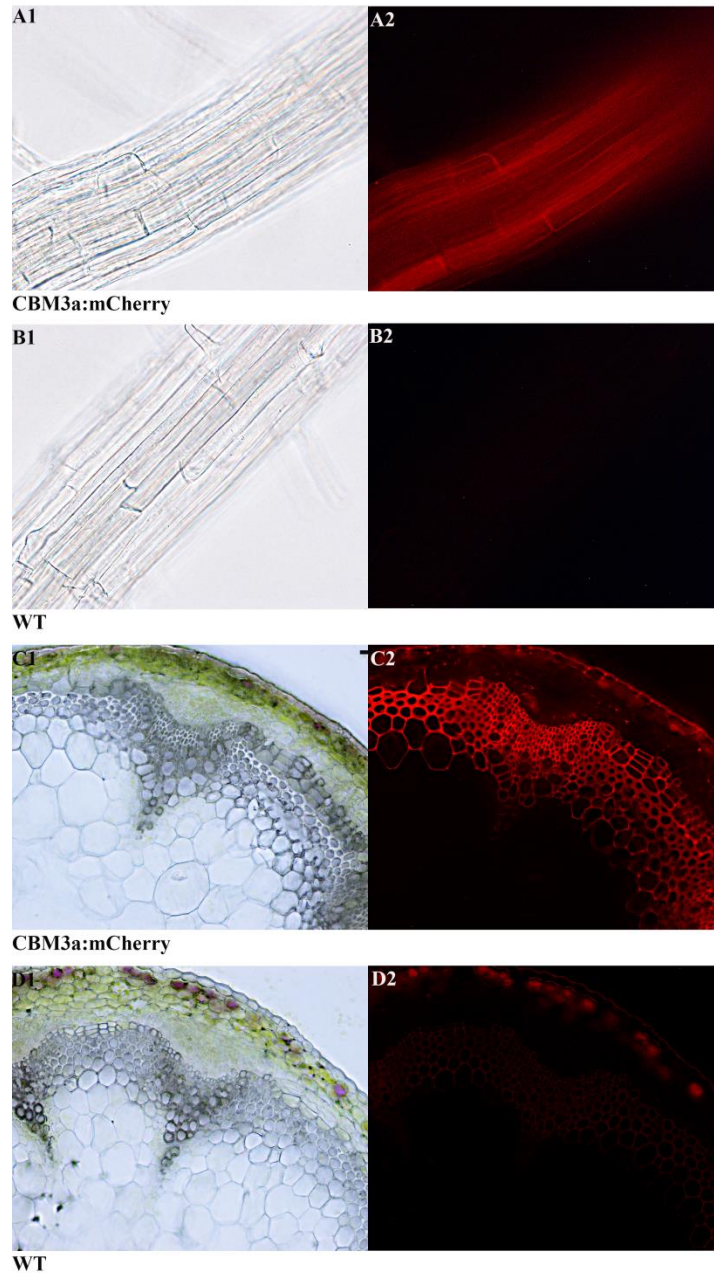


**Figure 4.5. Fluorescent images of root and stem of transgenic *Arabidopsis* plants expressing CBM3a:mCherry and of wild type plants. (A) Localization of CBM3a:mCherry fusion protein in the 3-day-old root. **A1** image of background without green light excitation, **A2** fluorescent image. (B) 3-day-old wild type root. **B1**, image of background without green light excitation, **B2** fluorescent image. (C) Localization of CBM3a:mCherry fusion protein in the 8-**

week-old stem. **C1** image of background without green light excitation, **C2** fluorescent image. **(D)** 8-week-old wild type stem. **D1** image of background without green light excitation, **D2** fluorescent image. (green light excitation = 528-553 nm, emission = 590-650 nm) Scale bar = 50  $\mu\text{m}$ .

### **Glycome Profiling Analysis**

To determine if expression of CBM3a:mCherry affected cell wall structure on a larger scale, glycome profiling (Zhu et al., 2010) was used to compare transgenic CBM3a:mCherry cell walls versus wild type cell walls. Stem cell walls from 2-month-old, 3-month-old and 4-month-old transgenic plants were analyzed to obtain a more comprehensive picture of possible changes in the cell wall composition (hemicellulose and pectin) and structure (Figure 4.6 and Supplementary Figure S4.2 and S4.3). Glycome profiling indicated subtle differences, primarily in epitope extractability patterns, in transgenic CBM3a:mCherry stem cell walls compared to wild type walls. For example, the 1M KOH extracts of transgenic CBM3a:mCherry stem walls contained less detectable levels of xylan epitopes, HG backbone epitopes and RG-I epitopes. There were also subtle changes in the levels of xyloglucan epitopes in the Carbonate extracts of transgenic CBM3a:mCherry stems compared with wild type stems.

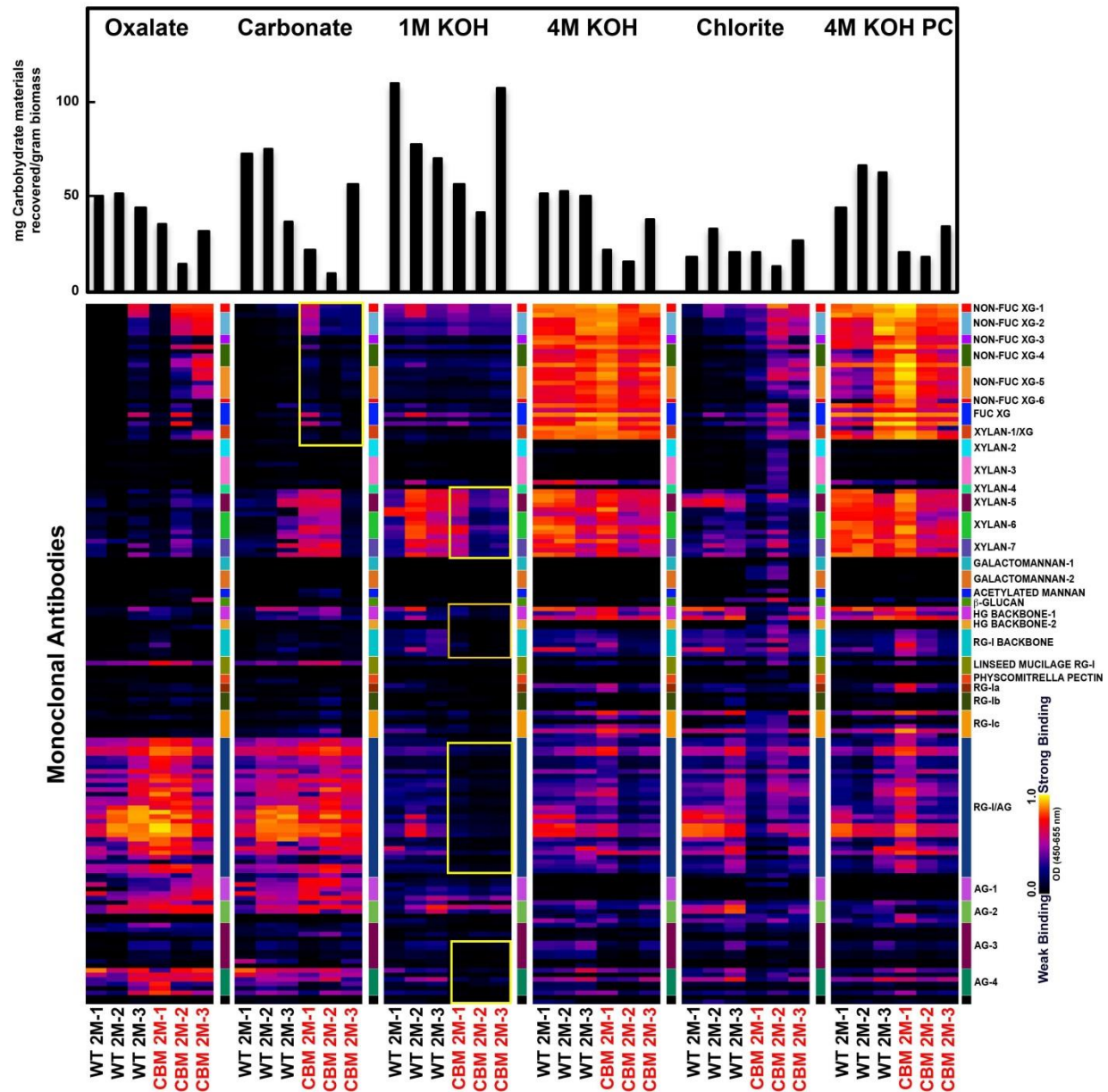


**Figure 4.6. Glycome Profiling of sequential cell wall extracts from 2-month-old Wild-Type and transgenic CBM3a:mCherry stems.**

Glycome profiling of sequential extracts prepared from total plant stem cell walls of three plants each of 2-month-old transgenic CBM3a:mCherry plants and wild-type plants. The presence of cell wall glycan epitopes in each extract was determined by ELISA using 150 glycan-directed monoclonal antibodies and the data were prepared as heat maps. The panel on the right lists the

array of antibodies used, grouped according to the principal cell wall glycan (right-hand side) recognized by antibodies.

## **Discussion**

We have investigated whether or not CBM3a:mCherry could be used as a tool to localize cellulose *in vivo* in the same way that we were able to localize xylans *in vivo* using CBM2b-1-2 (see Chapter 3). Previous literature on the effects of heterologous expression of cellulose-directed CBMs in plants yielded plants with altered growth phenotypes. In one case, transgenic expression of CBM29-1-2 was deleterious to plant growth in tobacco (Obembe et al., 2007). In the other case, transgenic expression of CBM4 resulted in enhanced growth in potatoes (Safra-Dassa et al., 2006). Thus we were interested in testing whether expression of fluorescent protein mCherry-tagged cellulose-binding CBM3a in Arabidopsis has any effect on the growth and development of the plant, and if so, what changes in composition or structure of plant cell wall networks might have occurred. In this study, we generated transgenic Arabidopsis plant expressing CBM3a:mCherry and demonstrated that expression of CBM3a:mCherry affected plant development and cell wall composition in Arabidopsis, as reflected by a dwarfed growth habit of the transgenic plants, decreased cellulose content, decreased xylose content, and changes in glycan epitope extractability patterns compared to wild type plants. Thus, CBM3a cannot be used as a benign tool for tagging cellulose *in vivo*. Instead, it appears that CBM3a can be used as a tool to selectively target cellulose, thereby modulating wall structure and consequently plant growth and development.

Unlike non-cellulosic polysaccharides, which are assembled within the Golgi and then transported to the apoplast via secretory vesicles, cellulose is synthesized at the plasma

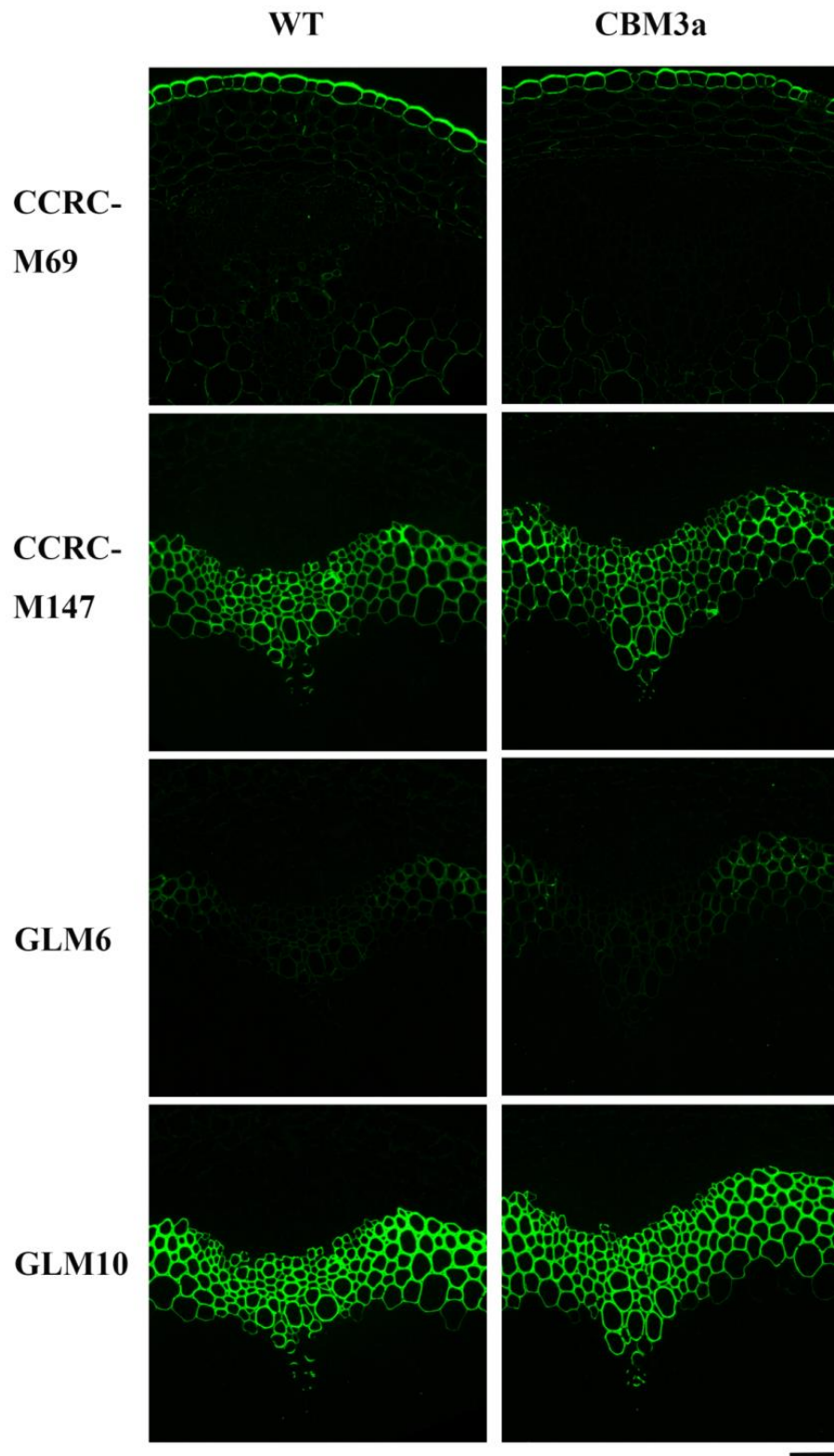
membrane by plasma membrane resident cellulose synthase (CESA) complexes (Mutwil et al., 2008). In our study, CBM3a was fused with a signal peptide to direct the newly translated protein into the endoplasmic reticulum (ER) and hence into the secretory pathway. Newly translated CBM3a proteins are transferred from the ER to the Golgi, and then secreted into the apoplast by fusion of Golgi-derived vesicles with the plasma membrane. Thus, the heterologously expressed CBM3a can interact with cellulose only after the protein has reached the cell wall, where it could bind to cellulose microfibrils as they are newly synthesized by the CESA complexes or to already existing cellulose microfibrils in the wall.

Previous studies using the bacterium, *Acetobacter xylinum*, indicated that the fluorescent dye Calcofluor alters the crystallization of cellulose by hydrogen bonding with individual glucan chains, thereby preventing their assembly into a microfibril (Haigler et al., 1980). The alteration of microfibril assembly led to an increase in the rate of glucan chain polymerization, suggesting polymerization and crystallization are coupled processes, and that the rate of crystallization determines the rate of polymerization (Benziman et al., 1980). Changes in the assembly of the cellulose microfibrils might further affect composition and mechanical properties of cell walls. Arabidopsis mutants in CESA1<sup>A903V</sup> and CESA3<sup>T942I</sup>, have reduced width and lower microfibril crystallinity of cellulose, suggesting different chain assembly during microfibril formation (Harris et al., 2012). These mutants also display decreased cellulose content (Harris et al., 2012). Cellulose-binding CBM3a presents a planar hydrophobic face that likely binds to the surface of the cellulose crystal (Murashima et al., 2005) and CBM3a is also suggested to make few significant hydrogen bonds with cellulose structures (Blake et al., 2006). The polar side chains in the binding face of CBM3a are suggested to interact with matrix polysaccharides that are in intimate contact with the cellulose microfibrils (Blake et al., 2006). Thus, one could speculate

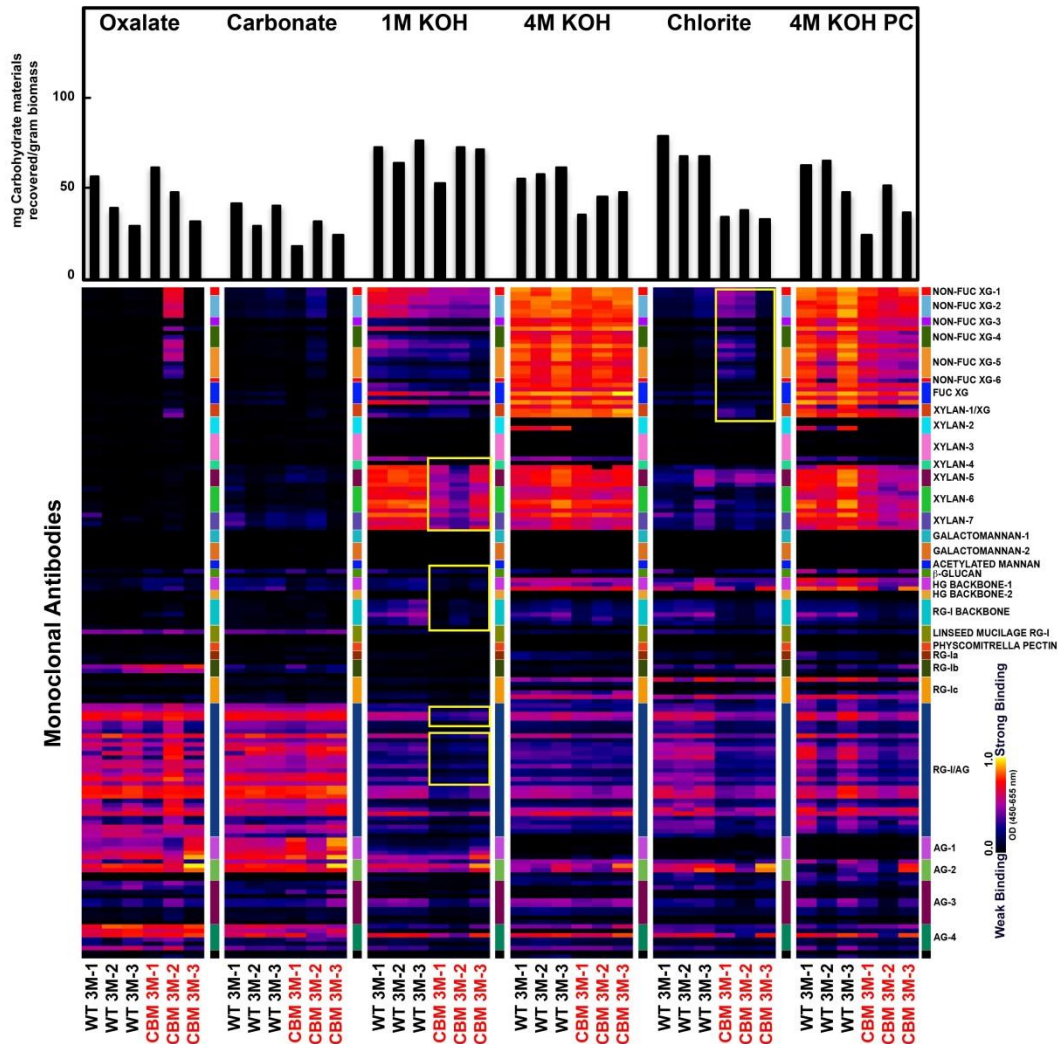
that the presence of the CBM3a in the Arabidopsis cell wall has an influence on the assembly of cellulose microfibrils and/or on the interactions of cellulose with other wall polymers, resulting in decreased cellulose content, decreased xylose content, and changes in glycan epitope extractability patterns. Further measurement of the cellulose crystallinity index and analysis of glycosyl linkage composition are planned to interpret the effects of the heterologously expressed CBM3a on the Arabidopsis cell wall.

The continuous presence of CBM3a protein could also result in cell wall structures being held more loosely, thereby affecting the rate of wall extension and possibly leading to a remodeling of cell wall structure. During cell expansion, a delicate balance between cell wall biosynthesis and cell wall remodeling needs to be maintained. That is, cell walls are loosened enough to allow extension, but the integrity of the cell is not jeopardized (Bashline et al., 2014). Once the balance is disturbed via the presence of CBM3a protein, cell wall biosynthesis could be affected with resulting functional and structural alterations in the cell wall. In some cases, the modulated wall itself could act as feedback signal to the cell. Although compensatory mechanisms of cell wall integrity sensing are not well understood, it is noteworthy that the cell wall responds to either chemically or genetically reduced cellulose by increasing the amount of pectin (Albersheim et al., 2011). Thus, cell wall modification caused by the transgenically expressed CBM3a may activate signaling pathways to affect cell wall synthesis by up- or down-regulating polysaccharide biosynthesis genes. Detailed transcriptional analysis of transgenic CBM3a:mCherry plant by next generation high-throughput sequencing methodology (RNAseq) is planned to define whether the transcription levels of genes involved in cell wall biosynthesis/modification are affected by the heterologously expressed CBM3a.

In this study, we have shown that it is possible to apply a cell wall engineering approach to plants by transgenic expression of the cellulose-binding CBM3a protein in Arabidopsis. Investigation of cell wall modifications caused by expression of CBM3a has given some insight into the impact of this approach on cell wall integrity and plant fitness. Creation of a broad collection of Arabidopsis plants expressing diverse microbial CBMs and/or single-chain antibody fragments (ScFvs) by cloning the variable domains of the heavy and light antibody chains from hybridoma cell lines secreting plant glycan-directed antibodies (in progress in our lab) may serve as polysaccharide-selective agents to alter cell wall structure in the future.

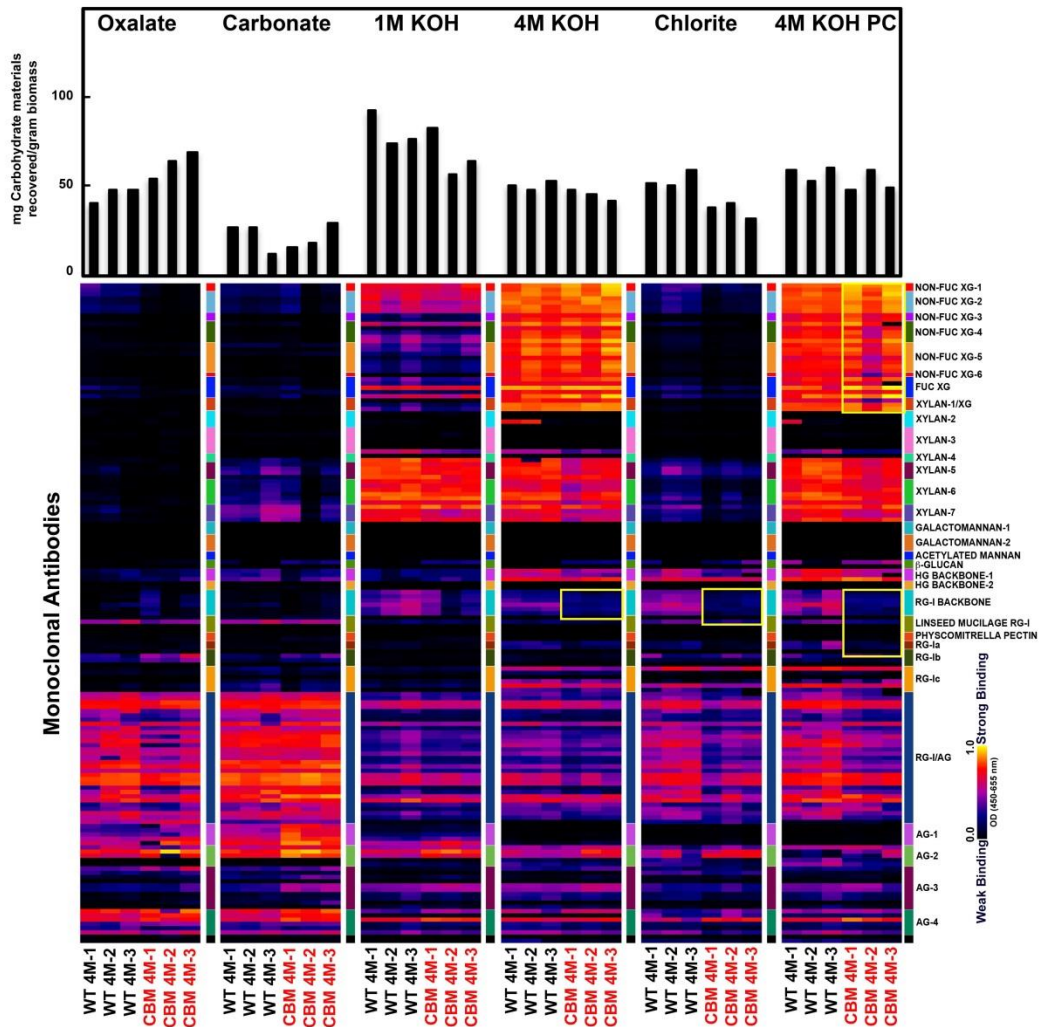


**Supplemental Figure S4.1. Pectin, xylan and lignin deposition in transgenic CBM3a:mCherry stems.** Transverse sections of the basal part of 2-month-old transgenic CBM3a:mCherry plants labeled with the pectin RG-I backbone-directed monoclonal antibody CCRC-M69, the xylan-directed monoclonal antibody CCRC-M147, and the lignin-directed monoclonal antibodies GLM6 and GLM10.



**Supplemental Figure S4.2. Glycome Profiling of sequential stem cell wall extracts from 3-month-old Wild-Type and transgenic CBM3a:mCherry plants**

Glycome profiling of sequential extracts prepared from total stem plant cell walls of three plants each of 3-month-old transgenic CBM3a:mCherry plants and wild-type plants. The presence of cell wall glycan epitopes in each extract was determined by ELISA using 150 glycan-directed monoclonal antibodies and the data were prepared as heat maps. The panel on the right lists the array of antibodies used, grouped according to the principal cell wall glycan (right-hand side) recognized by antibodies.



**Supplemental Figure S4.3. Glycome Profiling of sequential stem cell wall extracts from 4-month-old Wild-Type and transgenic CBM3a:mCherry plants**

Glycome profiling of sequential extracts prepared from total stem plant cell walls of three plants each of 4-month-old transgenic CBM3a:mCherry plants and wild-type plants. The presence of cell wall glycan epitopes in each extract was determined by ELISA using 150 glycan-directed monoclonal antibodies and the data were prepared as heat maps. The panel on the right lists the array of antibodies used, grouped according to the principal cell wall glycan (right-hand side) recognized by antibodies.

**Supplemental Table S4.1 List of primer**

<b>Primer</b>	<b>Sequence</b>
AtSP-F	/5Phos/CTAGAATGGGTCATCTTGGGTTCTTAGTTATGATTATGG TAGGAGTCATGGCTTCTTCTGTGAGCGGCTACGGTG
AtSP-R	/5Phos/GATCCACCGTAGCCGCTCACAGAAGAAGCCATGACTCC TACCATAATCATAACTAAGAACCCAAGATGACCCATT
PT linker Forward	/5Phos/CCGTACTCGAGGGCGGCACGGCGACCCCGACCCC CACGCCGACGCCGACGCCGGAATTCGAGCTCGTCGACGTA
PT linker Reverse	/5Phos/CCGGTACGTCGACGAGCTCGAATTCCGGCGTCGGCGTC GGCGTGGGGGTCGGGGTCGCCGTGCCGCCGCCCTCGAGTA
mCherry Forward	5'-ACCGGTCGCCACCATGGTGAGCA-3'
mCherry Reverse	5'-ACCGGTCTTGACAGCTCGTCC-3'
CBM3a Forward	5'-GGATCCATGGTATCAGGCAATTTG-3'
CBM3a Reverse	5'-CTCGAGACCGGGTTCTTTACCCC-3'
RT-CBM3aM F	5'-GTATCAGGCAATTTGAAGG-3'
RT-CBM3aM R	5'-ACCGGGTTCTTTACCCC-3'
Actin2-1	5'-ATCCTCCGTCTTGACCTTGC-3'
Actin2-2	5'-GACCTGCCTCATCATACTCG-3'
pETCBM3aM F	5'-GGGAATTCCATATGGTATCAGGCAATTTGAAGG-3'
pETCBM3aM R	5'-ATAAGAATGCGGCCGCTTGTACAGCTCGTCC-3'

## References

- Abramson M, Shoseyov O, Shani Z** (2010) Plant cell wall reconstruction toward improved lignocellulosic production and processability. *Plant Science* **178**: 61-72
- Albersheim P, Darvill A, Roberts K, Sederoff R, Staehelin A** (2011) *Plant Cell Walls*. Garland Science, New York
- Anderson CT, Carroll A, Akhmetova L, Somerville C** (2010) Real-time imaging of cellulose reorientation during cell wall expansion in Arabidopsis roots. *Plant Physiol* **152**: 787-796
- Bashline L, Lei L, Li S, Gu Y** (2014) Cell Wall, Cytoskeleton, and Cell Expansion in Higher Plants. *Molecular Plant* **7**: 586-600
- Benziman M, Haigler CH, Brown RM, White AR, Cooper KM** (1980) Cellulose biogenesis: Polymerization and crystallization are coupled processes in *Acetobacter xylinum*. *Proc Natl Acad Sci U S A* **77**: 6678-6682
- Bertani G** (1951) STUDIES ON LYSOGENESIS I.: The Mode of Phage Liberation by Lysogenic *Escherichia coli*. *Journal of Bacteriology* **62**: 293-300
- Blake AW, McCartney L, Flint JE, Bolam DN, Boraston AB, Gilbert HJ, Knox JP** (2006) Understanding the Biological Rationale for the Diversity of Cellulose-directed Carbohydrate-binding Modules in Prokaryotic Enzymes. *Journal of Biological Chemistry* **281**: 29321-29329
- Blake AW, McCartney L, Flint JE, Bolam DN, Boraston AB, Gilbert HJ, Knox JP** (2006) Understanding the biological rationale for the diversity of cellulose-directed carbohydrate-binding modules in prokaryotic enzymes. *J Biol Chem* **281**: 29321-29329
- Bootten TJ, Harris PJ, Melton LD, Newman RH** (2004) Solid-state <sup>13</sup>C-NMR spectroscopy shows that the xyloglucans in the primary cell walls of mung bean (*Vigna radiata* L.)

- occur in different domains: a new model for xyloglucan-cellulose interactions in the cell wall. *J Exp Bot* **55**: 571-583
- Boraston AB, Bolam DN, Gilbert HJ, Davies GJ** (2004) Carbohydrate-binding modules: fine-tuning polysaccharide recognition. *Biochem J* **382**: 769-781
- Cavalier DM, Lerouxel O, Neumetzler L, Yamauchi K, Reinecke A, Freshour G, Zabolina OA, Hahn MG, Burgert I, Pauly M, Raikhel NV, Keegstra K** (2008) Disrupting Two *Arabidopsis thaliana* Xylosyltransferase Genes Results in Plants Deficient in Xyloglucan, a Major Primary Cell Wall Component. *The Plant Cell Online* **20**: 1519-1537
- Cho H-T, Cosgrove DJ** (2000) Altered expression of expansin modulates leaf growth and pedicel abscission in *Arabidopsis thaliana*. *Proceedings of the National Academy of Sciences* **97**: 9783-9788
- Choi D, Lee Y, Cho H-T, Kende H** (2003) Regulation of Expansin Gene Expression Affects Growth and Development in Transgenic Rice Plants. *The Plant Cell Online* **15**: 1386-1398
- Clough SJ, Bent AF** (1998) Floral dip: a simplified method for *Agrobacterium*-mediated transformation of *Arabidopsis thaliana*. *Plant J* **16**: 735-743
- Cosgrove DJ** (2005) Growth of the plant cell wall. *Nat Rev Mol Cell Biol* **6**: 850-861
- Dick-Perez M, Zhang Y, Hayes J, Salazar A, Zabolina OA, Hong M** (2011) Structure and interactions of plant cell-wall polysaccharides by two- and three-dimensional magic-angle-spinning solid-state NMR. *Biochemistry* **50**: 989-1000
- Filonova L, Kallas AM, Greffe L, Johansson G, Teeri TT, Daniel G** (2007) Analysis of the surfaces of wood tissues and pulp fibers using carbohydrate-binding modules specific for crystalline cellulose and mannan. *Biomacromolecules* **8**: 91-97

- Foster CE, Martin TM, Pauly M** (2010) Comprehensive compositional analysis of plant cell walls (lignocellulosic biomass) part II: carbohydrates. *J Vis Exp*
- Haigler CH, Brown RM, Jr., Benziman M** (1980) Calcofluor white ST Alters the in vivo assembly of cellulose microfibrils. *Science* **210**: 903-906
- Harris DM, Corbin K, Wang T, Gutierrez R, Bertolo AL, Petti C, Smilgies DM, Estevez JM, Bonetta D, Urbanowicz BR, Ehrhardt DW, Somerville CR, Rose JK, Hong M, Debolt S** (2012) Cellulose microfibril crystallinity is reduced by mutating C-terminal transmembrane region residues CESA1A903V and CESA3T942I of cellulose synthase. *Proc Natl Acad Sci U S A* **109**: 4098-4103
- Herve C, Rogowski A, Blake AW, Marcus SE, Gilbert HJ, Knox JP** (2010) Carbohydrate-binding modules promote the enzymatic deconstruction of intact plant cell walls by targeting and proximity effects. *Proc Natl Acad Sci U S A* **107**: 15293-15298
- Knox JP** (2008) Revealing the structural and functional diversity of plant cell walls. *Current Opinion in Plant Biology* **11**: 308-313
- Levy I, Shani Z, Shoseyov O** (2002) Modification of polysaccharides and plant cell wall by endo-1,4-beta-glucanase and cellulose-binding domains. *Biomol Eng* **19**: 17-30
- Marga F, Grandbois M, Cosgrove DJ, Baskin TI** (2005) Cell wall extension results in the coordinate separation of parallel microfibrils: evidence from scanning electron microscopy and atomic force microscopy. *Plant J* **43**: 181-190
- Masuko T, Minami A, Iwasaki N, Majima T, Nishimura S, Lee YC** (2005) Carbohydrate analysis by a phenol-sulfuric acid method in microplate format. *Anal Biochem* **339**: 69-

- McCann MC, Knox JP** (2010) Plant Cell Wall Biology: Polysaccharides in Architectural and Developmental Contexts. *In Annual Plant Reviews*. Wiley-Blackwell, pp 343-366
- McCartney L, Blake AW, Flint J, Bolam DN, Boraston AB, Gilbert HJ, Knox JP** (2006) Differential recognition of plant cell walls by microbial xylan-specific carbohydrate-binding modules. *Proceedings of the National Academy of Sciences of the United States of America* **103**: 4765-4770
- Murashima K, Kosugi A, Doi RH** (2005) Site-directed mutagenesis and expression of the soluble form of the family IIIa cellulose binding domain from the cellulosomal scaffolding protein of *Clostridium cellulovorans*. *J Bacteriol* **187**: 7146-7149
- Mutwil M, Debolt S, Persson S** (2008) Cellulose synthesis: a complex complex. *Curr Opin Plant Biol* **11**: 252-257
- Nishiyama Y, Langan P, Chanzy H** (2002) Crystal Structure and Hydrogen-Bonding System in Cellulose I $\beta$  from Synchrotron X-ray and Neutron Fiber Diffraction. *Journal of the American Chemical Society* **124**: 9074-9082
- Obembe OO, Jacobsen E, Timmers J, Gilbert H, Blake AW, Knox JP, Visser RG, Vincken JP** (2007) Promiscuous, non-catalytic, tandem carbohydrate-binding modules modulate the cell-wall structure and development of transgenic tobacco (*Nicotiana tabacum*) plants. *J Plant Res* **120**: 605-617
- Park YB, Cosgrove DJ** (2012) A Revised Architecture of Primary Cell Walls Based on Biomechanical Changes Induced by Substrate-Specific Endoglucanases. *Plant Physiology* **158**: 1933-1943

- Pattathil S, Avci U, Miller J, Hahn M** (2012) Immunological Approaches to Plant Cell Wall and Biomass Characterization: Glycome Profiling. *In* ME Himmel, ed, Biomass Conversion, Vol 908. Humana Press, pp 61-72
- Safra-Dassa L, Shani Z, Danin A, Roiz L, Shoseyov O, Wolf S** (2006) Growth modulation of transgenic potato plants by heterologous expression of bacterial carbohydrate-binding module. *Molecular Breeding* **17**: 355-364
- Sambrook J, Fritsch EF, Maniatis T** (1989) *Molecular Cloning: A Laboratory Manual*, Ed 2nd. Cold Spring Harbor Laboratory Press, Plainview, N.Y
- Shaner NC, Steinbach PA, Tsien RY** (2005) A guide to choosing fluorescent proteins. *Nat Methods* **2**: 905-909
- Tomme P, Warren RA, Gilkes NR** (1995) Cellulose hydrolysis by bacteria and fungi. *Adv Microb Physiol* **37**: 1-81
- von Schantz L, Gullfot F, Scheer S, Filonova L, Cicortas Gunnarsson L, Flint JE, Daniel G, Nordberg-Karlsson E, Brumer H, Ohlin M** (2009) Affinity maturation generates greatly improved xyloglucan-specific carbohydrate binding modules. *BMC Biotechnol* **9**: 92
- York WS, Darvill, A.G., McNeil, M., Stevenson, T.T., Albersheim, P.** (1985) Isolation and characterization of plant cell walls and cell wall components. *Methods Enzymol* **118**: 3-40
- Zabotina OA, Avci U, Cavalier D, Pattathil S, Chou YH, Eberhard S, Danhof L, Keegstra K, Hahn MG** (2012) Mutations in multiple XXT genes of Arabidopsis reveal the complexity of xyloglucan biosynthesis. *Plant Physiol* **159**: 1367-1384

- Zabotina OA, van de Ven WT, Freshour G, Drakakaki G, Cavalier D, Mouille G, Hahn MG, Keegstra K, Raikhel NV** (2008) Arabidopsis XXT5 gene encodes a putative alpha-1,6-xylosyltransferase that is involved in xyloglucan biosynthesis. *Plant J* **56**: 101-115
- Zhu X, Pattathil S, Mazumder K, Brehm A, Hahn MG, Dinesh-Kumar SP, Joshi CP** (2010) Virus-induced gene silencing offers a functional genomics platform for studying plant cell wall formation. *Mol Plant* **3**: 818-833
- Zykwinska A, Thibault JF, Ralet MC** (2007) Organization of pectic arabinan and galactan side chains in association with cellulose microfibrils in primary cell walls and related models envisaged. *J Exp Bot* **58**: 1795-1802

## CONCLUSIONS

The complex and dynamic nature of the plant cell wall has led to the need for novel tools and approaches to characterize wall structure, and the genes responsible for its synthesis and modification. As imaging tools develop in scope and sophistication, efforts are now focusing on observation of structurally and functionally diverse cell walls during plant development. *In vivo* imaging of polysaccharides is severely limited, since unlike protein or nucleic acid synthesis, where sequences are directly encoded by gene sequences, the biosynthesis of plant polysaccharides occurs from the combined action of specific enzymes including not only the ones involved in the biosynthesis, but also ones that function in degradation and modification (Fry, 2010). Also, the biosynthesis of plant polysaccharides depends on the availability of the necessary precursors and whether these precursors will confine the reactions in specific cells, cellular locations, compartments or tissues (Stone et al., 2010). We have demonstrated that heterologous expression of CBMs can provide a platform for tracking cell wall polysaccharides *in vivo*. Our transgenic CBM2b-1-2:mCherry plant is enabling a new approach to monitor active xylan deposition *in vivo* without unnecessarily disturbing plant physiology and development. In this respect, CBM2b-1-2:mCherry constitutes a novel imaging tool for xylan detection in living plants, and is in contrast to traditional immunolabeling of fixed plant sections, where the activity and distribution of cell wall polysaccharides during the dynamics of plant development as cells grow, divide, and differentiate cannot be observed because these tissues are “dead”. The *in vivo* feature of transgenic CBM expression provides scientists with a substantial advantage in studies of the detailed alterations of plant cell walls during development and during cell expansion and cell separation processes. This year, the development of super-resolved fluorescence microscopy

was awarded the Nobel Prize in chemistry. Super-resolved fluorescence microscopy enables scientists to visualize the pathways of individual molecules inside living cells. We expect our *in vivo* polysaccharide tracking tool, in combination with recent microscopic advances, will provide important new insights into the biosynthesis of cell walls, and the contribution of polysaccharides in cellular processes.

On the other hand, we also demonstrated that heterologous expression of cellulose-binding CBM3a modifies the cell wall in transgenic plants. Future investigations of cell wall modifications caused by heterologously expressed specific CBMs and their impact on cell wall structure and plant development will help us to understand the contribution of different polysaccharides to the biology of plant cells. Currently, steady progress is being made in characterizing polysaccharide biosynthesis genes in order to enable the design of plants biomass with higher yield and altered cell wall composition suited for various biotechnological applications, including biofuel production. However, there are still technical difficulties in the genetic engineering of plant cell walls due to the complexity of polysaccharide metabolism, which is regulated through the balance between biosynthesis, modification, and degradation. More than 2000 genes are involved in these processes. Heterologous expression of specific CBMs may provide an effective alternative strategy to modify biomass quality and quantity by use of CBMs to alter cell wall structure and content in the future. Whether the heterologous expression of fluorescent protein tagged CBMs is suitable for utilization as an *in vivo* tracking tool or as a cell wall modification tool depends on the CBM itself and the polysaccharide that the CBM binds to. Indeed, even within the same polysaccharide binding group, different CBMs could lead to different results, since these modules can display very different specificities in cell walls due to their different topologies (Gilbert et al., 2013).

## References

**Fry SC** (2010) Cell Wall Polysaccharide Composition and Covalent Crosslinking. *In Annual Plant Reviews*. Wiley-Blackwell, pp 1-42

**Gilbert HJ, Knox JP, Boraston AB** (2013) Advances in understanding the molecular basis of plant cell wall polysaccharide recognition by carbohydrate-binding modules. *Current Opinion in Structural Biology* **23**: 669-677

**Stone BA, Jacobs AK, Hrmova M, Burton RA, Fincher GB** (2010) Biosynthesis of Plant Cell Wall and Related Polysaccharides by Enzymes of the GT2 and GT48 Families. *In Annual Plant Reviews*. Wiley-Blackwell, pp 109-165